DISSERTATION

Titel der Dissertation

Functional Analysis of the Plasma Membrane
Alr1 and Alr2 Proteins in Yeast *Saccharomyces cerevisiae*

angestrebter akademischer Grad

Doktor/in der Naturwissenschaften (Dr. rer.nat.)

Verfasserin / Verfasser:	Mag. Ing. Marcin Wachek
Matrikel-Nummer:	0247179
Dissertationsgebiet (lt. Studienblatt):	Molekulare Biologie
Betreuerin / Betreuer:	Univ.-Prof. Dr. Rudolf Schweyen, Dr. Anton Graschopf

Wien, im März 2009

TABEL OF CONTENTS

1. SUMMARY

Proteins Alr1 and Alr2 of *Saccharomyces cerevisiae* encode a very sophisticated system to take up magnesium, one of the most abundant cations, into the cell. Together with the distantly related bacterial CorA and the mitochondrial Mrs2 subfamily they form the 2-TM-GxN type family of metal ion transporters that regulate the Mg^{2+} homeostasis. They are composed of a cytoplasmic amino terminal domain followed by a two trans-membrane domain segment connected by a short periplasmatic loop and the canonical (Y/FGMN) signature in the carboxyl terminus of the first TM.

In this thesis a series of biochemical and genetic analyses support the functional and structural homology of Alr1p and its close homolog protein Alr2 to the CorA-Mrs2-Alr1 family. Both proteins reside in the plasma membrane. Whereas Alr1p acts as the main Mg^{2+}-transporter, Alr2p contributes poorly to Mg^{2+}-uptake. Only overexpression of *ALR2* overcomes the Mg^{2+} dependent growth phenotype of cells mutated in *ALR1*. Substitution of a single arginine with a glutamic acid residue in the loop between the two TM domains at the cell surface greatly improves its activity. Recent determination of the CorA crystal structure yielded clear confirmation for the function of 2-TM-GxN members in oligomerized complexes. Both, Alr1 and Alr2 proteins are shown to form homo- and hetero-oligomers when treated with chemical cross-linkers. Using the *in vivo* mating-based split ubiquitin system, protein interactions between these proteins were demonstrated. The ability of the proteins to form homo- and hetero-oligomers can have dominant-negative effects on the function of wild-type Alr1p when Alr2p is overexpressed, most likely as a result of the interaction between low-function and full-function proteins. Furthermore, this assay also showed that the orientation of Alr proteins is consistent with CorA, where both N-terminal and C-terminal ends are exposed to the cell interior.

Successive truncations were constructed from N- and C-terminal tails of Alr1p to dissect the role in protein function. The analysis of carboxyl truncations affirmed the importance of this region for Alr1p Mg^{2+} transport activity and its critical impact on channel formation. In contrast, consecutive shortening of N-terminal domain of Alr1p accounted for striking abnormalities concerning protein stability and subcellular localization. Particularly, mutants deleted of a sequence stretch between E271 and Q318 showed an extremely changed phenotype. Further analysis using short amino acid intragenic deletions led to the identification of a sequence element of about 50 amino acids in the amino

terminal tail essential for protein translocation and stability. Proteins missing this region were blocked in translocation to the plasma membrane and undergo Mg^{2+} independent degradation, most likely via sorting mechanisms of the ER and subsequential proteasomal decay. However, the degradation is strictly excluded from the endosomal/vacuolar compartment as shown by the use of mutants hampered in the PVC pathway.

2. ZUSAMMENFASSUNG

Die Bäckerhefe *Saccharomyces cerevisiae* besitzt ein sehr raffiniertes System für den Magnesiumtransport in die Zelle, kodiert durch die Gene *ALR1* und *ALR2*. Gemeinsam mit den Unterfamilien der prokaryotischen CorA-Proteine und mitochondrialen Mrs2-Proteine, bilden sie die ubiquitäre 2-TM-GxN Familie der Metallionentransporter, die die Magnesium-Homöostase regulieren. Die Topologie dieser Proteinfamilie ist durch eine N-terminale Domäne mit niedriger Komplexität und zwei Transmembrandomänen in der C-terminalen Domäne charakterisiert. Am Ende der ersten Transmembrandomäne befindet sich die Konsensussequenz Y/FGMN, charakteristisch für alle Mitglieder dieser Proteinfamilie.

In der vorliegenden Arbeit bestätigt eine Reihe von biochemischen und genetischen Analysen eine funktionelle und strukturelle Homologie von Alr1p und seinem nahen Homolog Alr2p mit der CorA-Mrs2-Alr1 Familie. Beide Proteine wurden in der Plasmamembran lokalisiert. Während Alr1p als der primäre Mg^{2+}-Transporter fungiert, trägt das Alr2-Protein unter Standardbedingungen nur wenig zur Mg^{2+}-Aufnahme bei. Bei Überexpression des *ALR2* Gens kann Alr2p allerdings den Mg^{2+} abhängigen Phänotyp von *alr1Δ* Zellen supprimieren. Weiters haben Untersuchungen gezeigt, dass der Alr2p vermittelte Mg^{2+}-influx durch die Substitution einer einzelnen Aminosäure von Arg_{xy} zu Glu_{xy} in der „loop-Region" zwischen beiden Transmembranhelices signifikant gesteigert werden konnte.

Mittels chemischer „cross-link Studien" und *in vivo* „mating-based split-ubiquitin Studien" konnte sowohl die Ausbildung von Homo- als auch Heterooligomere zwischen Alr1p und Alr2p beobachtet werden. Eine Interaktion beider Proteine konnte weiters durch die Ausprägung eines dominant negativen Phänotyps bezüglich der intrazellulären Magnesiumkonzentration bei Überexpression von Alr2p nachgewiesen werden. Dies führte in Folge zu einer verringerten Wachstumsrate der betroffenen Zellen. Durch die Aufklärung der Proteinstruktur von *St*-CorA mittels Röntgenstrukturanalyse wurden diese Proteininteraktionen bestätigt und weiters die Ausbildung von Pentameren mit einer N-in/C-in Topologie für die Proteine der 2-TM-GxN Familie postuliert.

Um die Funktion unterschiedlicher Proteinabschnitte zu analysieren wurden sequenzielle Deletionen sowohl am C- als auch am N-terminus des Proteins durchgeführt und die Funktion bzw. deren Ausfall untersucht. Veränderungen am C-terminalen Ende, nahe der

2. Transmembrandomäne hatten meist einen Funktionsverlust des Proteins zur Folge. Hingegen wurde die Deletion von Aminosäuren am C-terminalen Ende des Proteins toleriert. Deletionen, die Transmembrandomänen betreffend, zerstörten die Funktion des Proteins wohl dadurch, dass die Verankerung des Proteins in der Plasmamembran und damit die Ausbildung eines Kanals nicht mehr möglich war.

Konsekutive Verkürzungen am N-terminus bis zu einem Ausmaß von ca. 270 Aminosäuren hatten keinen Einfluss auf die Funktion des Proteins. Weder kam es zu einer Reduktion der intrazellulären Mg^{2+} Konzentration, noch zu reduzierten Wachstumsraten. Allerdings zeigten sich signifikante Abweichungen in der Proteinstabilität und Lokalisation dieser Isomere. Die Reduktion potentieller Modifikationsorte führte zu verzögerter und geringerer Phosphorilierung was wiederum die Endozytose der Proteine negativ beeinflusste. Deletionen von mehr als 270 aa führten zu einem totalen Funktionsverlust. Durch die Konstruktion von intramolekularen Deletionen von ca. 20 – 30 Aminosäuren gelang es uns eine essentielle Domäne begrenzt durch die Aminosäuren E271 und Q318 zu charakterisieren. Proteine mit einer Deletion in diesem Abschnitt wurden nicht mehr zur Plasmamembran transloziert und wiesen eine sehr geringe, von Magnesium unabhängige, Stabilität auf. Durch die Analyse dieser veränderten Proteine in Zellen mit einem Defekt in der Ausbiludung des PVC (pre vacuolar complex) konnte ein Abbau über das endosomale Kompartment und in der Vakuole ausgeschlossen werden. Mit größter Wahrscheinlichkeit werden diese defekten Proteine durch „Sorting Prozesse" des Endoplasmatischen Reticulums bzw. des Golgiapparates erkannt und dem proteosomalen Abbau zugeführt.

3. INTRODUCTION

3.1 Unusual Nature of Magnesium – Chemistry and Biology

Magnesium is the eighth most abundant element on earth, the fourth most abundant element in vertebrates and the most abundant divalent cation within cells (Cowan, 1995; Maguire & Cowan, 2002; Wolf & Cittadini, 2003). The total magnesium content in various cell types ranges from 5 to 30 mM, thus making Mg^{2+} the second most abundant cellular cation after potassium (Hartwig, 2001). Major compartments in which magnesium appears to be widely distributed are mitochondria, the nucleus, and the endoplasmatic reticulum (Grubbs, 1990; Guenther, 1990; Romani & Scarpa, 1992). In biological systems, the vast majority of the magnesium in both intracellular and extracellular biological environments is complexed with other molecules, leaving only a small fraction as the free solvated ion (reviewed in (Kehres & Maguire, 2002)), (see Figure 3.1, (McCarthy & Kumar, 1999)). Intracellular free Mg^{2+} concentrations are in the range of 0.5 mM, which is 1-2% of the total cellular magnesium (Quamme, 1997). Accordingly, intracellular Mg^{2+} is maintained below the concentration predicted from the transmembrane electrochemical potential. Free ionized magnesium concentration is finely regulated by precise controls of Mg^{2+} entry, Mg^{2+} efflux and intracellular storage compartments (Cole & Quamme, 2000). As a consequence, the free magnesium content remains relatively constant whereas total concentrations can change significantly following the intracellular milieu and metabolic stimulation by hormones and other factors (Fatholahi et al, 2000; Romani & Scarpa, 1992). The vast majority of magnesium is complexed in a relatively non-specific way with macromolecules like nucleic acids, protein complexes, polysaccharides, and the polar group regions of membranes. About half of cellular Mg^{2+} is associated with small energy-rich compounds like ATP and other phosphonucleotides (Scarpa & Brinley, 1981). In addition, to serve as an essential cofactor that mediates enzyme-substrate interactions, or stabilizes intermediate metabolites or bridges distinct reactive substrates, a small fraction of Mg^{2+} may also bind directly to enzymes. Such effects allow Mg^{2+} to allosterically modify enzyme structures or gain a catalytic role (Tevelev & Cowan, 1995). The best-known cases of this tight and specific binding are interactions with ribonuclease H, exonuclease and topoisomerase II, but a comprehensive listing of Mg^{2+}-enzyme ligand-

binding interactions would probably include more than 300 different examples (Williams, 1993).
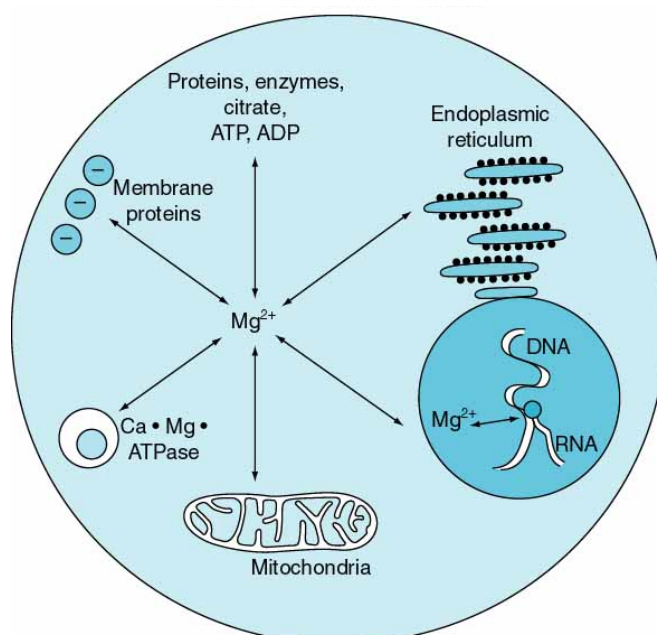
Figure 3.1. Intracellular distribution of magnesium (Mg^{2+}). Only 1% to 3% of the total intracellular Mg^{2+} exists as the free ionized form of Mg^{2+}, according to a cellular concentration of 0.5 to 1.0 mM. The total cellular Mg^{2+} concentration can vary from 5 to 20 mM, depending on the type of tissue studied, with the highest Mg^{2+} concentrations being found in skeletal and cardiac muscle cells. Our understanding of the concentration and distribution of intracellular Mg^{2+} has been facilitated by the development of electron microprobe analysis techniques and fluorescent dyes using microfluorescence spectrometry. Intracellular Mg^{2+} is predominantly complexed to organic molecules (*e.g.* adenosine triphosphatase [ATPase], cell and nuclear membrane-associated proteins, DNA and RNA, enzymes, proteins, and citrates) or sequestered within subcellular organelles (mitochondria and endoplasmic reticulum). A heterogeneous distribution of Mg^{2+} occurs within cells, with the highest concentrations being found in the perinuclear areas, which is the predominant site of endoplasmic reticulum. The concentration of intracellular free ionized Mg^{2+} is tightly regulated by intracellular sequestration and complexation. Very little change occurs in the concentration of intracellular free Mg^{2+}, even with large variations in the concentrations of total intracellular or extracellular Mg^{2+} (al-Ghamdi et al, 1994; de Rouffignac & Quamme, 1994; Romani et al, 1993). ADP— adenosine diphosphate; ATP—adenosine triphosphate; Ca+—ionized calcium (adapted from (McCarthy & Kumar, 1999)).

Virtually, all biological processes require Mg^{2+} not only as an essential cofactor in reactions involved in transfer, storage and utilization of energy. Magnesium acts also as a major cellular and subcellular stabilizing agent, which is necessary for the integrity of

cytoskeleton, mitochondria, lysosomes and polysomes. It exerts also membrane stabilizing and protecting effect by the binding of substances to the plasma membrane (reviewed in (Saris et al, 2000)). Mg^{2+} frequently modulates ion transport by pumps, carriers and channels and thereby may modulate signal transduction and the cytosolic concentrations of other ions (Saris et al, 2000)). As an intrinsic component of Na^+, K^+ – ATPase, HCO_3^- ATPase and Ca^{2+}, Mg^{2+} –ATPase, magnesium regulates Na^+/K^+, proton and Ca^{2+} transport, respectively (Nakajima et al, 1997; Ryan, 1991). It is an important modulator of intracellular free Ca^{2+} concentration and pH_i, which are major determinants of cell concentration, motility, and proliferation (Schmitz et al, 2007). With respect to genomic stability, several important aspects include the role of Mg^{2+} in DNA replication and protein synthesis, its function as a cofactor in DNA repair proteins, its role in maintaining the anti-oxidative status of the cell and finally its effect on the cell cycle regulation and apoptosis. Magnesium deficiency or the displacement of Mg^{2+} by other toxic divalent metal ions leads to an increased genomic instability, as evident by inhibited DNA repair, oxidative stress, aging and carcinogenicity (Hartwig, 2001).

The widespread distribution of Mg^{2+} in soil has also favoured its utilization by plants. Thus, magnesium is an integral component of chlorophyll and serves an essential function for photosynthesis (Wolf & Cittadini, 2003).

The basic chemical properties of Mg^{2+} make it highly unique amongst biological cations (Maguire & Cowan, 2002). Its size, charge density, structure in aqueous solutions and aqueous chemistry differ greatly from other monovalent or divalent cations of biological relevance. Mg^{2+} is a very hard Lewis acid. It readily interacts with carboxylate and phosphate anions in solutions or on proteins (Black et al, 1994; Maguire & Cowan, 2002). Mg^{2+} strongly prefers oxygen as a ligand, although the relative few examples of binding via nitrogen are of obvious importance, as in chlorophyll. Unlike most other cations, Mg^{2+} does not bind via sulfur.

Mg^{2+} has the largest hydrated radius of any common cation (*e.g.* 4.76 Å for Mg^{2+} *vs* 2.95 Å for Ca^{2+}), while the ionic radius of Mg^{2+} is among the smallest of all cations (*e.g.* 0.65 Å for Mg *vs* 0.99 Å for Ca^{2+}). The hydrated Mg^{2+} cation is approximately 400-fold larger than its ionic, dehydrated form. In contrast, Na^+ and Ca^{2+} are only 25-fold larger and the hydrated K^+ cation only 4-fold larger than the dehydrated forms (Maguire & Cowan, 2002).

In aqueous solutions and biological systems, Mg^{2+} shows almost always hexacoordinate conformation like Na^+, binding water or other ligands in a regular octahedral geometry. In contrast, Ca^{2+} is relatively promiscuous and can adopt bonding arrangements of 6 to 9 coordination bonds (Williams, 1970). This makes Ca^{2+} more flexible in binding with other molecules in comparison to Mg^{2+} that attracts water molecules in a more constrained way. Ca^{2+} is generally a signalling molecule that must bind to a variety of proteins and modulate a conformational change. This implies that the geometry of the Ca^{2+} binding site must exhibit some flexibility to accommodate Ca^{2+} bound to at least 2 states of a protein in question (Ashby & Tepikin, 2001; Bootman et al, 2001; Brown & MacLeod, 2001). In contrast, the most common physiological role of Mg^{2+} is to bind ATP or another nucleotide triphosphate in the catalytic pocket of an enzyme. The relatively weaker strength of Mg^{2+} binding to proteins and other molecules coupled with the very slow exchange rate of solvent water around the hydrated Mg^{2+} together with above mentioned properties renders the Mg^{2+} ion multifaceted and unusual among cations.

3.2 Biological Magnesium Transport Systems

Due to the unique nature, the movement of magnesium ions across biological membranes is a great challenge. The Mg^{2+} transporters identified so far, amply confirm the postulation that proteins transporting this ion would constitute a novel and highly unusual family of integral membrane proteins. This section portrays constituents of Mg^{2+} transport pathways in prokaryotic and eukaryotic cells, including mammals.

3.2.1 CorA-Mrs2-Alr Family of Mg^{2+} Transporters

The first indications of a system for magnesium transport across the biological membranes were brought in 1969 and 1971 by two laboratories of Silver and Kennedy both working with *Escherichia coli*. They identified the primary Mg^{2+} uptake system of prokaryotes by transport kinetic studies using the radioisotope $^{28}Mg^{2+}$ (Lusk & Kennedy, 1969; Silver, 1969; Silver & Clark, 1971). They screened mutants, which showed an increased resistance to the toxic effects of cobalt ions (Nelson & Kennedy, 1971), which beside nickel and cadmium, are co-transported with Mg^{2+} via the same system. Until recently, at least three distinct classes of Mg^{2+} transporters were reported to occur in Bacteria and

Archea: CorA, MgtA/B, and MgtE (Romani, 2007; Smith & Maguire, 1998; Smith et al, 1995; Townsend et al, 1995). Although all of these systems mediate Mg^{2+} translocation across bacterial cell membranes, their mechanisms are different (see Figure 3.2.1).
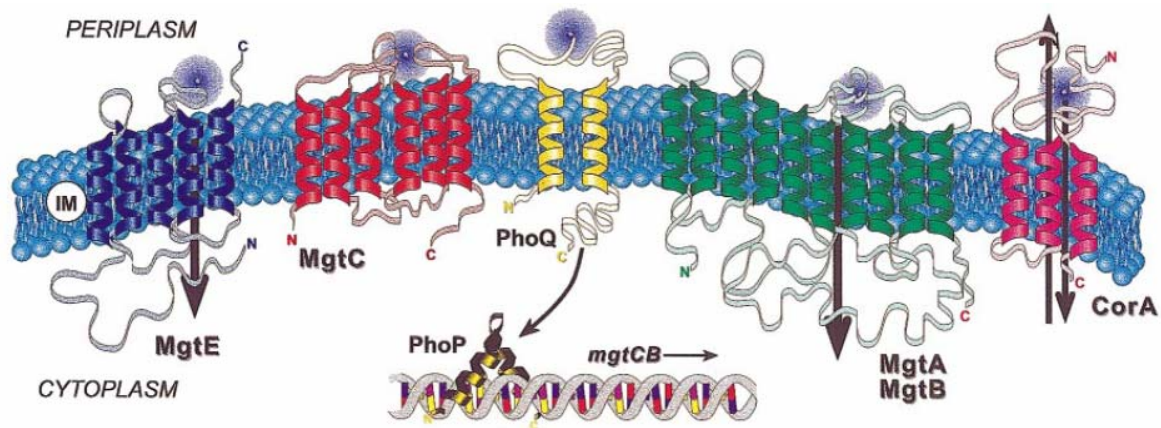
Figure 3.2.1. Bacterial Mg^{2+} receptor and transport systems. The Mg^{2+} transport systems of the Bacteria are shown with their membrane topologies. The topology for CorA, MgtA, MgtB, and PhoQ have been experimentally determined. That for MgtE is inferred from hydropathy analysis (Kyte & Doolittle, 1982). CorA has been found in all branches of the Bacterial and Archaeal kingdoms. The others are currently known only in Gram-negative bacteria. MgtA and MgtB are P-type ATPases which utilize the hydrolysis of ATP to provide energy for transport. CorA and MgtE probably use the cell's proton gradient. The function of MgtC is unknown. In *S. typhimurium mgtC* is in an operon with *mgtB,* that is regulated by Mg^{2+} via *phoPQ,* and is essential for *S. typhimurium* virulence. Mg^{2+} is shown as a central atomic ion-surrounded by a large hazy cloud representing its hydration shell to illustrate the relative sizes of the two forms. Adapted from (Moncrief & Maguire, 1999).

The CorA family is ubiquitous within both Kingdoms where it constitutes the primary Mg^{2+} uptake system. The gene was named after the mutant phenotype of increased resistance against usually toxic levels of Co^{2+} (Cor = <u>Co</u>balt <u>r</u>esistance) (Park et al, 1976). As a result of intensive studies in *Salmonella enterica* serovar Typhimurium (*S. enterica*) from which it was cloned in 1986 (Hmiel et al, 1986), CorA is the best-characterized Mg^{2+} transporter to date. As one of three members of CorA-Mrs2-Alr superfamily CorA is the prototypical member of the entire 2-TM-GxN type family of metal ion transporters (MIT). Members of this family are composed of two C-terminal transmembrane (TM) domains and a conserved G(M,I,V)N motif towards the C-terminal end of the first TM. However, Y/FGMN variant of this conserved signature occurs in common. Other characterized

members include the prokaryotic ZntB, the yeast Alr1/2 and Mnr2, *Arabidopsis thaliana* *At*MGT and Mrs2, which is found from yeast to human.

The CorA system is encoded by the *corA* gene that constitutively expresses a 316 aa, 37 kDa integral membrane protein. Its promoter does not respond to changes in magnesium concentration or to any other stimuli (Smith et al, 1998; Tao et al, 1998). CorA was shown to mediate Mg^{2+} ion influx by the utilization of the membrane potential (Froschauer et al, 2004; Kolisek et al, 2003). CorA can also transport Co^{2+} and Ni^{2+}. The affinity for Mg^{2+} is (K_m of 15 μM) compared with 20-40 and 200-400 μM for Co^{2+} and Ni^{2+}, respectively, suggesting that transport of these latter ions is not the primary function of CorA (Kehres & Maguire, 2002). As mentioned above, the CorA, Mrs2 and Alr1/2p representatives of the 2-TM-GxN family are essentially two-domains transporters, with a large soluble N-terminus and a small C-terminal tail, both protruding into the cytoplasm (Smith et al, 1993; Warren et al, 2004). They share the conserved GMN motif within their transmembrane region, but most other CorA-related prokaryotic proteins conserve either an MPEL sequence in close proximity (Kehres & Maguire, 2002; Knoop et al, 2005). Single mutations within the GMN signature are known to abolish Mg^{2+} transport, however naturally occurring variants might be associated with the transport of other divalent cations (Knoop et al, 2005). In general, sequence homology between distantly related members of this family is weak showing as little as 15-20% of identity (Kehres et al, 1998). Sequence similarity is most pronounced in the C-terminal membrane-spanning domain and less significant within the N-terminal soluble region. Recently, the crystal structure of the full length CorA homologue from *Thermotoga maritima* was solved almost simultaneously by three independent research groups at high-resolution 2.9Å (Eshaghi et al, 2006) and lower resolutions 3.7Å and 3.9Å (Lunin et al, 2006; Payandeh & Pai, 2006). This was the first structure not only of a member of the 2-TM-GxN family, but of any divalent cation channel reinforcing conclusions about a number of proteins of other ion channels. Although presenting the very low sequence conservation among CorA family, these diverse transporters share a common secondary structural scaffold that agrees well with the three-dimensional arrangement of *Tm*CorA. To constitute a functional transporter within the plasma membrane, CorA needs to oligomerize. *Tm*CorA presents a funnel-shaped pentameric assembly, forming the ion conduction pathway, build by the TM1 segment of each monomer. This central pore is surrounded by a ring of TM2 helices. Both N- and C-terminal ends are facing the cytosol. 10 metal binding-sites located within the cytoplasmic

funnel domain, characterized as physiologically tuned divalent cation sensors, supervise the CorA selectivity. Furthermore, the protein is equipped in molecular appliance that might discriminate between size and preferred coordination geometry of hydrated cations (Payandeh & Pai, 2006). Figure 3.2.2 depicts the structure of CorA Mg^{2+} channel together with predicted metal binding sites. Biochemical evidence for functional oligomeric complexes exists also for other members of the CorA-Mrs2-Alr superfamily, *e.g.* the Mrs2p as a pentamer (Kolisek et al, 2003) and Alr1/2 proteins as an at least homo- or heterotetramer (Wachek et al, 2006). These strongly suggest that the crystal structure of *Tm*CorA is representative for the entire CorA family.
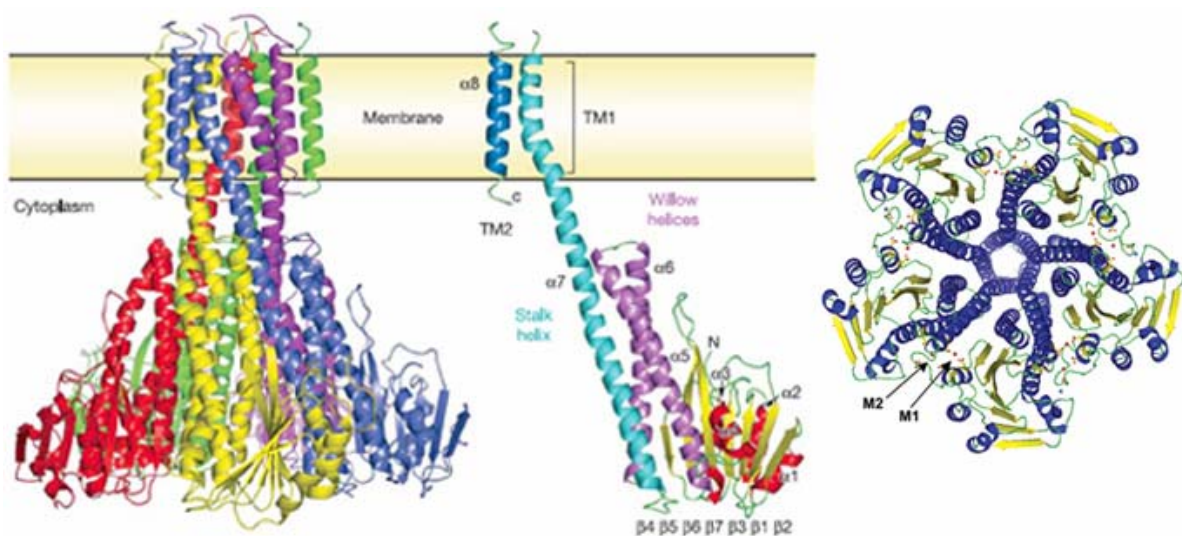
Figure 3.2.2. Structure of the CorA Mg^{2+} channel. (a), Ribbon diagram of the CorA pentameric complex, viewed in the plane of the membrane. On the right is a single unit of the CorA channel highlighting the following structural features: stalk helix and inner TM1 helix (turquoise), outer helix (dark blue), willow helices (purple) and the remaining a-helices (red) and b-sheets (yellow). The membrane surface is indicated (Lunin et al, 2006). (b), Metal binding sites. Top view of the overall structure with metal binding sites, M1 and M2, indicated with arrows (adapted from (Eshaghi et al, 2006)).

Further members of the CorA-Mrs2-Alr superfamily, Mrs2p and Alr1/2p proteins, were found in yeast *Saccharomyces cerevisiae* and represent the best-characterized eukaryotic homologues of CorA. They share a similar overall membrane topology with two adjacent TM spans and the short Y/FGMN peptide motif. In case of Mrs2p, several conserved

primary sequence domains of importance for Mrs2p activity were identified additionally in the central part near the TMs (Weghuber et al, 2006).

The nuclear gene *MRS2* encodes an integral protein of the inner mitochondrial membrane involved in Mg^{2+} homeostasis in yeast mitochondria (Bui et al, 1999). Mrs2p was described for the first time in a screen for genes suppressing mitochondrial RNA splicing of group II introns in yeast mutants (Koll et al, 1987; Wiesenberger et al, 1992). The crucial role of Mrs2p in this process is carried out indirectly through the establishment of matrix Mg^{2+} concentration permissive for RNA splicing (Gregan et al, 2001b; Wiesenberger et al, 1992) and was identified before its function as a Mg^{2+} transporter (Koll et al, 1987).

The potential role of Mrs2p as a Mg^{2+} transporter was suggested by the ability to partially complement the *pet-* phenotype of Mrs2-deficient yeasts by a CorA version fused to the mitochondrial N-terminal leader sequence of Mrs2, ensuring proper insertion of CorA into the mitochondrial inner membrane (Bui et al, 1999; Gregan et al, 2001a; Schock et al, 2000). Other homologues that can functionally substitute for its yeast counterpart are *Arabidopsis thaliana At*Mrs2-1p (Schock et al, 2000) and human hMrs2p (Zsurka et al, 2001). In plants, *MRS2* related genes are strongly represented with 15 homologues, at least three of which are functional in yeast (Drummond et al, 2006), whereas mammalian genomes contain only one single representative of the Mrs2 family. Direct evidence for Mrs2p as a major component of the mitochondrial Mg^{2+} flux system has been shown by using the fluorescent Mg^{2+} indicator Mag-fura 2 (Kolisek et al, 2003). The monitoring of matrix Mg^{2+} levels $[Mg^{2+}]_m$ in isolated mitochondria from wt and *MRS2* deficient yeast cells revealed a rapid Mg^{2+} influx system of high capacity, driven by the membrane potential. It was shown that the rapid increase in $[Mg^{2+}]_m$, as much as 25% within the first second, observed upon elevation of the external Mg^{2+} levels is almost abolished in *mrs2Δ* mitochondria, but significantly elevated upon Mrs2p overexpression. Thus, this experiment together with cross-linking analysis revealing presence of homo-oligomeric pentamers (Kolisek et al, 2003) demonstrated first evidences for the channel-like behaviour of yeast Mrs2p. Finally, this notion was recently confirmed by electrophisiological analysis. Data gained from single channel patch-clamping studies clearly revealed that Mrs2p forms a Mg^{2+}-selective channel of high conductance (155 pS) (Schindl et al, 2007). Mg^{2+} uptake is controlled by an intrinsic negative feedback mechanism what is in accordance with the hypothesis of CorA channel pore gating (Lunin et al, 2006; Payandeh & Pai, 2006). The

Mrs2 channel is also permeable for Ni^{2+} but with lower conductance of about 45 pS. However, in contrast to Alr1p or CorA no permeability has been observed either for Ca^{2+}, Mn^{2+} or Co^{2+}.

For tight regulation of the intracellular Mg^{2+} levels, the Alr proteins, which constitute another subclass of the CorA family, has been evolved in yeast. Two genes, first identified from their ability to confer aluminium resistance, designated *ALR1* and *ALR2*, encode proteins involved in Mg^{2+} uptake (MacDiarmid & Gardner, 1998). Both Alr1 and Alr2 proteins are closely related showing 69% sequence identity with similar lengths of 859 aa and 858 aa, respectively (MacDiarmid & Gardner, 1998). Alr proteins reveal low degree of overall amino acid similarity with the bacterial CorA (MacDiarmid & Gardner, 1998). Phylogenetic analyses indicates that they share a common polypeptide carboxy-terminus with CorA, with two transmembrane domains connected by a conserved short loop with a canonical sequence (Y/F)GMN (Kern et al, 2005). The destination of Alr proteins is the plasma membrane, which was determined by cell fractionation and fluorescence microscopy (Graschopf et al, 2001; Wachek et al, 2006). Alr1p and Alr2p behave similar with respect to Mg^{2+}-dependent mRNA expression and protein turnover. The mRNA level of *ALR1* is down-regulated in medium containing standard or high Mg^{2+} concentrations compared to Mg^{2+} limiting growth conditions. In addition, high Mg^{2+} triggers protein ubiquitination and endocytosis followed by vacuolar degradation (Graschopf et al, 2001).

Alr1p is essential for growth of yeast cells at Mg^{2+}-limiting conditions. Mutants lacking *ALR1* fail to grow in standard medium and show significant reduction of total intracellular Mg^{2+} compared to the wild-type. High Mg^{2+} concentration in the medium suppress the phenotype of *ALR1* gene disruption (Graschopf et al, 2001; MacDiarmid & Gardner, 1998). Unlike its homolog, Alr2p contributes poorly to Mg^{2+} uptake. Low activity may in part be evoked by very poor expression of *ALR2*. The affinity of Alr2p to Mg^{2+} is greatly improved by single amino acid substitutions in the loop between TM1 and TM2, which in turn enable a significant suppression of *alr1Δ* growth defect. A surplus of negatively charged residues is typically found in this loop, particularly a glutamate residue at position +6 after the GMN motif. The replacing of positively charged arginine with well conserved glutamic acid residue accounts for the apparently low Mg^{2+}-transport activity of Alr2p (Wachek et al, 2006).

Overexpression of *ALR1* and *ALR2* genes affects the tolerance of yeast cells to several metal cations. On the one hand, cells are more resistant to Al^{3+} and Ga^{3+}, on the other hand,

the sensitivity to divalent ions such as Co^{2+}, Mn^{2+}, Ni^{2+} and Zn^{2+} is increased (MacDiarmid & Gardner, 1998). Alr proteins are also suggested to have a central role in the heavy metal detoxification and cell survival in a high-toxicity environment, especially in case of Cd^{2+} (Kern et al, 2005).

First electrophysiological data for the function of Alr1p were provided by Liu and colleagues. By the use of the patch-clamp technique, Alr1p was characterized as an ion selective channel, mediating large influx and efflux Mg^{2+} currents (Liu et al, 2002). Additionally, the channel-like nature of the Mg^{2+} transporter was further supported by studies with chemical cross-linkers and split-ubiquitin assay, revealing the formation of di-, tri-, and tetramers at least (Wachek et al, 2006).

3.2.2 Non 2-TM-GxN family-related Mg^{2+} transport systems

In *Salmonella typhimurium* two classes of transporters MgtA/B and MgtE compose an additional uptake system for Mg^{2+} (see above Figure 3.2.1.). These proteins operate as P-type ATPases in mediating the cation influx down its large electrochemical gradient in contrast to other counterparts (Kuhlbrandt, 2004). Both MgtA/B classes are phylogenetically closer to eukaryotic than prokaryotic P-type ATPases. Like eukaryotic P-type ATPases, they are composed of 10 TMDs. Unlike constitutively expressed CorA and MgtE magnesium transporters, MgtA and MgtB expression is subjected to specific PhoPQ two-component regulatory system responding to external Mg^{2+} concentration fluctuations (reviewed in (Maguire, 2006)).

MgtE was initially identified in the bacteria *Bacillus firmus* OF4 (Smith et al, 1995; Townsend et al, 1995) and *Providencia stuartii* (Townsend et al, 1995) in a search for additional members of the CorA family, based on their ability to complement a magnesium transport deficiency in *S. typhimurium*. MgtE protein has an appropriate molecular weight of 40 kDa with 5-6 TMDs with a large hydrophilic domain at the N-terminus residing in cytosol and does not resemble any known class of proteins. The predicted topology was recently corroborated by solving the crystal structure of *Thermus thermophilus* MgtE at a resolution 3,5Å (Hattori et al, 2007). The transporter adopts homodimeric architecture, consisting of five transmembrane and amino-terminal cytosolic domains to form a functional unit. MgtE appears to have a conceptually similar Mg^{2+}-dependent gating mechanism as CorA, with intracellular Mg^{2+} concentration sensors, but with far different

architecture. The bacterial MgtE translocates Mg^{2+} and Co^{2+} inward. In contrast to CorA, Ni^{2+} seems not to be transported (Smith et al, 1995; Townsend et al, 1995). This family is ubiquitously distributed in all phylogenetic domains with at least 36 MgtE-like proteins identified so far.

Currently, human homologues have been functionally characterized and suggested to be involved in magnesium homeostasis (Goytain & Quamme, 2005b; Goytain & Quamme, 2005c; Sahni et al, 2007). They belong to the SLC41 subfamily of human solute carriers that include three members widely expressed in different human tissues. On the basis of the similarity to MgtE (Wabakken et al, 2003) the possible implication in Mg^{2+} transport was suggested and further supported by voltage-clamp analysis of SLC41A1 and SLC41A2 heterologously expressed in *Xenopus leavis* oocytes.

Over the past 2 years considerable advances were made to characterize molecular mechanisms and components involved in regulation of Mg^{2+} homeostasis in mammals. Two members of the transient potential melastatin receptor family TRPM6 and TRPM7 of cation channels have been demonstrated to be primarily Mg^{2+} channels (Nadler et al, 2001; Schmitz et al, 2003). TRPM7 protein is ubiquitously expressed among tissues and has been reported to be essential for cell viability, whereas TRPM6, predominantly expressed in intestinal epithelia and kidney tubules, has been implicated in Mg^{2+} absorption and whole body Mg^{2+} homeostasis (Schlingmann et al, 2002). TRPM6 and TRPM7 "chenzymes" possess a unique structure, containing a kinase domain in the carboxy-terminal region with an ascribed regulatory function in both active and passive transport by the sensitivity to intracellular Mg^{2+} or MgATP (Nadler et al, 2001; Schmitz et al, 2003; Voets et al, 2004). Goytain and Quamme identified two additional genes that code for a Mg^{2+} transport mechanism, *MagT1* and *ACDP2*. *MagT1* (Magnesium Transporter 1) encodes a Mg^{2+} transporter with no sequence identity to any known transporters. When expressed in oocytes, MagT1 is able to elicit large Mg^{2+}-dependent currents. It appears to display channel-like characteristics with selectivity towards Mg^{2+} and little permeability to other divalent cations. Differently to MagT1, ACDP2 (Ancient Conserved Domain Protein 2) exhibits a voltage-dependent transporter with a broad spectrum translocating beside Mg^{2+} also other divalent cations including Co^{2+}, Mn^{2+}, Sr^{2+}, Ba^{2+}, Cu^{2+} and Fe^{2+}. All members of this family are spread in numerous species from bacteria to man and share a evolutionary conserved domain with homology to the bacterial CorC. The levels of both MagT1 and

ACDP2 appear to be responsive to external Mg^{2+} concentrations (Goytain & Quamme, 2005a; Goytain & Quamme, 2005d).

The total body Mg^{2+} homeostasis in mammalian cells is also regulated by another gene product, namely PCLN-1. Paracellin-1 is a member of the claudin family of tight-junction proteins that control paracellular reabsorbtion in the kidney (Simon et al, 1999). The pore formed likely by PCLN-1 conducts Mg^{2+} fluxes directly as a result of the positive lumen potential generated after paracellular Na^{+} permeation (Hou et al, 2005).

3.3 Structure and Mechanism of a Membrane Trafficking Network in Yeast

A basic feature of eukaryotic cells is the presence of intracellular membranes creating compartments or organelles. The plasma membrane with its proteins defines the barrier between the cytosol and the extracellular environment. Together with proteins of the subcellular compartments, a controlled protein trafficking provides the physiological composition of the intracellular milieu. The importance of membrane proteins and such internal cell organization facilitated the ongoing development of sophisticated mechanisms precisely sorting and distributing newly synthesised proteins and metabolites to their appropriate target organelles.

Secretion and endocytosis are the mechanisms by which eukaryotic cells control membrane flow to and from the cell surface. The equilibrium is maintained by the fusion of secretory vesicles and by the invagination of endocytic vesicles. Hence, traffic along the secretory and endocytic pathways must be continuously balanced to maintain the appropriate lipid and protein composition of the plasma membrane and to coordinate cell surface expansion during growth and morphogenesis.

In contrast to soluble cytoplasmic proteins, membrane proteins, which are inserted into a lipid bilayer, cannot freely diffuse throughout the cell and therefore have to be targeted to their destination by specific mechanisms. These mechanisms, generally known as membrane transport or protein traffic between different cellular organelles, follow a common scheme in which protein cargoes are recruited into budding regions in a donor organelle. These regions then bud off as vesicles and move on to a recipient organelle, with which they fuse and to which they deliver the cargo proteins (Gruenberg, 2001; Jahn et al, 2003; Maxfield & McGraw, 2004; Whyte & Munro, 2002) Vesicular traffic is a predominant mechanism by which components are transported from one membrane-

bounded organelle to another and appears to be highly conserved in eukaryotic cells from yeast to mammals (Bennett & Scheller, 1993; Ferro-Novick & Jahn, 1994; Rothman & Warren, 1994) (see Figure 3.3.1, (Bonifacino & Glick, 2004)).
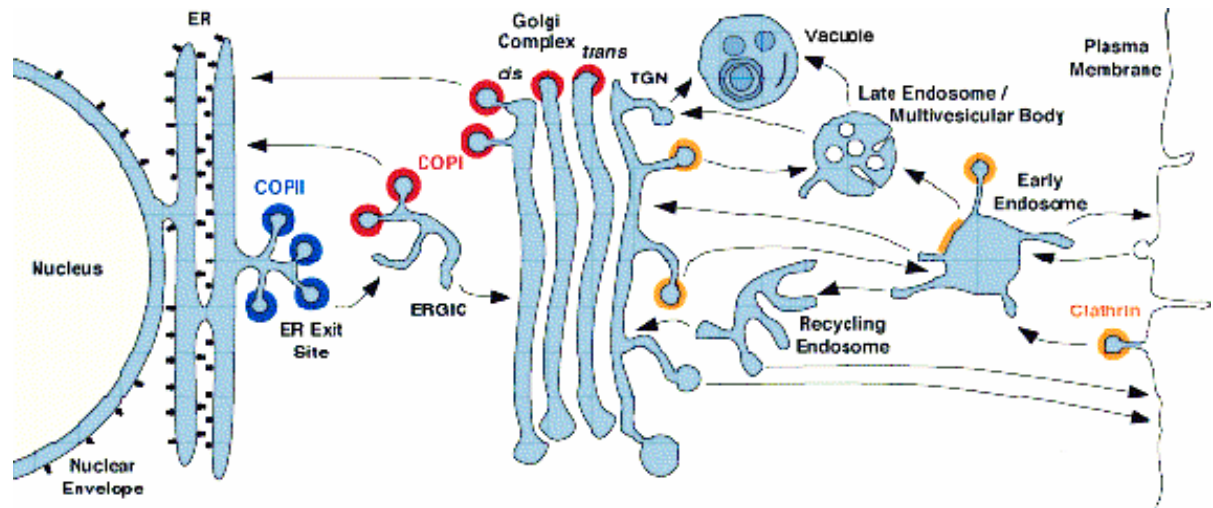
Figure 3.3.1. A model for intracellular transport along the secretory and endocytic pathways in yeast ((Bonifacino & Glick, 2004), modified). The scheme depicts the compartments of the secretory, lysosomal/vacuolar, and endocytic pathways. Transport steps are indicated by arrows. Colors indicate the known or presumed locations of COPII (blue), COPI (red), and clathrin (orange). Clathrin coats are heterogeneous and contain different adaptor and accessory proteins at different membranes. Only the function of COPII in ER export and of plasma membrane associated clathrin in endocytosis are known with certainty. Less well understood are the exact functions of COPI at the ERGIC and Golgi complex and of clathrin at the TGN, early endosomes, and immature secretory granules. Additional coats or coat-like complexes exist but are not represented in this figure.

3.3.1 Secretion of Membrane Proteins and Biosynthetic Degradation Pathway

The secretory pathway sorts and delivers a tremendous variety of proteins to their proper intracellular location. The port of entry into the secretory pathway in eukaryotic cells is the endoplasmic reticulum (ER), a compartment that is the first key checkpoint for protein quality. When *de novo* synthesized protein emerge in the lumen of the ER, nascent chains are immediately assisted by several ER chaperones like one of the best characterized lumenal binding proteins BiP or other factors (Matlack et al, 1999), that promote efficient translocation, protein folding and reduce aggregation by masking hydrophobic regions

(Hartl, 1996; Kleizen & Braakman, 2004). Properly folded proteins destined for distal compartments exit the ER via vesicular or tubular structures (Lee et al, 2004; Watanabe & Riezman, 2004). In yeast vesicular transport of correctly folded proteins involves concentration of proteins in specialized encounters followed by simple diffusion between ER-derived vesicles and single dispersed Golgi elements (Preuss et al, 1992). By contrast, in higher eukaryotes, transport from the ER is initiated at specialized subdomains of the ER, ER-export sites (ERES) (Bannykh et al, 1996; Hammond & Glick, 2000). Further, protein traffic moving from the ER to the Golgi passes through the tubulovesicular membrane clusters of the ER-Golgi intermediate compartment (ERGIC), which is the first station for anterograde and retrograde cargo separation (Appenzeller-Herzog & Hauri, 2006; Aridor et al, 1995; Hauri et al, 2000; Klumperman et al, 1998). The transport begins with the formation of vesicles at the ER surface followed by docking and fusion with the Golgi membrane (Schekman & Orci, 1996). This process is carried out by proteins classified as the *Sec* group together with accessory proteins belonging to the multiprotein complex TRAPP (Transport Protein Particle) (Barrowman et al, 2000; Cai et al, 2007; Morozova et al, 2006; Singer-Kruger et al, 1998; Wang et al, 2000) and a set of proteins known as coatomer proteins (COP) (Barlowe, 1997; Klumperman, 2000; Peng et al, 1999; Tang et al, 1997).

The trans-Golgi compartment is a major sorting station for newly synthesized proteins and lipids in the biosynthetic pathway of *S. cerevisiae*. From there a number of different constitutive and regulated routes emerge, that deliver proteins either to the plasma membrane or to a number of endosomal system compartments. The cargo from ER is further transported trough at least five routes that branch out at this point; these are two parallel secretory pathways to the cell surface (Harsay & Bretscher, 1995), the retrograde pathway to the early Golgi and ER (discussed above (Aridor et al, 1995; Harris & Waters, 1996; Klumperman et al, 1998)), and two that carry soluble and membrane vacuolar proteins to the vacuole either traversing the late endosome/prevacuolar compartment (the CPY pathway) or the alternative rout bypassing PVC (the ALP pathway) (Bryant & Stevens, 1998) and references therein, (Gurunathan et al, 2002).

Budding yeast, like polarized epithelial cells and other mammalian cells have two routes for biosynthetic cargo sorting from the Golgi to the separate membrane domains. Two different types of secretion vesicles, separated at the *trans*-Golgi stage, are isolated based on their differences in density and transported cargo, low density secretion vesicles

(LDSVs) and high density secretion vesicles (HDSVs), depicting constitutive and regulated secretion, respectively. In contrast to other defined vesicular transport steps in yeast, constitutive transport from the Golgi to the plasma membrane seems not to require any proteinaceous coats from clathrin or other adaptor complexes (*i.e.* adaptor proteins AP1, AP2 or AP3) and GGA (Golgi-associated, γ-adaptin homologues, Arf-binding) proteins to function (Black & Pelham, 2000; Chen & Graham, 1998; Costaguta et al, 2001; Cowles et al, 1997a; Gu et al, 2001; Seeger & Payne, 1992; Yeung et al, 1999). This light population of vesicles contains a plasma membrane H+-ATPase activity and β-glucanase Bgl2p among its cargo (David et al, 1998; Harsay & Bretscher, 1995). The content of the soluble secreted enzymes invertase Suc2p and acid phosphatase Pho5p (Gurunathan et al, 2002; Harsay & Bretscher, 1995; Harsay & Schekman, 2002) as well as the bulk of exoglucanase activity in vesicles subjected to regulated secretion is concentrated using a clathrin and dynamin dependent mechanisms, and these more dense vesicle population can be clearly distinguished by electron microscopy (Alberts et al, 2002).

It was recently discovered that in mutants that block access of vesicles subjected to regulated secretion to the endosome *e.g.* dynamin-like *vps1*, *vps4*, clathrin (*chc1Δ*) and the late endosomal t-SNARE *pep12*, the dense vesicles were not formed and invertase was shifted to the light Pma1p-containing transport vesicles instead. Dense carriers-specific cargo followed subsequently the constitutive secretion route to reach its destination (Gurunathan et al, 2002; Harsay & Schekman, 2002). Such fate of protein missorting in case of inactivation of HDSV biogenesis was also presented for other cargo molecules like GPI-anchored protein, Gas1, or carboxypeptidase CPY and its receptor, Vsp10 (Gurunathan et al, 2002).

The main pathway for the delivery of newly synthesized proteins to the vacuole is referred to as the carboxypeptidase Y (CPY) pathway based on the utilization of this pathway by CPY (reviewed by (Burd et al, 1998; Conibear & Stevens, 1998; Mullins & Bonifacino, 2001)). This pathway involves transport from the late-Golgi complex to a prevacuolar compartment (PVC). From the PVC some proteins are subsequently transferred to the vacuole, whereas others return to the late-Golgi complex for further rounds of transport. Another soluble hydrolase, proteinase A (PrA), as well as the membrane-bound hydrolase carboxypeptidase S are also transported to the vacuole via the CPY pathway. Vesicular transport between the late Golgi and endosomes clearly requires both clathrin and clathrin-adaptor proteins. The clathrin coat is required as a scaffold for vesicle budding, and the

adaptor proteins bind both clathrin and cargo to link vesicle formation with protein sorting (Robinson, 2004). A second pathway, referred to as the alkaline phosphatase (ALP) pathway, is followed by the membrane-bound hydrolase ALP and the t-soluble *N*-ethylmaleimide-sensitive factor attachment protein receptors (SNAREs) Vam3p and Nyv1p (Burd et al, 1998; Conibear & Stevens, 1998; Mullins & Bonifacino, 2001; Reggiori et al, 2000). In this pathway, ALP transport to the vacuole does not involve a prevacuolar compartment/late endosome and persists unaltered in mutant cells that are blocked in specific parts of the CPY pathway like vps4, vps27 and pep12 (Cowles et al, 1997b; Piper et al, 1997). Access to this pathway requires a specific cytoplasmic signal (reviewed by (Odorizzi et al, 1998)) and unlike sorting to endosomal compartments is not subjected to clathrin.

The complexity of intracellular protein trafficking and secretion reflects bulk of mutants found during mass scale genome analysis. Genetic screening for temperature-sensitive yeast mutants, defective at different steps along the secretory (*e.g. sec*), endosomal (*e.g. end*) and vacuolar transport pathways (*e.g. vps*, *vam* and *pep*), have defined a large number of gene products that function in vesicle biogenesis, transport, docking and fusion (Bryant & Stevens, 1998; Munn & Riezman, 1994; Novick et al, 1980; Wuestehube et al, 1996). Genetic studies in yeast have identified more than 70 gene products involved only in Vacuolar Protein Sorting (Vps). These genes encode transport components that function at distinct stages of protein traffic between the Golgi and the vacuole. According to the morphology of the vacuole, the mutants were classified into six groups (class A-F) (Raymond et al, 1992). Most of these Vps proteins are constituents of various complexes, like the retromer complex (Seaman, 2005), the retrograde GARP/VFT complex (Conibear et al, 2003; Conibear & Stevens, 2000; Reggiori et al, 2003; Siniossoglou & Pelham, 2002), the TRAPP and the COG complex (Grosshans et al, 2006), an endosomal sorting complex required for transport (ESCRT) (Babst, 2005; Babst et al, 2002a; Babst et al, 2002b; Katzmann et al, 2001), the class C core vacuole/endosome tethering (CORVET) complex (Peplowska et al, 2007) or class C/HOPS complex (Collins et al, 2005; Whyte & Munro, 2002), important for proper function of endosomal network.

3.3.2 Endocytosis

Endocytosis is the vesicular trafficking process by which cells internalize extracellular material by forming intracellular membrane-bound vesicles originating from the plasma membrane, and subsequently sort the vesicle contents to the appropriate destination. Internalized material includes membrane proteins, plasma membrane lipids, and extracellular fluid, and may also include other cells or apoptotic cell fragments, viruses, nutrients, or activated PM signalling complexes (Watson et al, 2004). This phenomenon conserved from yeast to human is required for divers cellular functions which include turnover and degradation of plasma membrane proteins and receptors, transduction and dispersal of signals within the cell and between cells of an organized tissue, spread of morphogens, cell-to-cell communication at synapses, elimination of pathogenic microorganisms, establishment of symbiosis with microorganisms, and nutrient uptake (Munn, 2001; Samaj et al, 2004). Several basic forms of endocytosis have been defined according to the type of cargo and molecular machinery driving its internalization. The endocytic pathways include clathrin-mediated, caveolae/lipid raft-mediated, clathrin-, and caveolae-independent endocytosis, fluid-phase endocytosis, and phagocytosis. Among them, mechanism of endocytosis mediated by clathrin-coated pits and vesicles constitutes the major mode of uptake from cell surface (Conner & Schmid, 2003; Kirchhausen, 2000; Mukherjee et al, 1997).

Endocytosis begins at the cell surface with the deformation and vesiculation of a region of the plasma membrane into which various membrane constituents are sequestered. The newly formed vesicle is then transported to and fused with a network of organelles called early endosomes (EE), where cargo destined for degradation is sorted out from material to be recycled. Recycling of material to the plasma membrane can occur from either the sorting endosome or the recycling endosome. Cargo destined for degradation is delivered to late endosomes (LE), which intersect with the biosynthetic pathway, and then to lysosomes where they are degraded.

At the molecular level, the process is orchestrated by a network of protein-protein and protein-membrane interactions, centred on the coat protein clathrin and the multisubunit adaptor complex AP-2 (Traub, 2005). The heterotetrameric plasma membrane adaptor AP-2 executes the pivotal task of connecting the clathrin scaffold to the designated cargo being concentrated within the membrane-bound vesicle and facilitates binding with other

accessory proteins involved in different stages of endocytosis (Owen et al, 2004; Traub, 2005). The operative complex of clathrin-adaptor-cargo represents the core of contemporary models for clathrin-mediated endocytosis (Ehrlich et al, 2004; Ohno, 2006), supported by the findings that targeted homozygous disruption or mutation of genes encoding AP-2 subunits is lethal in *C. elegans* (Kamikura & Cooper, 2003; Shim & Lee, 2000), *Drosophila* (Gonzalez-Gaitan & Jackle, 1997) and mice (Mitsunari et al, 2005). In addition to these three chief components, at least 20 other proteins referred as clathrin-coat-associated sorting proteins (CLASPs) contribute to the assembly of clathrin-coated vesicles (Traub & Lukacs, 2007).

Recruitment of transmembrane cargo to endocytic vesicles occurs through adaptor recognition of internalization signals present in cytoplasmic regions of the cargo proteins. In mammalian cells, several types of internalization signals have been extensively studied, including YxxΦ and NPxY motifs (where "x" is any residue and "Φ" a bulk hydrophobic residue) and ubiquitin (Hicke & Dunn, 2003; Owen et al, 2004; Traub, 2005). Two types of internalization signals have been defined in yeast: the ubiquitin-based signal recognized by monoubiquitin-binding domains (Hicke & Dunn, 2003) and the NPFxD signal (Howard et al, 2002; Mahadev et al, 2007; Piao et al, 2007; Tan et al, 1996).

Sites of endocytosis might be formed randomly by stochastic induction of protein and/or lipid clustering. Alternatively, endocytosis might initiate at specific positions. New insights into the mechanism, by which endocytosis initiates at particular locations on the plasma membrane were gained from studies of Walther (Walther et al, 2006). They described large protein assemblies at plasma membrane in yeast that mark endocytic sites. These structures, termed eisosomes are required for the proper spatial distribution of endocytic events. By contrast to other previously described endocytosis components, eisosomes are immobile static structures. Eisosomes thus provide a stable, functional link between the cytoplasmic components that catalyse endocytosis, and the plasma membrane, and may regulate when and where endocytosis occurs (Walther et al, 2006).

3.3.3 Signposts for the cell surface delivery and organelle identity

Due to the precise localization of membrane proteins to their respective compartments, organelles are able to generate and maintain their identity. Specific and regulated

mechanisms ensure proper sorting of membrane proteins and are fundamental for the establishment of cell polarity.

Little is known about the sorting determinants specifying protein transport to the plasma membrane and organelles uniqueness in yeast. Comprehensive work on epithelial polarized cells has established a role for lipid rafts, which are formed by lateral association of sphingolipids and cholesterol, and were first conceived in mammalian MDCK cells as platforms for polarized lipid and protein sorting (Simons & Ikonen, 1997; Simons & van Meer, 1988). These lipid raft planes are thought to be formed by tight packing of the long and highly saturated acyl chains of sphingolipids with sterols into which proteins specifically associate (Simons & Ikonen, 1997). It has been further shown that short motifs present on the cytoplasmic domain of transmembrane proteins (TMD) are recognized as determinants for the final destination of some membrane proteins (Matter & Mellman, 1994). Furthermore, *N-* and *O*-glycans attached to proteins are involved in apical exocytosis (Benting et al, 1999; Gut et al, 1998; Scheiffele et al, 1995; Spodsberg et al, 2001; Yeaman et al, 1997).

Recently, it was shown that in yeast cells similar to the apical sorting in mammalian cells, protein exocytosis is facilitated by such processes like lipid rafts association, *O*-glycosylation or TMD signal (Bagnat et al, 2000; Levine et al, 2000; Proszynski et al, 2004; Rayner & Pelham, 1997).

The plasma membrane of yeast as a specialized membrane exposed to the external environment contains high concentrations of ergosterol and sphingolipids. Of special interest in the exocytic pathway is phosphoinositide PtdIns(4)P, present on Golgi, where it is recognized by vesicle coat proteins and by the plectrins, which comprise homolog domains of proteins that deliver lipids to the Golgi. PtdIns(4)P is also found on the plasma membrane, where it is a substrate for the synthesis of lipid PtdIns(4,5)P – another major landmark for proteins that is needed to find the cell surface (Behnia & Munro, 2005). A clear indication that lipid rafts are associated with cell surface delivery was demonstrated for such yeast plasma membrane proteins like amino acid permease Tat2p (Umebayashi & Nakano, 2003), general amino acid permease Gap1p (Lauwers & Andre, 2006) and Pma1p where the last was missorted to the vacuole upon disruption of lipid raft (Bagnat et al, 2001; Bagnat et al, 2000; Lee et al, 2002b).

A difference in raft dependent secretory sorting between mammals and yeast is the biosynthetic pathway in protein segregation. Incorporation of proteins into DRMs

(detergent resistant membrane) in mammalian cells take place in the Golgi complex (Brown & London, 1998), whereas in yeast cells DRMs were detected already in the ER where ergosterol and ceramides are produced (Puoti et al, 1991).

The traffic accuracy and correct organelles recognition is defined either by other short-lived determinants GTPases with two main classes of the Rab and Arf families. These small GTPases function as molecular switches that after association with specific membranes can alternate in the state of activation, what in turn enables the recruitment of other peripheral membrane proteins contributing to the traffic regulation (Behnia & Munro, 2005).

3.3.4 Specificity of intracellular transport pathways - SNARE proteins and tethering factors

Protein targeting through the secretory pathway occurs as a complex sequence of transient protein-protein interactions controlling particular steps in the pathway. This sequence starts with the binding of cargo to specific receptors and the subsequent recruitment of coat proteins that form transport vesicles, (Bonifacino & Glick, 2004), which enable the exchange of information and protein cargo between membrane-encased organelles. The vesicles, with their accompanying protein cargo, are pinched off from the donor organelle by budding (Rothman & Orci, 1996), and are possibly guided by the cytoskeleton to the target compartment, where the content is released into it.

The delivery of cargo to the recipient organelle is accomplished by membrane recognition known as tethering, followed by docking and fusion. Tethering factors are peripherally membrane-associated protein complexes consisting of up to 10 different subunits. The docking step is thought to be mediated by the Rab/Ypt family of low molecular weight GTPases (Zerial & McBride, 2001) and a specific set of tethering factors that are capable of forming stable coiled-coil interactions (Gillingham & Munro, 2003; Pfeffer, 1999).

At the core of vesicle fusion events in the secretory and endocytic pathways is a family of membrane-associated proteins known as SNAREs (soluble *N*-ethyl maleimide sensitive-factor attachment protein receptor) (reviewed in (Gerst, 1999; Hay & Scheller, 1997; Pfeffer, 1996; Poirier et al, 1998; Rothman, 1996; Rothman & Warren, 1994; Sutton et al, 1998; Weber et al, 1998)). Originally identified as components of the 20S-fusion particle, required for neuronal exocytosis (Sollner et al, 1993), this family of type II integral

membrane proteins is evolutionarily well conserved among all eukaryotic species (Bock et al, 2001; Ferro-Novick & Jahn, 1994; Jahn et al, 2003; Pratelli et al, 2004; Surpin & Raikhel, 2004). In the yeast genome 24 different SNAREs has been identified and among them some yeast target complexes (t-SNAREs) assigned to specific traffic steps *i.e.*, Golgi to plasma membrane is marked with Sso1p/Sec9p, endoplasmic reticulum to Golgi is specified by Sed5p/Bos1p, and Sec22p, intra-Golgi is designated by Sed5p/Gos1p, and Ykt6p, vacuole fusion is accompanied by Vam3p/Vam7p, and Vti1p and early endosome to the trans-Golgi network shares the Tlg2p/Tlg1p, Vti1p complex (Burri & Lithgow, 2004; McNew et al, 2000; Parlati et al, 2002; Paumet et al, 2001). From a residence perspective and situation in which fusion occurs between a transport vesicle and a larger compartment, the SNAREs can be classified as v-SNAREs on vesicles (synaptobrevin-related receptors/VAMP families on the vesicle membrane) or t-SNAREs on fusion targets (plasma membrane syntaxin related receptors). According to the SNARE model (Sollner et al, 1993; Weber et al, 1998) complementary SNAREs localized to opposing membranes and interact to form a tetrameric bundle of coiled helices that draws the membrane surfaces together, providing a mechanism for fusion (Nichols et al, 1997; Ungermann et al, 1998, Sutton, 1998 #318). SNAREs also have been typed according to the charged amino acid (*i.e.*, glutamine [Q] or arginine [R]), which are present in the ionic layer within the bundle of the SNARE complex (Chen & Scheller, 2001; Fasshauer, 2003; Fasshauer et al, 1998; Hong, 2005).

Due to their importance in the last step of vesicle docking and fusion, SNAREs are also required to supervise the specificity of membrane fusion events that must be carefully regulated to allow proper communication between the organelles of the secretory and endocytic pathways while avoiding inappropriate fusion events which might degrade the organization of membranes within a cell. Such regulatory mechanism to prevent undesired membrane interactions was suggested for recently identified inhibitory SNAREs (i-SNAREs) (Varlamov et al, 2004).

3.4 Down-regulation of plasma membrane proteins

Degradation of membrane proteins is an important aspect of cellular physiology. It is used both as a quality control mechanism, to eliminate damaged or misfolded proteins (reviewed by (Trombetta & Parodi, 2003)), and as a regulatory process to remove proteins

that are no longer required (Hicke & Dunn, 2003). A common phenomenon is the down-regulation of transporters in the presence of their substrates. Such substrate-induced destruction protects cells from self-poisoning, a particular problem with components such as heavy metals, which are essential for cell physiology but toxic in excess. The activities of such proteins that move various molecules across membranes are controlled by a combination of transcriptional, translational, and post-translational mechanisms. In general, genes encoding transporters that facilitate the uptake of different metal ions are all activated by transcription factors that specifically respond to the depletion of cognate metal. Supplementation with the specific substrate rapidly switches off this transcriptional activation. In addition to this transcriptional regulation, increased concentration of respective metal substrate also exerts a posttranslational effect by the intracellular trafficking alterations or at the cell surface level by the internalization of transporter proteins followed by transport to the degradative compartment (reviewed in (Haguenauer-Tsapis & André, 2004)).

The sorting of transmembrane proteins to intended compartments of the endosomal-vacuolar system is mediated by complex system of sorting signals presented within the cytosolic domains of the protein. Most signals consist of short, linear sequences of amino acid residues. Such complex array of specific signals and recognition elements of the internalization and vacuolar targeting machinery ensure dynamic but accurate taking up of protein from plasma membrane into the cell and ensuing degradation (Bonifacino & Traub, 2003).

Despite number kinds of sorting motifs and signals, contained within the cytosolic domains of transmembrane proteins such as tyrosine-based (NPXY or YXX∅), dileucine-based ([DE]XXXL[LI] or DXXLL), acidic cluster, lysosomal avoidance signals, NPFX(1,2)D-Type signals or ubiquitin, characteristic for endocytic and lysosomal machinery, apparently the major endocytic signal in budding yeast is ubiquitin (Bonifacino & Traub, 2003).

Ubiquitin is a small 76 amino acid polypeptide that is highly conserved in the evolution. It is the best characterized member of a class of small protein modifiers, ubiquitin and ubiquitin-like proteins, that regulates the activity of diverse arrays of cellular proteins (Hershko & Ciechanover, 1998; Hochstrasser, 2000; Jentsch & Pyrowolakis, 2000; Kerscher et al, 2006). Proteins of the ubiquitin pathway are covalently modified by the attachment of ubiquitin to the ε-amino groups of internal lysine residues in target substrates. This process usually requires the successive action of three enzymes: a

ubiquitin-activating enzyme (E1), a ubiquitin-conjugating enzyme (E2), and a ubiquitin-protein ligase (E3) (reviewed in (Hershko & Ciechanover, 1998; Staub & Rotin, 2006; Weissman, 2001)).

The key regulatory determinants in the ubiquitination reaction are E3 ligases that are thought to specify the timing and substrate selection (Fang & Weissman, 2004; Pickart, 2001; Schwartz & Hochstrasser, 2003). There are two main types of E3 for ubiquitin, the RING class and the HECT class (Pickart, 2001; Weissman, 2001). The first family, characterized by the zinc-binding RING (really interesting new gene) finger domain and related U-box or PHD domains, carries ubiquitination by simultaneous binding of the substrate and an E2 (Joazeiro & Weissman, 2000). The second family, defined by the HECT (homologous to E6-AP carboxy terminus) domain, participates directly in catalysis by forming an obligate thiolester bond with ubiquitin during the ubiquitination reaction (Huibregtse et al, 1995). In a number of cases, the ligase responsible is a HECT domain-containing family represented by Nedd4/Rsp5 members (Blondel et al, 2004; Dunn & Hicke, 2001; Hettema et al, 2004; Rougier et al, 2005; Springael & Andre, 1998). The Nedd4/Rsp5 family is widely conserved from human to the yeast, where a single family member Rsp5 is found (Shearwin-Whyatt et al, 2006). These ligases are characterized by the presence of three distinct domains: a N-terminal phospholipid-binding C2 domain, implicated in membrane association, a variable (1-4) of WW domains, and a C-termianl HECT domain that contains the active site for ubiquitin ligation (Shearwin-Whyatt et al, 2006). The WW domains found in Nedd4/Rsp5 are the type that bind short "PY" motifs typically with the sequence PPxY (Harty et al, 2000; Sudol, 1996), and it has been shown that the addition of a PY motif can make a protein a substrate for Rsp5 *in vitro* (Saeki et al, 2005). Many substrates of Nedd4/Rsp5, however, lack PY motifs, and they must rely on other interactions to be recognized. In yeast, protein linking ligase with its substrate is the Bsd2 protein containing PY motif, that is required for such specific protein targeting (Hettema et al, 2004; Sullivan et al, 2007).

To date, Rsp5 is the only ubiquitin ligase that in yeast impacts regulation of endocytosis and lysosomal degradation of plasma membrane proteins such as Gap1p, Put4p, Dal5p, Gnp1p, Tat2p, Hxt6/p, Gal2p, Mall11p, Mal61p, Fur4p, Zrt1p, Itr1p, Alr1p, Can1p, Ste2p, Ste3p and Ste6p (Beck et al, 1999; Galan & Haguenauer-Tsapis, 1997; Gitan & Eide, 2000; Gitan et al, 1998; Graschopf et al, 2001; Grenson, 1992; Hein & Andre, 1997; Horak & Wolf, 2001; Kelm et al, 2004; Krampe et al, 1998; Lucero & Lagunas, 1997;

Matejckova-Forejtova et al, 1999; Medintz et al, 1998; Robinson et al, 1996). Recently, numerous novel ubiquitinated substrates of this E3 ligase were identified, *e.g.*, Ymr171c, Rcr1/2p, Sna3/4p, Yip5p, Ydl012C, Alg6p (reviewed in (Gupta et al, 2007)). Rsp5 also ubiquitinates a components of the endocytic machinery (Dunn & Hicke, 2001; Gajewska et al, 2001; Kaminska et al, 2002; Stamenova et al, 2004). Morover, Rsp5-dependent ubiquitination is involved in sorting at the Golgi apparatus (Helliwell et al, 2001) and into the multivesicular bodies (Katzmann et al, 2004; Morvan et al, 2004).

Rsp5 plays also well characterized roles in numerous other cellular functions, which are tightly linked to the type of chain generation. Ubiquitin has seven lysine residues, all of which are potentially involved in generation of structurally and functionally distinct chains (Haglund & Dikic, 2005; Peng et al, 2003). Polyubiquitination involving ubiquitin lysines 48 and 29 directs short lived, damaged, misfolded, or misassembled proteins to the 26S proteosome for degradation (Hershko & Ciechanover, 1998; Hochstrasser, 1996). In contrast, polyubiquitination, involving lysine 63, regulates post-replicative DNA repair, transcription, cell cycle transition, and endocytosis of plasma membrane proteins. Yet the monoubiquitination affects endocytosis/lysosomal degradation, meiosis, and chromatin remodeling (Hicke, 2001; Lindsten et al, 2002; Weissman, 2001). The reversibility of ubiquitination is ensured by a large group of deubiquitinating enzymes that have important regulatory functions (Amerik & Hochstrasser, 2004; Nijman et al, 2005).

4. MATERIAL AND METHODS

The following chapter is devoted to supplement the materials and experimental techniques specified in publications presented here (see chapter "RESULTS").

4.1. Bacterial strains and media

Table 4.1. *Escherichia coli* strains used in this thesis.

Strain	Genotype	Reference
DH5α	*F- endA1 glnV44 thi-1 recA1 relA1 gyrA96 deoR nupG Φ80dlacZΔM15 Δ(lacZYA-argF)U169 hsdR17(rK- mK+) λ–*	D. Hanahan (1983)
DH10β	*F- mcrA Δ(mrr-hsdRMS-mcrBC) φ80lacZΔM15 ΔlacX74 recA1 araD139 Δ(ara-leu)7697 galK rpsL(StrR) endA1 nupG*	Invitrogen, Paisley, UK

Growth media for *E. coli*

Rich medium (LB): 1% Tryptone
0,5% Yeast extract
0,5% NaCl

For selection of cells carrying plasmids, 150 μg/ml ampicillin was added to the media after autoclaving (LB-Amp). Solid media contained 2% agar in addition. Cells were incubated at 37°C.

4.2. Yeast strains and media

Table 4.2. *Saccharomyces cerevisiae* yeast strains used in this thesis.

Strain	Genotype	References
GA74-1A	MAT a, *leu2, ura3::CTT1-lacZ, his3, trp1, ade8, cta1-2, can1*	laboratory stock
JS74A	isogenic wild-type to JS74	Graschopf et al., (2001)
JS74B	MAT a, *leu2, ura3::CTT1-lacZ, his3, trp1, ade8, cta1-2, can1, alr1::URA3*	Graschopf et al., (2001)
AG02	MAT a, *leu2, ura3::CTT1-lacZ, his3, trp1, ade8, cta1-2, can1, alr1::URA3, alr2::HIS3*	Graschopf et al., (2001)
AG012	MAT a, *leu2, ura3::CTT1-lacZ, his3, trp1, ade8, cta1-2, can1, alr1::URA3, alr2::HIS3*	Graschopf et al., (2001)
FY1679	MAT a; *ura3-52 trp1D63 leu2Δ1 his3 Δ200 GAL2*	Winston et al., (1995)
BY4742	MAT a; *his3D1 leu2D0 lys2D0 ura3D0*	Brachmann et al., (1998)
BY*pep12 Δ*	Mat a; *his3D1 leu2D0 lys2D0 ura3D0 YOR036w::kanMX4*	EUROSCARF
THY.AP4	MAT a; *ura3 leu2 lexA::lacZ::trp1 lexA::HIS3 lexA::ADE2*	Obrdlik et al., (2004)
THY.AP5	MAT α; *URA3 leu2 trp1 his3 loxP::ade2*	Obrdlik et al., (2004)

Growth media for *S. cerevisiae*

Rich medium (YPD): 1% yeast extract

2% peptone

2% glucose

Standard medium (SD): 2% glucose

0,5% $(NH_4)SO_4$

0,4% KH_2PO_4 (212,5 mg/ml)

0,4% K_2HPO_4 (37,5 mg/ml)

0,2% NaCl (50 mg/ml)

0,2% $CaCl_2$ (50 mg/ml)

Vitamins and amino acids supplementation

Synthetic complete medium (SM): 2% glucose

0,67% yeast nitrogen base

Vitamins and amino acids supplementation

Low pH, low phosphate medium (LPP): 2% glucose

0,5% $(NH_4)SO_4$

6,4% KH_2PO_4 (212,5 mg/ml)

0,5% KCl (1 M)

0,2% NaCl (50 mg/ml)

0,2% $CaCl_2$ (50 mg/ml)

Vitamins and amino acids supplementation

Vitamin and amino acid drop out solutions were prepared as described in Sherman (Sherman, 2002). To solidify, the media are supplemented with 2% agar. For selection of cells that carried plasmids appropriate amino acids were excluded from the growth medium. Yeast strains were grown at 30°C.

4.3. Plasmids and oligonucleotides

Table 4.3. Plasmids used in this thesis.

Plasmid name	Description	Reference
pFA6a-His3MX6	Template for PCR amplification of fragments for gene deletion with *S. cerevisiae HIS5*-selection marker	Longtine et al., (1998)
YEp351-HA	2μ-plasmid with *LEU2* marker	Bui et al., (1999)
YEpM351-HA	2μ-plasmid with *LEU2* marker, 449 bp Sac*I*/Sal*I* of pUG23 p_{Met25} promoter	Wachek et al., (2006)
YIplac204	integrative vector with *TRP1* marker	Gietz and Sugino, (1998)
YCplac22	*ARS*1 *CEN*4 vector with *TRP1* marker	Gietz and Sugino, (1998)
YCplac111	*ARS1 CEN4* vector with *LEU2* marker	Gietz and Sugino, (1998)
pUG23	*HIS3* marker, yEGFP3	Niedenthal et al., (1996)
pMetYCgate	fusion to C-terminal part of ubiquitin for use with mbSUS	Obrdlik et al., (2004)
pN-Xgate	fusion to N-terminal part of ubiquitin for use with mbSUS	Obrdlik et al., (2004)

Generated constructs and the sequences of the oligonucleotides used throughout this work are found in the respective publications attached in this work (see chapter "RESULTS").

4.4. Protocols used in this study

4.4.1. Preparation of E. coli competent cells

Electro-competent cells

1. Inoculate 10 ml of *E. coli* cells in LB medium and incubate overnight at 37°C
2. Transfer 5-10 ml of *E. coli* cells to 1000 ml LB medium in 2000 ml flask and incubate for 3-4 hours to OD_{600} of about 0,7
3. Transfer the cell cultures to 2 x 500 ml tubes and centrifuge at 4°C, 4000 rpm for 5 min.
4. Wash the cells in 200 ml of ice-cold 10% glycerol, centrifuge as in the step 3 and discard the supernatant
5. Wash the pellet in 20 ml of ice-cold 10% glycerol, centrifuge as above and discard the supernatant
6. Wash the cells in 2 ml of ice-cold 10% glycerol, transfer suspension from both tubes to one and aliquot suspension in volume of 100 μl to microfuge tubes
7. Prepared cells store at -80°C

CaCl$_2$-competent cells

1. Inoculate 10 ml *E. coli* cells in LB medium and incubate overnight at 37°C
2. Add 5 ml of overnight cultured *E. coli* cells to 500 ml LB medium and incubate cells for 3-4 hours to OD_{600} of about 0,7
3. Spin the cells down at 4°C, 3000 rpm for 10 min. and discard the supernatant
4. Resuspend the pellet in original volume of ice-cold 100 mM $MgCl_2$, centrifuge as in the step 3 and discard the supernatant
5. Resuspend the cells in 250 ml of ice-cold 50 mM $CaCl_2$ and put on ice for at least 30 min.
6. Spin the cells down as in the step 3 and discard the supernatant
7. Resuspend the cells in 20 ml of ice-cold 50 mM $CaCl_2$ and follow the step 3
8. Add to the pellet 2 ml of 50 mM $CaCl_2$ and 2 ml of 50% glycerol
9. Aliquot suspension in volume of 150 μl to microfuge tubes and store at -80°C

4.4.2. Transformation of E. coli cells

Electroporation

1. Thaw the aliquots with electro-competent cells on ice
2. Add your plasmid DNA and mix gently
3. Transfer individual aliquots of cell and DNA into chilled electroporation cuvette and hold them on ice
4. Place cuvette onto controller and electroshock under optimal conditions for the strain (voltage 2,5 kV, capacitance 25 ΩF, resistance 200 Ω)
5. Add 1 ml of LB medium to the cells directly after electroshock and transfer them with a micropipette from chamber to the chilled glass falcon
6. Incubate at 37°C for 30 min.
7. Plate 100 µl of the transformed cell suspension on agar containing medium
8. Incubate at 37°C to establish colonies

Standard *E. coli* transformation protocol

1. Thaw the aliquots with $CaCl_2$-competent cells on ice
2. Add your plasmid DNA, mix gently and incubate on ice for 20 min.
3. Heat shock at 42°C for 90 sec.
4. Cool down immediately the samples on ice for 2 min.
5. Add 150 µl LB medium and incubate at room temperature (or 37°C) for 30 min.
6. Plate the suspension with transformed cells on appropriate medium
7. Incubate overnight at 37°C

4.4.3. Plasmid DNA extraction from E.coli

1. Inoculate 5 ml of cell cultures in LB medium (with antibiotic supplementation if required) and allow to grow overnight at 37°C
2. Harvest the cells by centrifugation at room temperature, 14000 rpm for 30 sec.
3. Add 300 µl Solution I with RNAse A (50-100 µg/ml) and resuspend the pellet completely by vortexing

4. Add 300 µl of Solution II and mix suspention gently by 3-4 times tube inversion

5. Incubate at room temperature for 5 min.

6. Add 300 µl of Solution III and mix suspension gently by 3-4 times tube inversion

7. Incubate on ice for 15 min.

8. Centrifuge at room temperature, 12000 rpm for 5 min.

9. Transfer supernatant to the fresh microfuge tube

10. Add 540 µl of absolute isopropanol, mix and precipitate DNA at -70°C for 10 min.

11. Centrifuge at 4°C, 16000 rpm for 15 min.

12. Discard the supernatant and wash the DNA pellet with ice-cold 70% ethanol

13. Centrifuge at 4°C, 16000 rpm for 5 min.

14. Discard the supernatant and allow the pellet to air-dry

15. Resuspend DNA in 20-50 µl of sterile H_2O or TE buffer (pH 8,0)

16. Check DNA on an Agarose gel

Solution I – 50 mM glucose

        25 mM Tris-Cl (pH 8,0)

        10 mM EDTA (pH 8,0)

Solution II – 0,2 N NaOH

        1% SDS

Solution III – 5 M potassium acetate

        Glacial acetic acid

        H_2O

4.4.4. Hydroxylamine Mutagenesis of Plasmid DNA

1. Prepare the hydroxylamine solution just before use and store on ice until needed

2. Add 10 µg of CsCl - purified plasmid DNA to 500 µl of hydroxylamine solution in a microfuge tube

3. Incubate at 37°C for a time as desired

4. Stop the reaction by adding 10 µl of 5 M NaCl , 50 µl of 1 mg/ml BSA and 1 ml of 100% ethanol

5. Precipitate the DNA at -70°C for 10 min.

6. Centrifuge the precipitated DNA in a microfuge at 15000 rpm for 10 min. and carefully remove all of the supernatant

7. Resuspend the DNA in 100 µl of TE (pH 8,0), then add 10 µl of 3 M sodium acetat and 250 µl of 100%

8. Precipitate the DNA at -70°C for 10 min. and centrifuge as in the step 6

9. Allow the pellet to air-dry and then resuspend it in 100 µl of TE (pH 8,0)

10. The DNA can be used directly for transformation of either *E. coli* or yeast.

Hydroxylamine solution – Hydroxylamine HCl 0,35 g

NaOH 0,09 g

Ice-cold distilled water 5 ml

The pH of prepared solution should be about 7,0

TE buffer (pH 8,0) – 10 mM Tris-Cl (pH 8,0)

1 mM Na$_2$EDTA

4.4.5. Yeast plasmid rescue

1. Grow about 3 ml culture overnight under selective conditions

2. Harvest the cells in microfuge tubes at 5000 rpm for 5 min.

3. Discard the supernatant and resuspend pellet in 100 µl STET

4. Add 0,2 g of 0,45 mm glass beads (~200 µl) and put tubes on ice

5. Vortex vigorously at 4°C for 5-10 min.

6. Add further 100 µl STET and vortex briefly again

7. Boil samples 3 min.

8. Cool briefly on ice and spin at 4°C, 10000 rpm for 10 min.

9. Prepare fresh tubes and dispense 50 µl of 7,5M ammonium acetate to each, then transfer 100 µl of supernatant to the prepared tubes

10. Incubate at -20°C for 1 hour

11. Centrifuge at 4°C, 16000 rpm for 10 min.

12. Prepare fresh tubes and precipitate with 2,5 volume of ice-cold ethanol at -70°C for 10 min.

13. Centrifuge at 4°C, 16000 rpm for 10 min. and remove the ethanol

14. Wash pellet with 100 µl of 70% ethanol

15. Centrifuge at 4°C, 16000 rpm for 10 min. and remove the ethanol

16. Dry the pellet and resuspend in 20 µl sterile H_2O

17. Transform into *E. coli*

STET solution – 8% sucrose

                 50 mM Tris pH 8,0

                 50 mM EDTA

                 5% Triton X-100

Preparation of glass beads – 1. Soak the glass beads for 16 hours in concentrated HCl

                 2. Rinse thoroughly in distilled water

                 3. Bake them for 16 hours at about 150°C

                 4. Chill the glass beads at 4°C or on ice before use

4.4.6. Transformation of S. cerevisiae

Standard protocol with DMSO use

1. Grow yeast cells at 28°C overnight in proper medium

2. Centrifuge 1 ml of culture for each transformation in a microfuge tube at room temperature, 4000 rpm for 3 min.

3. Wash cells pellet with 700 µl LiAc solution

4. Centrifuge at room temperature, 4000 rpm for 3 min. and discard the supernatant

5. Repeat 3 times steps 3 and 4

6. Add 5 µl carrier DNA (2 mg/ml), plasmid DNA, 500-700 µl LiAc/PEG solution and incubate at room temperature for 30 min.

7. Add 50-70 µl DMSO, then heat samples at 42°C for 5 min. and immediately put on ice for 2 min.

8. Centrifuge at room temperature, 4500 rpm for 5 min.

9. Resuspend pellet in 150 µl of TE or sterile H_2O, plate cells on selective madia and incubate at 30°C for 2-4 days

<u>LiAc solution</u> – 0.1 M LiAc

          10 mM Tris pH 7,4

          1 mM EDTA

<u>LiAc/PEG solution</u> – 0.1 M LiAc

          10 mM Tris pH 7,4

          1 mM EDTA

          40% PEG

<u>Carrier DNA (Salmon sperm DNA), 2 mg/ml</u> – dissolve 200 mg in 100 ml sterile TE buffer on a stir plate overnight in a cold room. Dispense 90 ml into sterile 15 ml screw-capped plastic centrifuge tubes and the remainder as 1,0 ml samples into 1,5 ml microfuge tubes. Store at -20°C.

High efficiency transformation

1. Inoculate strain to be transformed into liquid medium and grow overnight at 30°C
2. Determine the cell titer by measuring the optical density of 10 µl diluted into 1 ml. For most strains an OD_{600} of 0,1 is equivalent to about 1 x 10^6/ml cells. Pipette 2,5 x 10^8 cells into 50 ml of liquid medium.
3. Incubate at 30°C with vigorous aeration for 3-4 hours. During this time most yeast strains will undergo at least two divisions. Determine OD_{600} to ensure the correct cell concentration has been achieved. The total yield should be about 1 x 10^9 cells
4. Harvest the cells by centrifugation and wash them in 10 ml of sterile water
5. Transfer samples of 1 x 10^8 cells to microfuge tubes, one for each transformation, and centrifuge for 30 sec.
6. Remove the supernatant and resuspend the cells in 1 ml of 100 mM LiAc
7. Incubate the suspension at 30°C for 10 min.
8. Prepare a microfuge tube of carrier DNA (2 mg/ml) by denaturing in boiling water bath for 5 min. and chilling immediately in an ice/water bath
9. Centrifuge the cell suspension at top speed for 30 sec. and remove the LiAc

10. Add transformation mix to each cell pellet and resuspend the cells by vortexing vigorously. The reagents can either be added directly to the cell pellet in descending order and then vortexed or premixed in bulk for several transformations
11. Incubate at 30°C for 30 min.
12. Heat shock at 42°C for 20 min.
13. Centrifuge at top speed for 30 sec. and remove the transformation mix
14. Pipette 1 ml of sterile H_2O or SC drop-out medium onto the pellet and incubate at room temperature for 5 min. Resuspend the cells by vortexing vigorously
15. Dilute 10 µl into 1 ml of sterile H_2O and plate 100 µl samples of each transformation onto SC drop out medium
16. Incubate at 30°C for 2-4 days

Transformation mix – 50% PEG 240 µl

1 M LiAc 36 µl

Carrier DNA 52 µl

Plasmid DNA + H_2O 32 µl

Total volume 360 µl

4.4.7. Total protein extraction from yeast

Yeast protein extraction by TCA method (quick protocol)

1. Grow yeast cells overnight at permissive temperature (28°C)
2. Harvest about 50 µl of cells pellet from overnight culture in microfuge tube at 4°C, 4000 rpm for 3 min.
3. Wash cells with 200 µl of 0,02% NaN_3 solution, then vortex and centrifuge again at 4000 rpm for 3 min. in 4°C
4. Resuspend pellet in solution of 200 µl 2 M NaOH with 5% β-mercaptoethanol
5. Keep on ice for 10 min.
6. Add 40 µl of cold (4°C) 50% TCA
7. Keep on ice for further 10 min.
8. Spin at room temperature, 5000 rpm for 5 min.
9. Remove the supernatant and add to the pellet 200 µl of ice cold 90% aceton

10. Spin again at room temperature, 5000 rpm for 5 min.

11. Dissolve pellet in 40 µl of SDS-Loading buffer and boil 5 to 10 min.

12. Spin probes at room temperature, 5000 rpm for 5 min.

13. Load supernatant on gel or store at -20°C

SDS-Loading buffer - 1:1 Laemmli buffer and Tris pH 8,0

2 x Laemmli buffer – 5 ml 1 M Tris-Cl pH 6,8

                6 ml 20 % SDS

                4,6 ml 87 % Glycerin

                2 ml β-Mercaptoethanol

                2,4 ml H_2O

                Bromophenolblue

Yeast protein preparation by TCA method (with protein concentration assay)

1. Grow cells overnight in 2-5 ml YPD medium

2. Wash cells 2 x in SD medium with low magnesium content (5 µl Mg^{2+})

3. Grow cells further 3 to 4 hours in SD (5 µl Mg^{2+})

4. Aliquot cells, add 100 µg/ml CHX and Mg^{2+} as desired

5. Harvest cells at 4°C, 5000 rpm for 1 min.

6. Wash cells 2 x in ice-cold 1 mM EDTA and 1 x in H_2O (4°C)

7. Spin cells at 4°C, 5000 rpm for 1 min.

8. Resuspend the pellet in 200 µl ice-cold 2 M NaOH with 2,5 µl of β-mercaptoethanol

9. Incubate on ice for 10 min.

10. Add 80 µl of 100% TCA (final concentration 28 %), vortex

11. Incubate on ice for at least 60 min.

12. Spin at 14000 rpm for 5 min.

13. Take off the supernatant, wash pellet in 200 µl of ice-cold 90% aceton

14. Spin at 14000 rpm for 5 min.

15. Wash pellet in 100 µl of 1 M Tris-base

16. Spin at 14000 rpm for 5 min.

17. Resuspend the pellet in 80 µl hot 5% SDS and boil for 5 min.

18. Spin at 2500 rpm for 5 min. and transfer supernatant to a fresh tube

19. Determine the protein concentration (Biorad DC)

20. Add SDS-Loading buffer and boil further 5 min.

21. Let it cool to room temperature and load up on SDS-PAGE

<u>Cycloheximide (CHX) stock solution</u> – 10 mg/ml in sterile H_2O, prepare always freshly

Determination of protein concentration according to Biorad DC instruction manual (standard curve)

Standard concentration	10% SDS (µl)	H_2O (µl)	BSA stock 10 mg/ml (µl)
0	5	45	0
0,2	5	44	1
0,4	5	43	2
0,6	5	42	3
0,8	5	41	4
1,0	5	40	5
1,2	5	39	6

Take 25 µl of solutions for measurement

4.5. Application of the mating-based split-ubiquitin system to investigate membrane protein interactions

Protein-protein interactions play a fundamental role in the regulation of almost all cellular processes such as division, growth and signaling. Thus, the identification of interacting proteins can help to elucidate their regulation and function in the cellular context. Several methods, divided into biochemical and genetic, are available to detect possible protein interactions. Biochemical assays establish the state of interacting proteins by direct working with proteins to determine the composition of protein complexes. However, these methods require harsh treatment for cell disruption and therefore may not preserve weak or

transient interactions. To overcome technical difficulties associated with the biochemical characterization of physical protein-protein interactions, the alternative genetic methods are employed, that indirectly determine protein interactions based upon outputs generated through the manipulation of endogenous and exogenous gene networks.

The most powerful genetic method for *in vivo* detection of protein-protein interactions is the yeast two-hybrid system (YTH) described by Johnsson and Varshavsky (Johnsson & Varshavsky, 1994). The advantage of this system was later adopted for the study of membrane protein interactions by Stagljar and colleagues (Stagljar et al, 1998) and further modified by Obrdlik and colleagues (Obrdlik et al, 2004). The major benefit of improved YTH method is that protein-protein interactions can be analyzed at the site of their natural location in the cell, *i.e.* the proteins of interest do not need to enter the nucleus for activation of the reporter gene. The mating-based split-ubiquitin system (mbSUS) is found on the observation that the wild-type N-terminal ubiquitin domain (NubI) (amino acids 1-34) can spontaneously reconstitute a full-length ubiquitin protein when overexpressed with the C-terminal ubiquitin half (Cub) (amino acids 35-76). Ubiquitin-specific proteases (UBPs), present in the cytosol and nucleus of all eukaryotic cells, recognize such reconstituted ubiquitin and generally cleave off proteins attached to ubiquitin moieties. For protein interactions the assay is designed in such a way that the association of Nub and Cub is only efficient if the ubiquitin halves are linked to two proteins that interact *in vivo*. It was achieved by the single amino acid substitution of isoleucine at position 13 in NubI with that of glycine (NubG), thereby preventing the spontaneous reconstitution of a functional ubiquitin molecule. When both proteins of interest interact, the protein-protein interaction leads to an increase in the local concentration of NubG and Cub. Subsequently, a native-like ubiquitin is formed and recognized by UBPs followed by release of artificial transcription factor PLV (protein-LexA-VP16) fused to the C-terminus of Cub. The liberated PLV diffuses to the nucleus and activates a set of LexA-driven reporter genes *ADE2*, *HIS3* and *LacZ* (see Figure 4.5.1).
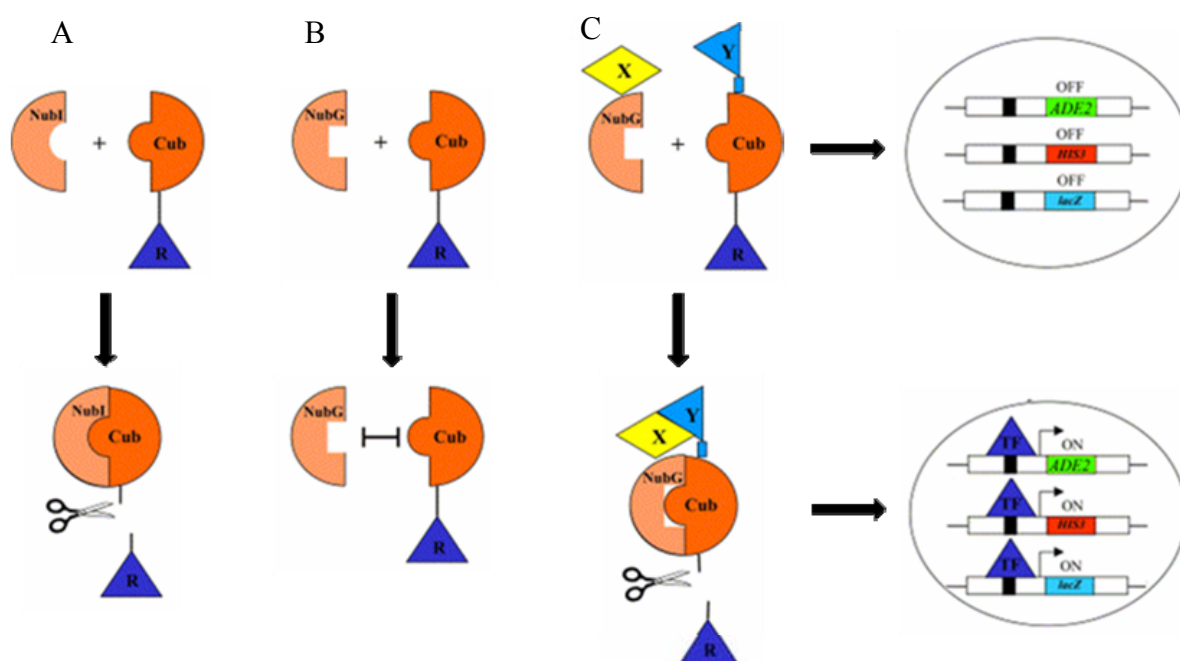
Fig. 4.5.1. Principle of the mating-based split-ubiquitin approach. (A) If wild-type ubiquitin is split into an N-terminal fragment (Nub, light orange semi-circle) and a C-terminal fragment (Cub, red orange semi-circle), the two halves will spontaneously associate. If a reporter construct is attached to the N-terminal of Cub (triangle, R), ubiquitin specific proteases (UBPs, scissors) will cleave the reporter from Cub upon re-association of ubiquitin. (B) If a mutation is generated in the Nub portion of ubiquitin (NubG), the NubG and Cub portions no longer spontaneously associate and therefore the reporter remains associated with the Cub domain. (C) If interacting proteins X and Y are fused to the NubG and Cub domains, the interaction between X and Y brings the NubG and Cub domain into close proximity which causes partial re-association of ubiquitin, recognition by the UBPs and release of the reporter from the membrane. Subsequently, TF diffuses into the nucleus and turns on the expression of *ADE2*, *HIS3* and *lacZ* resulting in cells which are able to grow on medium lacking adenine, histidine and which will turn blue in the presence of X-gal (adapted from (Fetchko & Stagljar, 2004), and modified).

With accordance to the manual for split ubiquitin system presented by Obrdlik and collegues (Obrdlik et al, 2004) we applied pMetYCgate vector in our study to fuse Alr1p, its C-terminally truncated isomers and Alr2p with bait Cub-PLV fusion peptide. The prey peptide was generated by the fusion of desired Alr1/Alr2 proteins, also mutated variants, with vector pNXgate-3HA. The mbSUS uses two haploid yeast strains, THY.AP4 (mating type a) and THY.AP5 (mating type α) (see Tables 4.1, 4.2, and Figure 4.5.1). The strain THY.AP4 carries the reporter genes *HIS3*, *ADE2*, and *lacZ* under the control of a PLV-regulated promoter. To perform interaction tests, THY.AP4 is transformed with bait Cub-

PLV fusion constructs, whereas THY.AP5 is transformed with Nub constructs. The interactions are tested in diploid cells by mating THY.AP4 bait with THY.AP5 prey. PLV-induced activation of *HIS3* and *ADE2* reporter genes can be visualized on media lacking adenine and histidine. In addition, the activation of *ADE2* can usually be observed on complete media due to a change of colony color from pink/red to white. The activity of the *lacZ* reporter gene can be monitored by means of qualitative as well as quantitative assays.
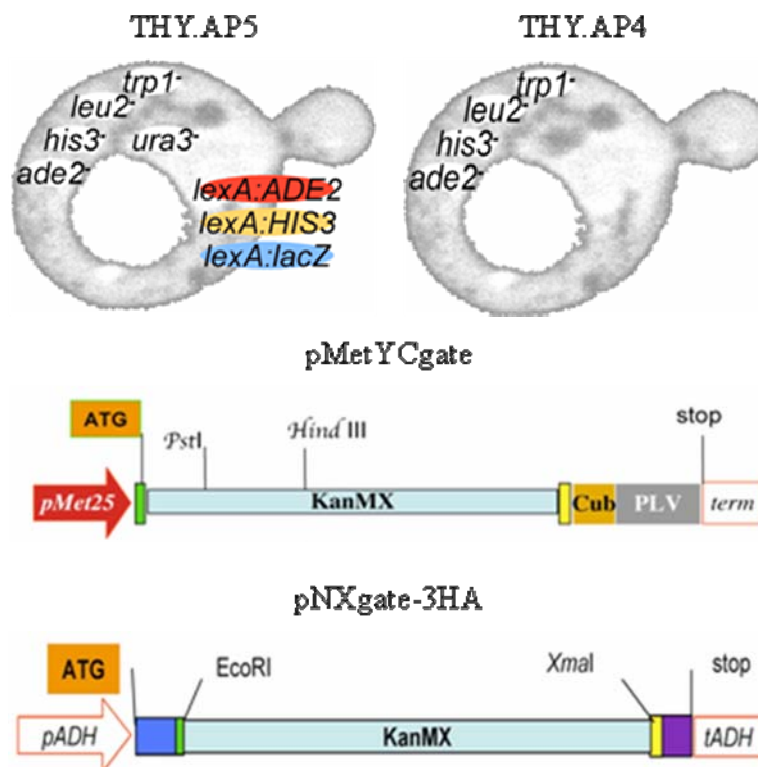

Figure 4.5.2. Yeast strains THY.AP5 and THY.AP4 and the maps of pMetYCgate and pNXgate-3HA vectors used in mbSUS approach. pMetYCgate vector is suited for Y-CubPLV fusion of bait peptide and pNXgate-3HA vector is suited for Nub-X fusion of prey peptide. In both vectors B1-KanMX-B2 cassettes are identical, the linkers B1 and B2 are green and yellow, respectively. In pMetYCgate promoter is red, *term* marks terminator. In pNXgate-3HA, pADH is the ADH1 promoter, tADH marks the ADH1 terminator. Marked restrictions sites are used to produce linear vectors for *in vivo* cloning. *ATG* and *stop* mark start and stop codon in the expression cassette (adapted from (Obrdlik, 2004)).

The detailed protocols are described in the "Manual for the use of mating-based Split ubiquitin system "mbSUS", version B, December 2004" by Petr Obrdlik available together with the components of the system (Obrdlik, 2004).

Analysis of Alr1p and Alr2p interactions with split-ubiquitin system demonstrated in this thesis (see *"Publication I"*) was performed according to the manual mentioned above. Figure 4.5.3 gives an overview of experimental procedure of mbSUS with different strategies for testing protein-protein interactions.
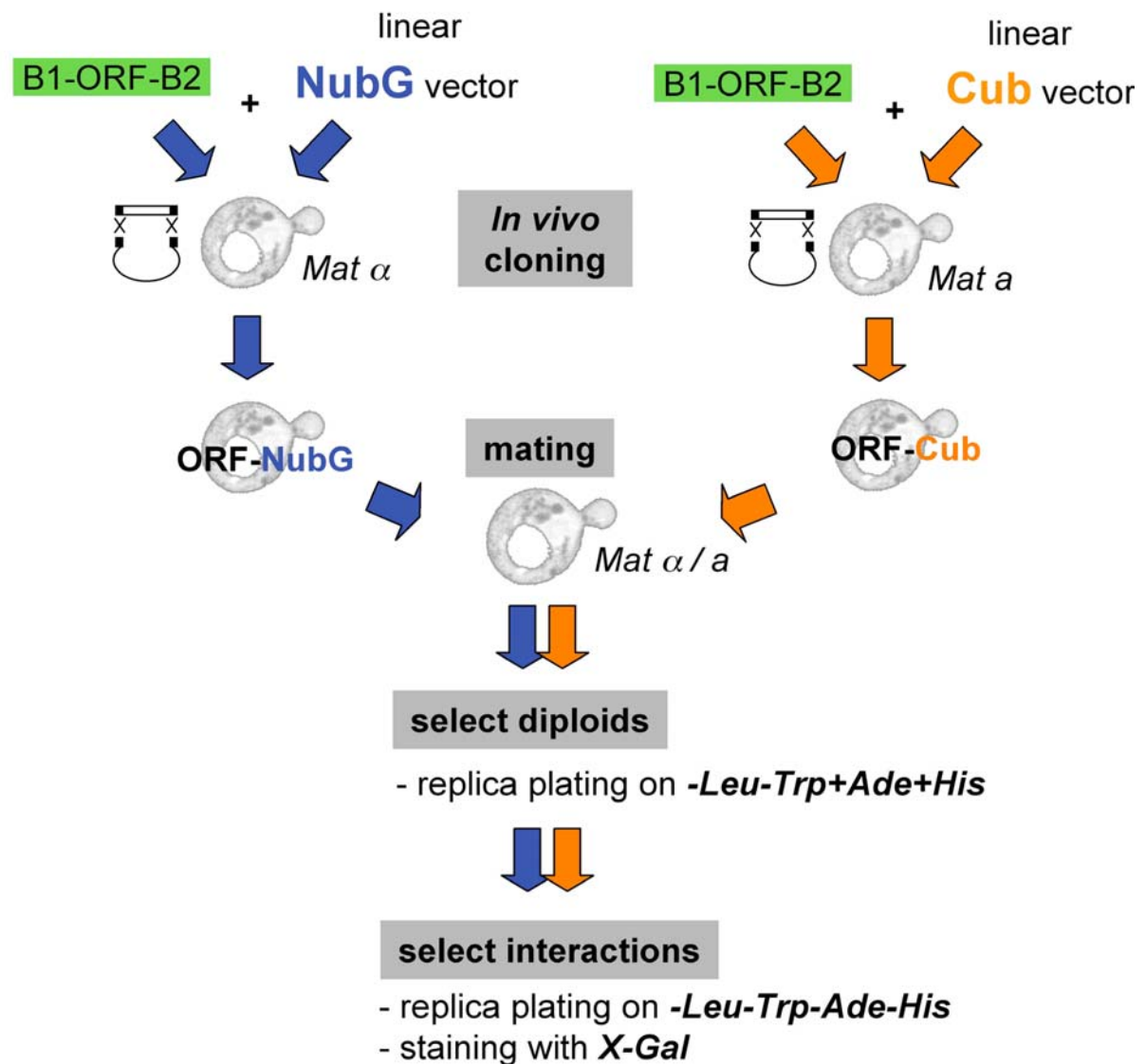

Figure 4.5.3. Flow chart of mbSUS interaction assay. Mat *α* strain is THY.AP5, Mat *a* strain is THY.AP4 (adapted from (Obrdlik, 2004)).

5. RESULTS

5.1. Publication I

Wachek M., Aichinger, M.C., Stadler, J.A., Schweyen R. and Graschopf A.

Oligomerization of the Mg^{2+}-transport Alr1p and Alr2p in yeast plasma membrane.

Febs J (2006), 273(18): 4236-49.

Oligomerization of the Mg^{2+}-transport proteins Alr1p and Alr2p in yeast plasma membrane

Marcin Wachek[1], Michael C. Aichinger[1], Jochen A. Stadler[2], Rudolf J. Schweyen[1] and Anton Graschopf[1]

1 Max F. Perutz Laboratories, Department of Genetics, University of Vienna, Austria
2 EMBL, Heidelberg, Germany

Alr1p is an integral plasma membrane protein essential for uptake of Mg^{2+} into yeast cells. Homologs of Alr1p are restricted to fungi and some protozoa. Alr1-type proteins are distant relatives of the mitochondrial and bacterial Mg^{2+}-transport proteins, Mrs2p and CorA, respectively, with which they have two adjacent TM domains and a short Mg^{2+} signature motif in common. The yeast genome encodes a close homolog of Alr1p, named Alr2p. Both proteins are shown here to be present in the plasma membrane. Alr2p contributes poorly to Mg^{2+} uptake. Substitution of a single arginine with a glutamic acid residue in the loop connecting the two TM domains at the cell surface greatly improves its function. Both proteins are shown to form homo-oligomers as well as hetero-oligomers. Wild-type Alr2p and mutant Alr1 proteins can have dominant-negative effects on wild-type Alr1p activity, presumably through oligomerization of low-function with full-function proteins. Chemical cross-linking indicates the presence of Alr1 oligomers, and split-ubiquitin assays reveal Alr1p–Alr1p, Alr2p–Alr2p, and Alr1p–Alr2p interactions. These assays also show that both the N-terminus and C-terminus of Alr1p and Alr2p are exposed to the inner side of the plasma membrane.

Mg^{2+} is the most abundant bivalent cation. It is involved in many cellular functions (as cofactor in numerous enzymatic reactions), particularly mediating phosphotransfer, and has extensive influence on macromolecular structures of nucleic acids, proteins and membranes. It also plays important roles in controlling the activities of the Ca^{2+} and K$^+$ channels in the plasma membrane.

Mg^{2+} uptake into cells and from cytoplasm into mitochondria and chloroplasts is mediated by specific transport proteins and is driven by the inside negative membrane potential. The CorA protein is the major Mg^{2+}-transport protein in bacteria and archaea [1,2]. A distantly related protein, named Mrs2, has been shown to mediate Mg^{2+} uptake into yeast mitochondria [3]. Orthologs of this protein also exist in mitochondria of mammals and plants as well as in plant chloroplasts and plasma membranes [4–6]. The yeast *Saccharomyces cerevisiae* makes use of another class of distant orthologs of CorA, named Alr1 and Alr2, for Mg^{2+} influx through the plasma membrane, and most members of ascomycota appear to encode proteins of the this subfamily of CorA-related proteins. In the absence of Alr1p, yeast cells undergo growth arrest in standard media when intracellular Mg^{2+} concentrations fall to $\approx 50\%$ of those in wild-type cells. Growth arrest can be suppressed by an increase in Mg^{2+} concentrations of growth medium above 20 mM or by overexpression of Alr2p [7,8]. The only Mg^{2+}-transport proteins that do not belong to the CorA

superfamily that are known to be essential for cells are the TRPM6 and TRPM7 proteins in mammalian plasma membrane [9,10].

Members of the CorA superfamily of Mg^{2+}-transport proteins are characterized by the presence of two adjacent transmembrane domains (TM-A, TM-B) near their C-terminus and a GMN motif at the end of TM-A [11]. The short sequence connecting the two TM domains appears to be oriented towards the outside of the bacterial plasma membrane or the outside of the mitochondrial inner membrane. A surplus of negatively charged residues is typically found in this loop, particularly a glutamate residue at position $+6$ after the GMN motif. The yeast Mrs2p appears to have both its short C-terminal and long N-terminal sequences inside the inner mitochondrial membrane [12]. Chemical cross-link studies revealed homo-oligomeric complexes of the bacterial CorA protein or the mitochondrial Mrs2 protein [3,13].

Heterologous expression of members of the CorA-Mrs2-Alr1 superfamily has repeatedly been shown to restore growth of cells lacking their cognate member of this family [8,12]. Accordingly, these proteins are functional homologs. It remains to be proven if these ion transporters themselves control Mg^{2+} influx into cells or organelles or if other factors mediate or contribute to flux control. Yeast cells have been shown to control expression of ALR genes and turnover of Alr1p via the Mg^{2+} concentration in the medium [8]. Limiting Mg^{2+} concentrations provokes an increase in *ALR1* expression and an enhanced concentration and stability of the protein at the plasma membrane, whereas the addition of Mg^{2+} to the growing cells induces rapid degradation of the protein via the endocytotic pathway, ending in the vacuole [8]. Recent patch clamp data in yeast suggest that the Alr1 protein acts as a Mg^{2+}-permeable ion channel [14].

Using *in vitro* chemical cross-linking and *in vivo* split-ubiquitin assays to analyze protein–protein interactions, we show here that Alr1p and Alr2p interact to form homo-oligomeric and hetero-oligomeric structures. These *in vivo* assays further revealed a N-in, C-in orientation of Alr1p. C-Terminal deletions of Alr1p lower the ability of Alr1p to homo-oligomerize. Alr2p is a close relative of Alr1p, but with reduced Mg^{2+}-transport activity due to the substitution of a conserved, negatively charged residue in the loop connecting the two TM domains.

Results

The genome of the budding yeast encodes two closely related proteins of the CorA superfamily, Alr1p and Alr2p. Overall sequence identity of these two proteins is 69% and exceeds 90% in the C-terminal part with its two predicted transmembrane domains (TM-A, TM-B) and the short connecting loop exposed to the outside, which are thought to form a major part of the ion channel.

Disruption of *ALR1* caused a growth dependence of yeast cells on high external Mg^{2+} concentrations, whereas a single disruption of *ALR2* did not affect cellular growth (Fig. 1A,B). The double knock out of *ALR1* and *ALR2* led to a slightly increased Mg^{2+} dependence (Fig. 1A). The *alr1Δ* growth defect was marginally suppressed by expression of Alr2p from a low-copy vector (YCp), but high copy expression of Alr2p (YEp) had a considerable suppressor effect (Fig. 1B). In addition, the determination of total cellular $[Mg^{2+}]$ of cells with low-copy expression of *ALR2* by inductively coupled plasma (ICP)-MS revealed a drastic reduction in the total cellular $[Mg^{2+}]$ to about half of wild-type levels (Fig. 1C). High-copy expression of *ALR2* increased the cellular $[Mg^{2+}]$, but not to wild-type levels (data not shown), corresponding to the growth ability on Mg^{2+}-limited media (Fig. 1B). Alr2p thus appears to mediate some Mg^{2+} uptake into yeast cells, but considerably less than Alr1p.

Poor expression of *ALR2*, as reported by MacDiarmid & Gardner [7], may in part account for the low Mg^{2+}-transport activity of Alr2p. Yet we observed that Alr1 and Alr2 protein sequences differ by few residues in their most conserved part, notably at the well conserved position $+6$ relative to TM-A (Fig. 2). Proteins of the CorA superfamily, which have previously been shown experimentally to transport Mg^{2+}, exhibit a negatively charged residue (mostly glutamic acid) at position $+6$ after the GMN motif, often followed by a second negatively charged residue. Yet in Alr2p the glutamic acid at position $+6$ is replaced by a positively charged residue (arginine, R768), which is followed by an asparagine. Thus it remains to be seen whether the inability of Alr2p to support normal Mg^{2+} uptake is due to this amino-acid substitution or to low gene expression, or to a combination of both.

A single amino-acid substitution accounts for low Mg^{2+}-transport activity of Alr2p
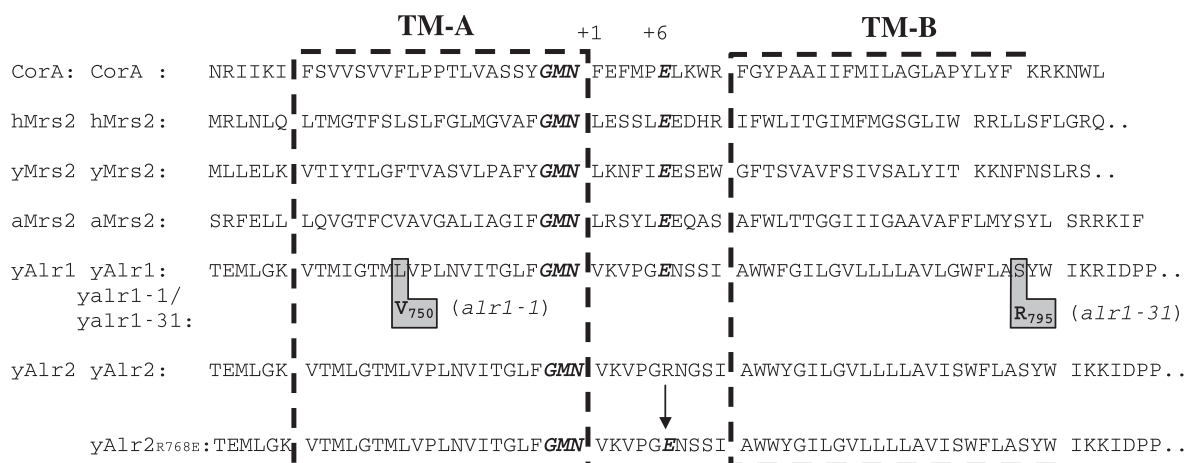
To analyse if the lack of a negatively charged residue at position 768 is relevant for the apparently low Mg^{2+}-transport activity of Alr2p, we introduced the substitution R768E by site-directed mutation in Alr2p (Fig. 2). Plasmids carrying genes *ALR1*, *ALR2* and *ALR2R768E* were transformed in either strain JS74-B (*alr1Δ*) or strain AG012 (*alr1Δ, alr2Δ*). Strikingly, expression
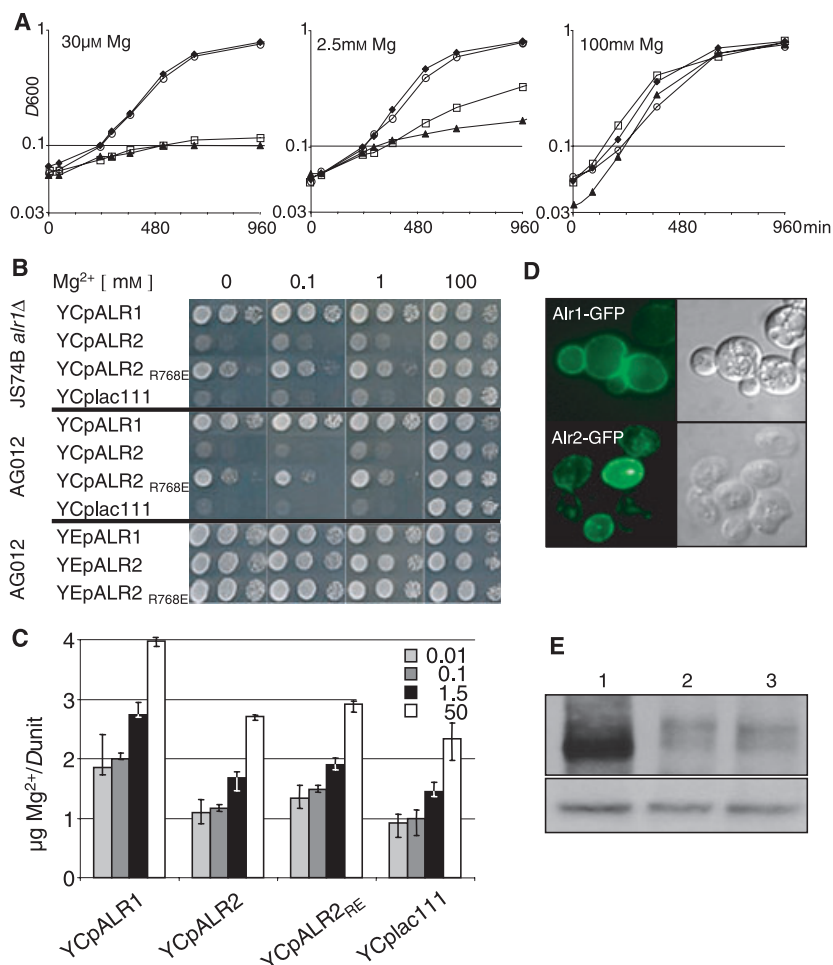
Fig. 1. Expression and activity of Alr1 and Alr2. (A) GA74B (wild-type; ◆), JS74B (*alr1Δ*; □), AG012 (*alr1Δ/alr2Δ*; ▲), and AG02 (*alr2Δ*; ○) cells were grown in synthetic SD medium supplemented with 100 mM Mg^{2+} to an D_{600} of 1.0. Cells were washed three times in synthetic SD medium lacking Mg^{2+} and inoculated at equal amounts into synthetic SD medium, supplemented with Mg^{2+} indicated in the figure. Cells were grown at 28 °C for 16 h with shaking, and growth was followed by measuring the D_{600}. (B) JS74-B (*alr1Δ*) and AG012 (*alr1Δ/alr2Δ*) cells expressing *ALR1*, *ALR2* and *ALR2R768E* either on a CEN plasmid or a 2 μ plasmid were grown in standard SD medium supplemented with 100 mM Mg^{2+} to an D_{600} of 1.0. Cells were washed three times in synthetic SD medium lacking Mg^{2+} and spotted in serial dilutions on to nominally Mg^{2+}-free synthetic SD or this medium supplemented with Mg^{2+} as indicated. Growth of cells was monitored after incubation for 2 days at 28 °C. (C) Total Mg^{2+} content was determined by ICP-MS measurement of JS74-B (*alr1Δ*) cells expressing *ALR1*, *ALR2* and *ALR2R768E* from a CEN (YCp) plasmid. The cells were incubated in medium containing Mg^{2+} (mM) as indicated for 12 h before determination of the Mg^{2+} concentration. Error bars indicate deviations of three independent measurements. (D) Subcellular localization of Alr1p and Alr2p by fluorescence microscopy. JS74A cells expressing C-terminally GFP-tagged *ALR1* from the centromeric vector pUG123-ALR1GFP and *ALR2* from the 2 μ vector YEpALR2-GFP were grown in synthetic SD medium containing 25 μM Mg^{2+} at 28 °C and examined by differential interference contrast/UV microscopy. GFP fluorescence (left panels) and corresponding differential interference contrast images (right panels) are shown. (E) Comparison of the protein concentration of cells expressing *ALR1-HA* (lane 1), *ALR2-HA* (lane 2) and *ALR2R768E-HA* (lane 3) from the multicopy plasmid YEplac351. Total cell extracts were prepared and equal amounts of protein were immunoblotted for HA-tagged proteins as well as hexokinase (Hxk1p).

of *ALR2R768E* from the centromeric plasmid YCpALR2$_{R768E}$-HA significantly suppressed the growth defect of *alr1Δ* cells in strain JS74B (*alr1Δ, ALR2*) and in strain AG012 (*alr1Δ, alr2Δ*) (Fig. 1B). Furthermore, the total Mg^{2+} content of *alr1Δ* cells expressing YCpALR2$_{R768E}$-HA was considerably increased com-

pared with cells expressing the original *ALR2* gene (Fig. 1C). A comparison of the cellular Alr2 (wild-type) and Alr2R768E protein content revealed no effect of the mutation on the expression level (Fig. 1E). We thus conclude that the R768E substitution results in stimulation of the Mg^{2+}-transport activity of Alr2p.

```
                        TM-A              +1    +6           TM-B
CorA: CorA :   NRIIKI FSVVSVVFLPPTLVASSYGMN FEFMPELKWR FGYPAAIIFMILAGLAPYLYF KRKNWL

hMrs2 hMrs2:   MRLNLQ LTMGTFSLSLFGLMGVAFGMN LESSLEEDHR IFWLITGIMFMGSGLIW RRLLSFLGRQ..

yMrs2 yMrs2:   MLLELK VTIYTLGFTVASVLPAFYGMN LKNFIEESEW GFTSVAVFSIVSALYIT KKNFNSLRS..

aMrs2 aMrs2:   SRFELL LQVGTFCVAVGALIAGIFGMN LRSYLEEQAS AFWLTTGGIIIGAAVAFFLMYSYL SRRKIF

yAlr1 yAlr1:   TEMLGK VTMIGTMLVPLNVITGLFGMN VKVPGENSSI AWWFGILGVLLLLAVLGWFLASYW IKRIDPP..
      yalr1-1/
      yalr1-31:                    V750  (alr1-1)                        R795  (alr1-31)

yAlr2 yAlr2:   TEMLGK VTMLGTMLVPLNVITGLFGMN VKVPGRNGSI AWWYGILGVLLLLAVISWFLASYW IKKIDPP..
                                                      ↓
        yAlr2R768E:TEMLGK VTMLGTMLVPLNVITGLFGMN VKVPGENSSI AWWYGILGVLLLLAVISWFLASYW IKKIDPP..
```

Fig. 2. Alignment of transmembrane parts of CorA-related proteins and mutational alterations Alr1p, and Alr2p. The TM domain sequences and flanking sequences shown are from *Salmonella typhimurium* CorA (Q9L5P6), yeast Mrs2p (yMrs2, Q01926), human Mrs2p (hMrs2, Q9HD23), *Arabidopsis thaliana* Mrs2–11 (aMrs2, Q9FPLO) and yeast Alr1 and Alr2 (yAlr1, Q08269; yALR2, P43553). The approximate position of transmembrane domains (TM-A and TM-B) is indicated by dashed lines. The highly conserved GMN motif and the conserved glutamic acid residue (E) at position +6 relative to TM-A are printed in italic. Single amino-acid exchanges in *alr1–1* and *alr1–31* at position 750 and 795, respectively, are indicated by grey boxes. The R768E substitution introduced into Alr2p is indicated by an arrow.

Subcellular localization and expression of *Alr1p* and *Alr2p*

Fluorescence of both Alr1-green fluorescent protein (GFP) and Alr2-GFP was visible in the plasma membrane of the cells, but Alr2-GFP fluorescence was detected only when expressed from the multicopy plasmid YEpALR2-GFP (Fig. 1D). Both *ALR1* and *ALR2* GFP fusions complement the *alr1Δ* phenotype when expressed in strain JS74B (data not shown). Western blotting of total yeast proteins followed by immunodecoration with an HA antibody confirmed the presence of low amounts of Alr2p compared with Alr1p (Fig. 1E).

Interference of Alr2p with Alr1p function

Reduced cellular Mg^{2+} contents are also observed when Alr2p was overexpressed in an *ALR1 ALR2* (wild-type) strain (Fig. 3A, lane 2), suggesting that the Alr2p exerts a dominant-negative effect on Alr1p expression or function. We compared the protein contents of cells expressing either *ALR1-myc* or *ALR2-HA* or both together. As can be seen in Fig. 3B, *ALR2* overexpression did not interfere with the cellular Alr1 protein content and *vice versa*. Hence Alr2p might have interfered with Alr1p function in Mg^{2+} uptake. Distant relatives of Alr1p and Alr2p, the bacterial
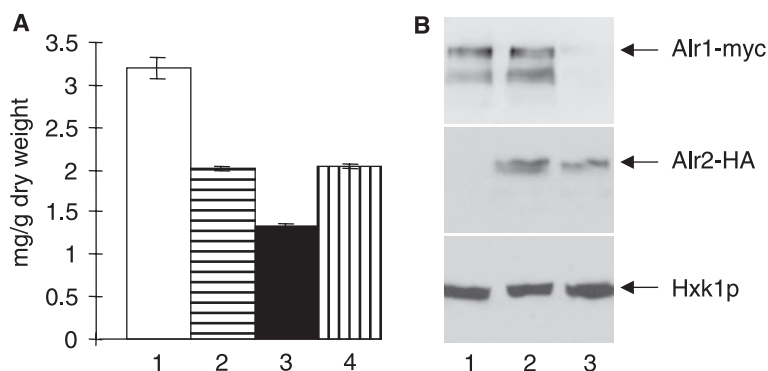
Fig. 3. Interference of *ALR2* overexpression with Alr1p function. (A) Total cellular Mg^{2+} concentration of cells expressing *ALR2*. Cells were incubated in standard SD medium before preparation for ICP-MS measurement: JS74A (wild-type, lane 1); JS74A, YEpALR2 (lane 2); JS74B (*alr1Δ*, lane 3); JS74B, YEpALR2 (lane 4). (B) Protein concentration of JS74A cells transformed with YCpALR1-myc and YEp351-HA (lane 1), YCpALR1-myc and YEpALR2-HA (lane 2), and YCp211-myc and YEpALR2-HA (lane 3). Total cell extracts were prepared, and equal amounts of protein were immunoblotted for HA-tagged and myc-tagged proteins as well as hexokinase (Hxk1p).

CorA and the mitochondrial Mrs2 Mg^{2+}-transport proteins, have been shown to form oligomeric complexes [3,13]. We hypothesize therefore that Alr2p may oligomerize with Alr1p and that, in the case of Alr2p overexpression, Alr1p–Alr2p hetero-oligomers may be formed abundantly, causing reduced activity because of the low activity of Alr2p with respect to Mg^{2+} uptake.

Dominant-negative Alr1 mutant proteins

Random *in vitro* mutagenesis of an *ALR1*-containing plasmid with hydroxylamine hydrochloride resulted in a series of mutants with altered cellular Mg^{2+} homeo-stasis. As shown in Fig. 4A, expression of the *ALR1* alleles *alr1–1* and *alr1–31* in JS74B (*alr1Δ*) did not suppress the Mg^{2+}-dependent phenotype when grown on media containing nominally 0 or 1.5 mM $MgCl_2$. Only on plates containing 100 mM $MgCl_2$ did all cells grow indistinguishably from cells expressing the wild-type *ALR1* gene. Sequencing of the mutated genes revealed single base substitutions in the *ALR1* gene, producing amino-acid exchange in TM-A and TM-B (L750V and S795R for *alr1–1* and *alr1–31*, respectively) (Fig. 2).

To investigate the expression of mutant Alr1 proteins, the centromeric plasmids YCpALR1, YCpalr1–1 and YCpalr1–31 tagged with a triple HA epitope were
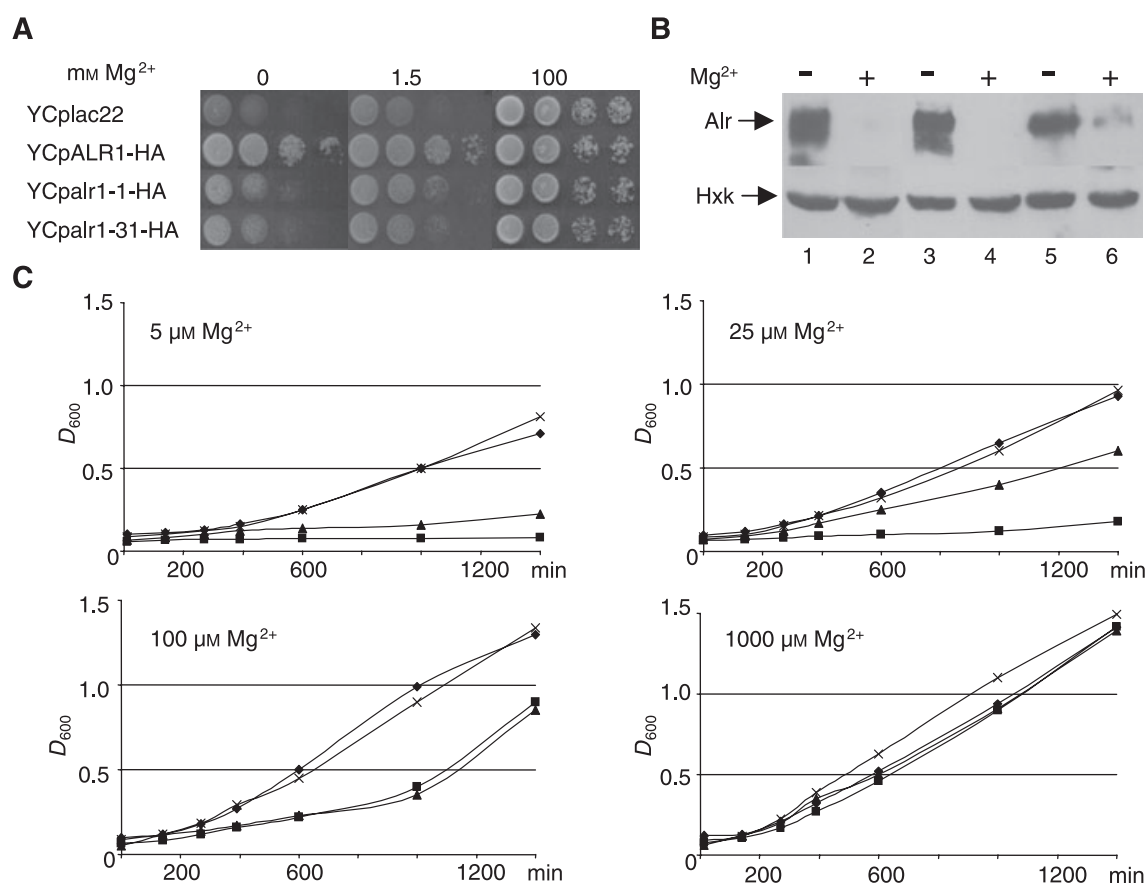
Fig. 4. Dominant-negative mutations in Alr1p. (A) Strain JS74B (*alr1Δ*), carrying plasmids indicated in the figure, was grown to mid-exponential phase in medium containing 100 mM Mg^{2+} before cells were washed and spotted in serial dilutions on to synthetic SD medium, containing the indicated Mg^{2+} concentrations. Cells were grown at 28 °C for 2 days. (B) Cells carrying plasmids YCpALR1-HA (lanes 1, 2), YCpalr1–1-HA (lanes 3, 4), and YCpalr1–31-HA (lanes 5, 6) were grown in synthetic SD medium supplemented with 50 mM Mg^{2+}. Before protein extraction, the cells were further incubated for 3 h at 28 °C in medium containing 25 μM Mg^{2+} or 50 mM Mg^{2+}. Equal protein amounts were separated by SDS/PAGE and analyzed by immunoblotting with an HA and a hexokinase (Hxk1p) antibody. (C) Expression of *alr1* mutant genes in JS74 wild-type cells reveals a dominant-negative effect. JS74 wild-type cells carrying plasmids YCplac22empty (◆), YCpALR1-HA (X), YCpalr1–1-HA (■), and YCpalr1–31-HA (▲) were grown in standard SD medium to D_{600} = 1. Cells were washed three times in synthetic SD medium without Mg^{2+} and inoculated in equal density into media containing 5, 25, 100, or 1000 μM Mg^{2+}. Cells were incubated at 28 °C with shaking. Growth was followed by measuring the D_{600} for 24 h.

transformed into the wild-type strain JS74A [8]. As shown in Fig. 4B, the mutant proteins were expressed in comparable amounts of the wild-type Alr1p, and the Mg^{2+}-dependence of Alr1p stability appeared to be unchanged, implying that the proteins are processed like wild-type Alr1p.

When growth of these transformants was observed, it became obvious that expression of *alr1–1* and *alr1–31* mutant alleles from a low-copy plasmid, along with their wild-type counterpart (chromosomal copy of *ALR1*), considerably decelerated growth at low medium concentrations of Mg^{2+} (Fig. 4C). At Mg^{2+} concentrations of 1 mM or more, expression of the mutant alleles had no influence on growth ability. These results imply that mutant Alr1 proteins interfere with wild-type Alr1p, affecting its expression, stability, or function. Similar results were recently obtained by Lee & Gardner [22] when overexpressing N-terminally deleted Alr1 proteins in an *ALR1* wild-type strain.

Protein–protein interactions detected by the split-ubiquitin system

To test for possible Alr1p–Alr1p interaction, we used the split-ubiquitin system, designed to assay interactions of membrane proteins *in vivo* [16,17]. Alr1p and Alr2p fusions were constructed by *in vivo* cloning the PCR fragments comprising genes *ALR1* and *ALR2* into the vectors pN-Xgate and pMetY-Cgate, where the latter is controlled by a methionine-repressible promoter. All constructs fused to NubG were checked for protein expression, and the function of full-length constructs was also confirmed (data not shown). The Alr1 and Alr2 fusion proteins carried either the N-terminal NubG ubiquitin part at their N-terminus or the C-terminal Cub ubiquitin part at their C-terminus. Interaction of membrane protein partners (Alr1–Alr1, Alr2–Alr2 or Alr1–Alr2) was expected to restore functional ubiquitin, which in turn should result in the release of the artificial transcription factor PLV and activation of lexA-driven reporter genes in the nucleus.

Avoiding repression of the p_{Met25}-driven Y-Cub construct in medium lacking methionine, we observed good growth of cells expressing NubG-ALR1 in combination with MetALR1-Cub on selective medium. This strongly indicated interaction of Alr1 proteins in the Nub and Cub constructs, restoring ubiquitin activity (Fig. 5A). Growth was considerably decreased when the expression of the p_{Met25}-driven ALR1-Cub was reduced by the addition of increasing methionine concentrations. In addition to our control samples, growth reduction with increasing methionine concentrations was taken as an internal control to exclude
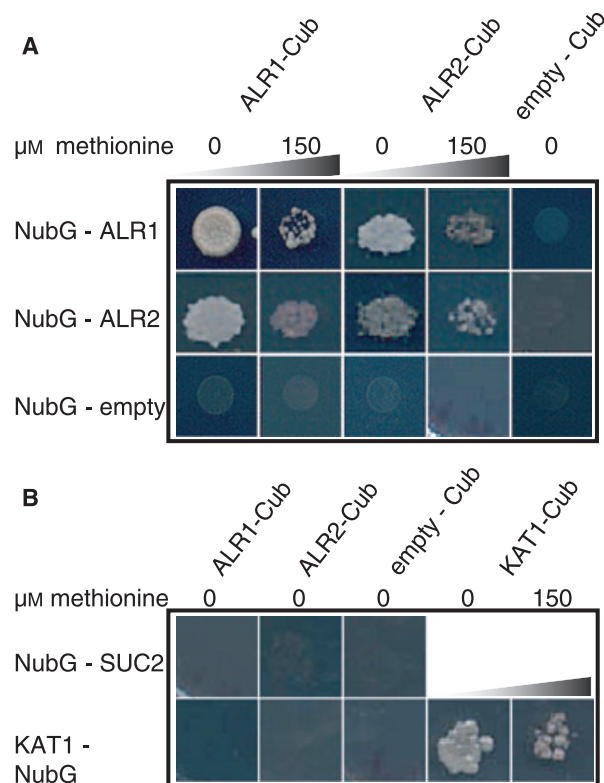
Fig. 5. Interactions of Alr1p and Alr2p in the split-ubiquitin system. Alr1p and Alr2p were analyzed using the split-ubiquitin system. Cells expressing NubG and Cub fusions of Alr1p and Alr2p were mated cross-wise and diploids were selected on plates lacking leucine and tryptophan. Diploid cells were resuspended and dropped in equal amounts on to plates lacking histidine and adenine with increasing methionine concentrations. (A) Interactions between Alr1–Alr1 pairs, Alr2–Alr2 pairs and Alr1–Alr2 pairs. Controls were performed using Alr1 or Alr2 fusion constructs in combination with the empty vectors (A), and the proteins Kat1 and Suc2 (B). As a positive control Kat1 pairs were analyzed in parallel (B). Growth was monitored after 3 days incubation at 28 °C.

false positive results, which usually also did not show any reduction at higher methionine concentrations. No growth was observed when either the Cub or the Nub vector lacked the *ALR1* sequence, or carried *SUC2* or *KAT1*, encoding a sucrose transporter or a potassium channel, either alone or combined with MetALR1-Cub (Fig. 5A,B). This confirmed that growth of cells was dependent on Alr1p–Alr1p interaction. Simultaneous expression of Kat1-NubG/MetKat1-Cub constructs resulted in growth activation and thus served as a positive control for the split-ubiquitin assay (Fig. 5B).

Coexpression of both NubG-ALR2 and MetALR1-Cub or NubG-ALR1 and MetALR2-Cub constructs resulted in significant cell growth, albeit somewhat reduced compared with the expression of *ALR1-ALR1*

pairs (Fig. 5A). Coexpression of MetALR2-Cub and NubG-ALR2 constructs also resulted in significant growth, again somewhat reduced compared with Alr1p interactions (Fig. 5A). No growth was observed in control experiments involving *SUC2* and *KAT1* constructs in combination with the *ALR2* construct (Fig. 5B).

Oligomerization of Alr1p

Chemical cross-linking has provided evidence for the formation of homo-oligomers of bacterial CorA or yeast mitochondrial Mrs2 proteins in their cognate membranes [3,13]. Together with other functional studies these findings were taken as evidence for the formation of Mg^{2+} channels by these proteins. In fact, Liu *et al.* [14] characterized yeast Alr1p as mediating large Mg^{2+} currents. We used the irreversible homo-bifunctional cross-linkers bismaleimidohexane and *o*-phenylenedimaleimide for chemical cross-linking of membrane proteins of cells overexpressing an Alr1-HA fusion protein, followed by SDS/PAGE and immunoblotting to detect Alr1p-containing products (Fig. 7).

Without the cross-linking agents, Alr1p was detected in two bands representing its monomeric form without and with a modification (apparent molecular mass of 100 kDa and 125 kDa). As shown previously, Alr1p modification precedes degradation of this protein [8]. When a yeast membrane fraction was treated with phosphatase (Fig. 6), the higher molecular mass band was greatly reduced. Although a minor part of this band resisted the treatment, this result indicated that the shift to a higher apparent molecular mass was essentially due to phosphorylation of Alr1p.
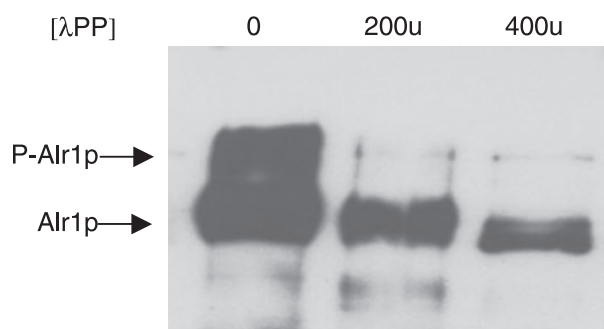
Fig. 6. λPP treatment of membranes expressing *ALR1-HA*. Equal amounts of membrane fractions of cells expressing *ALR1-HA* were incubated at 30 °C for 30 min with or without λPP at concentrations indicated in the figure. The positions of the phosphorylated protein (P-Alr1) and the unmodified protein (Alr1) are indicated by arrows. Samples were separated by SDS/PAGE (8% polyacrylamide) and analyzed by immunoblotting with an HA antiserum.

Upon addition of cross-linkers in increasing concentrations, additional high molecular mass products became detectable (Fig. 7). With increasing amounts of bismaleimidohexane cross-linker (Fig. 7B), the bands representing the unmodified and modified monomeric form were considerably diminished, and pairs of higher molecular mass bands appeared. Those with apparent molecular mass of 200–220 kDa most likely represented dimers of unmodified and modified Alr1p. Bands of ≈ 400 kDa were also visible, potentially indicating the presence of tetramers. The addition of *o*-phenylenedimaleimide also resulted in the appearance of products corresponding to dimers and tetramers, as found with the bismaleimidohexane cross-linker, with a slightly better resolution of the presumed tetramer (Fig. 7A). Poor resolution of higher molecular mass products in the gel did not allow us to distinguish between the presumed tetrameric products of an unmodified and modified form. Also, higher oligomeric products, if present, could not be visualized in our experimental system.

The C-terminus influences functionality of Alr1p

Alr1p sequence C-terminal to TM-B comprises 62 amino acids. To investigate the functional role of the C-terminus of Alr1p, we constructed truncations deleting 36 and 63 amino acids. Further deletions at the C-terminus comprised 96 and 137 amino acids, including either TM-B only or TM-A and TM-B, respectively (Fig. 8A). *ALR1* deletion constructs were expressed from a low-copy vector in mutant *alr1Δ* cells, and cell growth was monitored in synthetic media containing either 30 μM or 100 mM Mg^{2+}. Cellular free Mg^{2+} contents were determined after growth in the same media. Deletion of the very C-terminal sequences of *ALR1* (allele *alr-c36*) had no significant effect on growth or on the free Mg^{2+} content (Fig. 8B,C). Total deletion of the hydrophilic C-terminal sequence (allele *alr-c63*), however, caused a large reduction in growth and in cellular free Mg^{2+}. Finally, effects of C-terminal deletions including one or both TM domains (*alr-c96* and *alr-c137*, respectively) resulted in growth phenotypes and Mg^{2+} contents similar to *alr1Δ* deletion (Fig. 8B,C). To confirm expression of truncated proteins, similar amounts of total protein were immunoblotted, and the Alr1 as well as C-terminally truncated proteins were detected by the use of an HA antibody (Fig. 8D).

To follow the subcellular location of these proteins, we constructed fusions to GFP with the different C-terminal truncation alleles. When wild-type *ALR1* cells were starved of Mg^{2+} for 6 h before microscopic
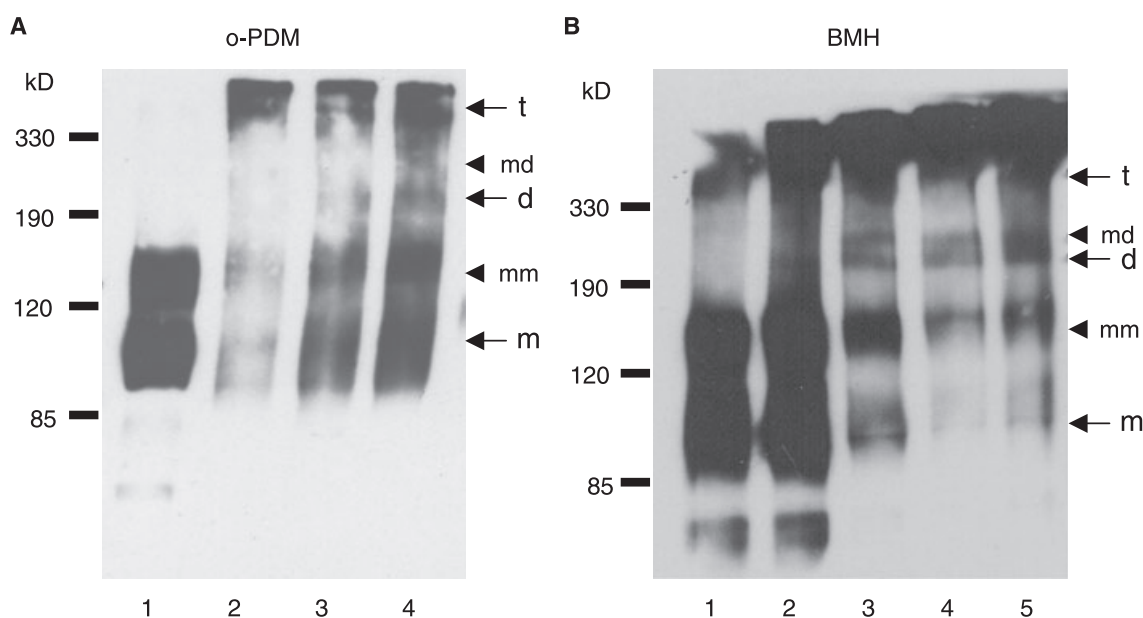
Fig. 7. Cross-linking of Alr1p. Membrane fractions were prepared from cells expressing *ALR1-HA*. The samples were treated with or without the cross-linking reagents *o*-phenylenedimaleimide at 0, 0.003, 0.03, and 0.3 mM (A; lanes 1–4) and bismaleimidohexane at 0, 0.05, 0.1, 0.5, and 1 mM (B; lanes 1–5), on ice for 30 min. The proteins were separated by SDS/PAGE and analyzed by immunoblotting with an HA anti-serum. The position of potential monomers (m), dimers (d), tetramers (t) and modified monomers (mm) and dimers (md) is indicated by arrows and arrowheads, respectively.

examination, Alr1-GFP fusion proteins were predominantly seen in the plasma membrane (Fig. 8E). Cells expressing the isomer Alr-c36p also showed plasma membrane localization of this protein, but it was also detected in the vacuolar membrane. The other three fusion proteins with larger C-terminal *ALR1* deletions (*alr-c63*, *alr-c96* and *alr-c137*) could hardly be detected in the plasma membrane but were associated with intracellular organelles or vesicles. Alr-c63 and Alr-c96 proteins appeared as punctuated structures, whereas the construct Alr-c137 in contrast is clearly misplaced, most likely to the nucleus. These observations indicated that total truncation of the C-terminus impeded delivery of mutant Alr1-GFP proteins to the plasma membrane.

The C-terminus is important for protein–protein interaction

Using the split-ubiquitin system, we investigated the interaction of the C-terminally truncated Alr1 isomers Alr-c36, Alr-c63 and Alr-c96. The protein lacking the very C-terminus of Alr1p (Alr–c36) showed interaction with itself (Fig. 9A), which was somewhat reduced compared with Alr1–Alr1 interaction. The combination of Alr-c36 with wild-type Alr1p shows fully conserved interaction (Fig. 9B). The Alr-c63/Alr-c63 pair

did not show any significant response, but this mutant protein, Alr-c63, showed almost full response when combined with Alr1 wild-type protein (Fig. 9), which might indicate an interaction domain with lower affinity proximal to the C-terminus. Finally, the Alr-c96/Alr-c96 pair failed to give any interaction signal, but surprisingly a strong signal was seen with the Alr-c96/Alr1 wild-type pair, and this signal was not repressed by methionine. Controls revealed that neither of the two proteins gave any positive signal when expressed alone. Apparently, the misplaced Alr-c96 exerts a direct or indirect effect on MetALR1-Cub, which causes transcriptional activation even when expression of the pMetY-Cgate vector in the presence of methionine is low.

Discussion

Members of the CorA-Mrs2-Alr1 superfamily of membrane proteins are likely to form ion-selective channels in their cognate membranes and to make use of the membrane potential as a driving force for Mg^{2+} flux. Arguments in favour of their role as channel proteins came first from Mg^{2+}-uptake studies with wild-type and mutant CorA of bacteria and Mrs2p of mitochondria [3,18]. This notion was then supported by patch-clamping studies, initially with whole yeast cells
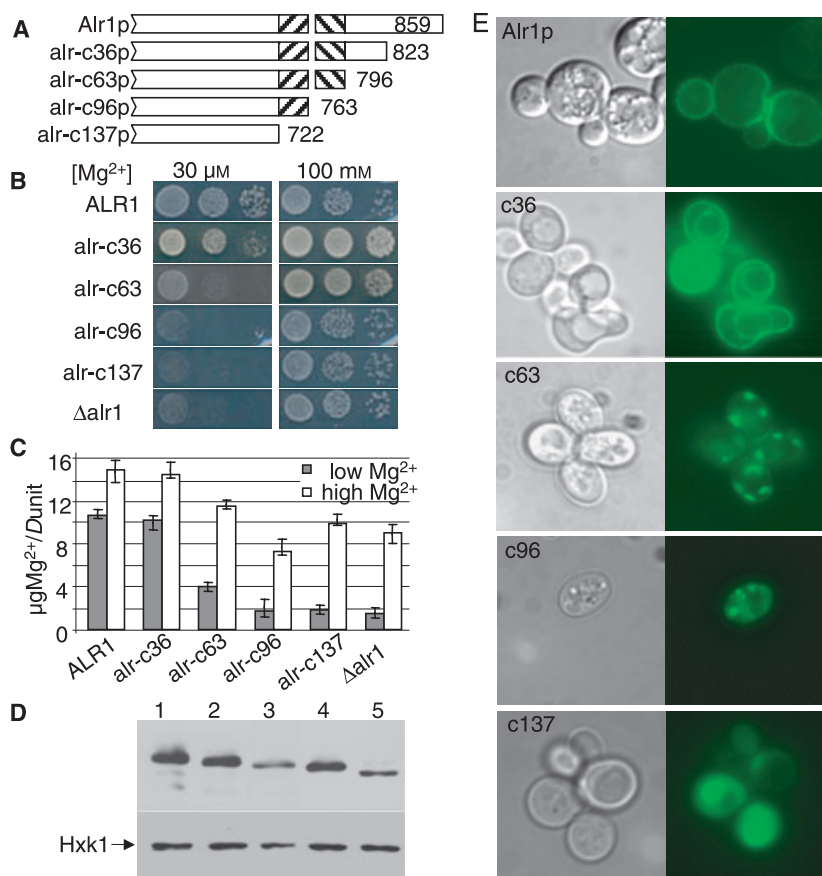
Fig. 8. Growth, localization, and Mg^{2+} content of Alr1p isomers. (A) Schematic illustration of C-terminally disrupted Alr1p. The length of molecules is indicated by the number of amino acids. Transmembrane domains are marked by hatched boxes. (B) Cells expressing *ALR1-HA* and truncated isomers *alr-c36-HA*, *alr-c63-HA*, *alr-c96-HA*, and *alr-c137-HA* were analyzed for their growth ability on synthetic SD medium containing 30 μM and 100 mM Mg^{2+}. Growth was monitored after 3 days at 28 °C. (C) The cellular free Mg^{2+} content of these cells was measured by the use of the indicator Eriochrome Blue. Therefore, the cells were incubated in synthetic SD medium with 30 μM or 100 mM Mg^{2+}, before the cells were prepared for the measurement (see Experimental procedures). Values given in the figure are the mean of at least three different measurements. (D) Protein concentration of cells expressing *ALR1* and c-terminally truncated isomers. Equal amounts of total protein were analyzed by SDS/PAGE (9% gel), immunoblotted, and Alr proteins were detected with HA antibody. Lanes 1–5, Alr1p, Alr-c36p, Alr-c63p, Alr-c96p, and Alr-c137. Detection of Hxk1p served as an internal loading control. (E) The subcellular localization of GFP-tagged proteins was analyzed by the use of UV/ differential interference contrast microscopy. JS74-A cells, expressing different *ALR1* alleles were incubated in low-Mg^{2+} medium 3 h before microscopical examination.

overexpressing or lacking Alr1p [14], and with reconstituted yeast wild-type and mutant mitochondrial Mrs2p in lipid vesicles [19]. Consistent with the proposed role of CorA and Mrs2p in constituting ion channels, they were shown by chemical cross-linking to form homo-oligomers in their cognate membranes [3,13]. Chemical cross-linking shown in this work also revealed the presence of Alr1p oligomers. A modified form of Alr1p, which we show to be due to phosphorylation, also appeared in oligomeric bands. The relatively large size and intrinsic instability of Alr1p prevented us from drawing final conclusions about the oligomerization state. However, bands corresponding

to dimers and most probably tetramers of the Alr1 monomer were detectable. Accordingly, homo-oligomerization appears to be a common feature of the CorA-Mrs2-Alr1 superfamily of proteins. Furthermore, during preparation of this paper, the crystal structure of the CorA protein of the bacterium *Thermotoga maritima* was published [20]. It reveals a homo-pentameric structure with two TM domains and both termini in the cytoplasm and the folding of the large N-terminal part into a large funnel-like structure with a potential binding site for Mg^{2+}.

As an independent approach to document protein–protein interaction, we used here the split-ubiquitin
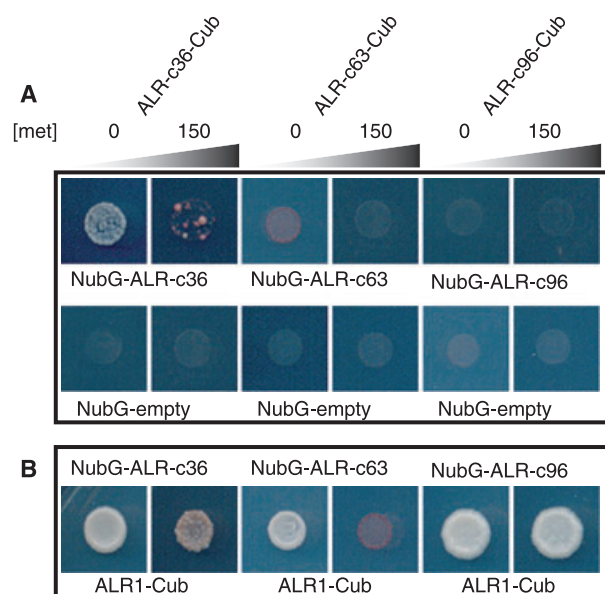
Fig. 9. Interaction of C-terminally truncated Alr1 isomers. (A) The constructs *alr-c36*, *alr-c63* and *alr-c96* were analyzed using the split-ubiquitin system. Cells expressing fusions of the respective proteins to NubG and Cub, as indicated in the figure, were grown on selective media containing 0 and 150 μM methionine (met). (B) NubG fusions of truncated Alr1p isomers (*alr-c36*, *alr-c63* and *alr-c96*) and full-length MetALR1-Cub were combined. Cellular growth mediated by protein–protein interaction was monitored after 3 days of incubation at 28 °C.

assay involving ubiquitin moieties, one ubiquitin moiety (NubG) added to the N-terminus and the other half (Cub) added to the C-terminus of Alr1 or Alr2. It revealed Alr1p–Alr1p, Alr2p–Alr2p homo-oligomeric as well as Alr1p–Alr2p hetero-oligomeric interactions. Accordingly, we conclude that both the N-terminus and C-terminus of Alr1 and Alr2 are in the same compartment, i.e. in the cytoplasm. A N-in, C-in orientation has previously also been concluded for the distant ortholog of Alr1p in mitochondria, Mrs2p [12,19].

Data from split-ubiquitin assays also imply that the N-terminus and C-terminus of a pair of interaction partners are sufficiently close to each other to allow reconstitution of functional ubiquitin. Given that Alr1 and Alr2 have very long N-terminal but short C-terminal extensions (742 and 62 amino acids, respectively) from their membrane parts, N-termini are likely to fold back to get close to the C-termini near the plasma membrane.

In contrast with Alr1p and the truncated construct lacking 36 amino acids at the C-terminus, C-terminally deleted versions of Alr1 missing 63, 96, and 137 amino acids were no longer able to homo-oligomerize. Surprisingly, the truncated isomer Alr-c63p was found to

still oligomerize with full-length (wild-type) Alr1p. We speculate that the C-terminal deletion affects the anchoring of the protein in the plasma membrane, leading to misplacement of the protein *per se*, but upstream sequences in Alr-c63p might achieve transient interactions with the correctly folded wild-type Alr1 protein.

Although Alr2p behaves similarly to Alr1p with respect to Mg^{2+}-dependent expression, Mg^{2+} sensitivity of RNA and protein content, and oligomerization, it apparently has low activity in mediating Mg^{2+} influx. The reduced expression of Alr2p, compared with Alr1p, had previously been invoked to explain this difference in activity. However, overexpression of *ALR2* only partially suppresses the *alr1Δ* growth phenotype, and moreover, provokes a negative effect on Alr1p-mediated Mg^{2+} uptake. This suggested that low Mg^{2+} transport activity is intrinsic to the Alr2p sequence and that its overexpression somehow reduces Alr1p function. In fact, we show here that a single amino-acid substitution, replacing an arginine residue with a glutamic acid residue in the loop connecting the two TM domains in Alr2p, accounts for most of the reduction in Mg^{2+}-transport activity. This glutamic acid residue at position +6 in the loop (relative to the GMN motif) is well conserved among bacterial CorA proteins and among mitochondrial Mrs2 proteins, where a second negatively charged or polar residue often follows it. About half of the available Alr1-related sequences of ascomycota also have the E residue at position +6, whereas the other half has a Q residue or another polar residue, but none of them has a positively charged residue at this position. Replacement of E-E by K-K residues, but not by D-D, in yeast Mrs2p dramatically reduces its ability to mediate Mg^{2+} uptake into mitochondria [19]. We propose a role for the negatively charged residue(s) in the TM-A–TM-B loop in attracting Mg^{2+} to the surface of the ion channel.

The observed dominant negative effect of Alr2p overexpression on Mg^{2+} uptake by Alr1p is likely to reflect abundant formation of Alr1p–Alr2p hetero-oligomers with reduced activity due to the presence of Alr2. Dominant negative effects were also exerted by the mutations L750V and S795R of the mutant alleles *alr1–1* and *alr1–31*, which are located in the first and second TM domain, respectively. The conservative mutation from L750V is likely to affect the flexibility and integrity of a predicted hydrophobic core [21], which is presumably critical for Mg^{2+} binding. The introduction of a positive charged amino acid in mutation S795R in the second TM domain is likely to alter the conformation of the transmembrane domain. Thus,

it remains possible that these amino-acid alterations influence the channel architecture of formed hetero-oligomers, when expressed in combination with the wild-type protein. Similarly, Lee & Gardner [22] observed dominant-negative effects by overexpression of other Alr1 mutant proteins along with the wild-type Alr1p and speculated that this effect might be due to the formation of hetero-oligomers of (defective) mutant and wild-type Alr1p.

According to the data presented here, Alr1 and Alr2 proteins also have two TM domains (not three as suggested previously for CorA), C-termini and N-termini oriented inside of the membrane and form oligomeric complexes. This confirms the phylogenetic relationship between CorA proteins of bacteria and Alr1-type proteins.

Experimental procedures

Strains, growth media and genetic procedures

Yeast strains were grown at 28 °C in YPD medium (yeast extract/peptone/glucose), standard SD medium (0.67% yeast nitrogen base, 2% glucose, and amino acids), or synthetic SD medium [23], supplemented with MgCl₂ where indicated. *Escherichia coli* strain DH10b (Invitrogen, Paisley, UK) was cultivated at 37 °C in Luria–Bertani medium supplemented with 150 μg·mL⁻¹ ampicillin when appropriate, and the following plasmids were used for subcloning: YEp351-HA [12], YIplac204, YCplac22, YCplac111 [15], and pUG23 [24]. For cloning of C-terminally truncated *ALR1* isomers, plasmid YEpM351-HA was constructed by the insertion of a *Sac*I/*Sal*I 449-bp fragment of pUG23, containing the p$_{\text{MET25}}$ sequence into the *Sac*I/*Sal*I-opened vector YEp351-HA. Genes *ALR1*, *alr-c36*, *alr-c63*, *alr-c96*, and *alr-c137* were amplified by PCR using primers listed in Table 1, and cloned via *Spe*I/*Sal*I into plasmid YEpM351-HA, using the same restriction sites. For fluorescence examinations, fragments containing the respective genes *ALR1*, *alr-c36*, *alr-c63*, *alr-c96*, and *alr-c137*, were subcloned as *Sac*I/*Bam*HI fragments into vector pUG23, opened by the same enzymes. *ALR2* was PCR amplified using primers ALR2-SacI-f and ALR2-PstI-r, listed in Table 1, and cloned via *Sac*I/*Pst*I into plasmid YEp351-HA, opened by the same enzymes. For fluorescence microscopy, the HA tag was exchanged by a 985-bp *Sal*I/*Xma*III fragment from pUG23, containing the GFP tag, resulting in plasmid YEpALR2-GFP. The plasmid YEp351-myc was created by the exchange of the 111-bp HA-tag-containing fragment via *Not*I restriction with the 366-bp myc-tag-containing fragment, originating from plasmid p3292 (laboratory stock), using the same restriction site.

Yeast strains JS74A (*ALR1*, *ALR2*) and JS74B (*alr1*Δ, *ALR2*) have been described previously [8]. To create

Table 1. Primers used in this study. Primers are listed in groups A (amplification of C-terminally truncated ALR1 isomers), B (*in vivo* cloning), C (disruption of *ALR2*), D (mutagenesis and cloning of *ALR2*), and E (RT-PCR). Restriction sites used for cloning are shown in italic.

Group	Primer	Sequence (5′– to 3′)
A	ALR1	AAAGCG*ACTAGT*CATTTTACCATG
	ALR-c36	TGTTTC*GTCGAC*GCAAGAAGCTCG
	ALR-c63	TTCT*GTCGAC*CCAATAGCTGG
	ALR-c96	ATTAATCCG*GTCGAC*TAACATTCATACC
	ALR-c137	TTAAA*GTCGAC*CTAAGTAGTTTGTATGG
	ALR1-revers	AAA*GTCGAC*TGTCGTAGCGGC
B	ALR1-SU5′	B1-linker-ATGTCATCATCCTCAAGTTC
	ALR1-SU3′	B2-linker-GTCGTAGCGGCTATATCTAC TAGG
	ALR2-SU5′	B1-linker-ATGTCGTCCTTATCC
	ALR2-SU3′	B2-linker-ATTGTAACGGCTATATCTACTGG
	ALR-c36SU3′	B2-linker-GGCAAGAAGCTCGAAATAACC
	ALR-c63SU3′	B2-linker-CCAATAGCTGGCCAAGAACC
	ALR-c96SU3′	B2-linker-ATTCATACCGAAAAGACC
C	ALR2-HIS-f	ATTTTTATGAGAAAACGTGAAAAAACTTC GTAATGTCGTCCTTATCGTACGCTGCA GGTCGAC
	ALR2-HIS-r	AAAGATCTGCCGACCTACCATAGCGGTC ATGTTAATTGTAACGGCATCGATGAATT CGAGCTCG
	ALR2-up	TTCGAAAAATGCAGCATT
	HIS3-r	TCTACAAAAGCCCTCCTACC
D	ALR2 mutR-Efor	CCAGGAGAGAATTCAAGTATTGC
	ALR2 mutR-Erev	GCAATACTTGAATTCTCTCCTGG
	ALR2-5′SacII-f	ATTGCAGTTGTCC
	ALR2-SalI-r	ATGCGGCCGC*GTCGAC*GATTGTAACG
	ALR2-SacI-f	TTTCTGCAG*GAGCTC*GAAAAATGCA GCATTTGG
	ALR2-PstI-r	AAA*CTGCAG*GATTGTAACGGCTATAT CTAC
E	Alr1-rtp	CAGGGTATGGATGAAACGGTTGC
	Alr1-rtm	TGATCCCGAAGTGGAAGTAGAGC
	Alr2-rtp	TTAAGTTCTAATGCGAGGCCATCC
	Alr2-rtm	TTCGTTCACTGTGCCTTTGATGG
	ACT1_plus	ACCAAGAGAGGTATCTTGACTTTACG
	ACT1_minus	GACATCGACATCACACTTCATGATGG

strains AG02 and AG012 (*alr1*Δ, *alr2*Δ), a disruption cassette was amplified, using the pFA6a-His3MX6 cassette [25], and oligonucleotide primers ALR2-HIS-f and ALR2-HIS-r (listed in Table 1) of sequences flanking the *ALR2* (*YFL050c*) gene. The PCR product was transformed into yeast strains FY 1679 (EUROSCARF) and JS74B, and His + colonies were selected. Correct insertion of the cassette was verified by PCR analysis using primers ALR2-up in combination with HIS3-r, resulting in a 770-bp fragment indicating correct insertion of the *HIS3* gene at the *ALR2* locus (data not shown). Strains THY.AP4 and THY.AP5, as well as plasmids pMetYCgate and pN-Xgate, used for *in vivo* cloning, and the cloning of

PCR products by recombinational *in vivo* cloning have been described elsewhere [26].

Random plasmid mutagenesis with hydroxylamine hydrochloride

Purified plasmid DNA was incubated in hydroxylamine hydrochloride solution (70 mg·mL^{-1} hydroxylamine hydrochloride, 18 mg·mL^{-1} NaOH) for 6 h at 37 °C. The reaction was quenched by the addition of NaCl (100 mM) and 0.1 mg·mL^{-1} BSA. DNA was recovered by precipitation with ethanol and transformed into yeast strain JS74B. Cells were grown on standard SD-Trp supplemented with 100 mM MgCl$_2$. Colonies dependent on Mg^{2+} for growth were screened upon replica plating on the same media and nominally Mg^{2+}-free medium. Relevant plasmids were recovered, and the *ALR1-HA* fusion genes were subcloned into the empty vector YCplac22 via *Sac*I/*Hin*DIII fragments, to exclude plasmid-based alterations of gene expression.

PCR-mediated site-directed mutagenesis of ALR2

A two-step PCR reaction involving mutagenic primers ALR2mutR-Efor and ALR2mutR-Erev plus primers ALR2-5′SacII-f and ALR2-SalI-r resulted in a PCR product with the R768E substitution. This PCR product was cleaved with *Sac*II/*Sal*I and cloned as a 1141-bp fragment into the *Sac*II/*Sal*I-opened vectors YCpALR2-HA and YEpALR2-HA, resulting in plasmids YCpALR2$_{R768E}$-HA and YEpALR2$_{R768E}$-HA.

Interaction tests with the split-ubiquitin assay

ALR1, *alr-c36*, *alr-c63*, *alr-c96* and *ALR2* alleles were amplified by standard PCR procedures using gene-specific forward primers (Table 1) flanked by a B1-linker (acaag tttgtacaaaaaagcaggctctccaaccaccATGxxx-5′-strand cDNA) and gene-specific reverse primers (Table 1) flanked by a B2-linker (tccgccaccaccaaccactttgtacaagaaagctgggtaxxx-3′-strand cDNA deleting the stop codon). The vectors pMetY-Cgate and pN-Xgate, yeast strains THY.AP4 and THY.AP5 and the cloning of PCR products by recombinational *in vivo* cloning have been previously described [27]. NubG fusions were constructed by cleaving the split ubiquitin vector pN-Xgate with *Eco*RI/*Sma*I, which was used with the appropriate PCR products to transform strain THY.AP5. Transformants were selected on SD medium lacking tryptophan and uracil. For Cub fusions, the vector pMetY-Cgate was cleaved with *Pst*I/*Hind*III and used with the appropriate PCR products to transform yeast strain THY.AP4. Transformants were selected on SD medium lacking leucine. Several clones from each THY.AP5 and THY.AP4 transformation were incubated in appropriate

SD medium with and without G418. Plasmids with resulting NubG-X and MetY-Cub constructs were re-isolated, amplified in *E. coli*, and controlled for the correct inserts. They were again transformed into strains THY.AP5 or THY.AP4, respectively, and used for subsequent interaction assays. Plasmids containing the constructs Kat1-NubG, MetKat1-Cub, and NubG-Suc2 were kindly provided by P. Obrdlik (Universität Tübingen, Germany).

Interaction assay

Stationary yeast cultures were harvested and resuspended in YPD. The strains THY.AP4 and THY.AP5, transformed with the relevant plasmids, were mated by plating on YPD. After 6–8 h at 28 °C, cells were selected for diploids by replica plating on standard SD medium-Leu/Trp/Ura, and incubated at 28 °C for 2–3 days. For growth assays, diploid cells were replica plated on SD minimal medium with or without methionine (0 mM, 0.15 mM). Growth was monitored for 2–4 days.

Analysis of cellular free Mg^{2+} content

Cellular free Mg^{2+} was measured spectrophotometrically by the use of Eriochrome Blue (Sigma-Aldrich Handels GmbH, Vienna, Austria). Cells were grown in synthetic SD medium supplemented with 100 mM Mg^{2+}. The cells were harvested and washed three times in SD medium lacking Mg^{2+} and further incubated with or without the addition of Mg^{2+}. After an incubation period of 16 h, the cells were harvested and washed by centrifugation at 4 °C twice with high performance liquid chromatography (HPLC) grade water (Pierce, Vienna, Austria), Eriochrome Blue/buffer (0.1 M KCl, 10 mM Pipes, pH 7.0), 1 mM EDTA to remove extracellular bivalent cations and then with Eriochrome Blue/buffer to remove EDTA. Cells were resuspended to an D_{600} of 0.9–1.0 and treated with 10 μg·μL^{-1} digitonin at room temperature for 1 h. Cells were pelleted, and the supernatants were taken for Mg^{2+} determination using a Hitachi U-2000 photometer measuring the difference in absorbance at 592 nm and 554 nm calibrated against increasing Mg^{2+} concentrations.

Phosphatase assay

Cells were grown in synthetic SD medium with low Mg^{2+} content (25 μM) to support high Alr1 protein stability. The cells were resuspended (1 g wet weight·mL^{-1}) in buffer A (25 mM Hepes, pH 8.2, 5 mM EDTA, pH 8.0, 1 mM phenylmethanesulfonyl fluoride) and disrupted by vortex-mixing for 6 min with permanent cooling, using acid-washed glass beads (0.45–0.6 μM). From the supernatant, unbroken cells were removed by low-speed centrifugation and further treated with buffer B (10 mM Hepes, pH 7.5, 0.2 mM

EDTA, pH 8.0, 0.5 mM phenylmethanesulfonyl fluoride) by vortex-mixing for a further 2 min. The supernatants were combined and centrifuged for 20 min at 20 000 *g*. The crude membrane pellet was resuspended in buffer C (10 mM Hepes, pH 7.5, 0.2 mM EDTA, pH 8.0, 0.5 mM phenyl-methanesulfonyl fluoride, 20% glycerol). The solution was loaded on a discontinuous sucrose gradient (25/43/53%) and centrifuged in an SW40Ti rotor at 100 000 *g* for 90 min. The interphase between 43% and 53% sucrose was recovered, diluted 4 times in ice-cold double distilled water and centrifuged again at 20 000 *g* for 20 min. The pellet was resuspended in 10 mM Hepes, pH 7.4. The membrane fraction was used for treatment with lambda phosphatase (λPP; New England Biolabs, Ipswich, MA). With the use of 0, 200, and 400 units of λPP, the samples were incubated for 30 min at 30 °C. The reactions were stopped with the addition of Laemmli buffer at 65 °C. The phosphoryla-tion status of equal amounts of the protein was analyzed on a 10% polyacrylamide/SDS gel followed by immuno-blotting.

Chemical cross-linking

Identical membrane fractions as for the phosphatase assay were used for chemical cross-linking of proteins. Protein (20 µg) was incubated with or without the homo-bifunc-tional cross-linking reagents *o*-phenylenedimaleimide (3, 30, and 300 µM final concentration) or 1,6-bismaleimidohexane (50, 100, 500, and 1000 µM final concentration) for 30 min on ice in 10 mM Hepes, pH 7.4. The reactions were stopped by the addition of *N*-ethylmaleimic acid (1 mg·mL^{-1}) for 10 min on ice. SDS loading buffer containing 2-mercapto-ethanol was added and samples were heated to 65 °C for 5 min before loading on SDS/polyacrylamide gels. Alr1-HA protein-containing bands were visualized by use of an anti-HA serum.

Microscopy

GFP fluorescence was analyzed with a Zeiss Axioplan UV microscope (Carl Zeiss, Oberkochen, Germany) using the METAVUE Software (Universal Imaging Corp., Downington, PA). Before microscopic examination, cells were grown in medium limited for Mg^{2+}.

Antibodies

The antibodies used in this study were mouse anti-HA [12], rabbit anti-Hxk1p (Biotrend, Kölu, Germany) and anti-myc (kindly provided by G. Adam, Zentrum für Angewandte Genetik, Universität für Bodenkultur, Vienna, Austria); and horseradish peroxidase-conjugated goat anti-mouse IgG and horseradish peroxidase-conjugated goat anti-rabbit IgG (Promega, Mannheim, Germany).

Miscellaneous

Sequencing of DNA was performed by the Automated DNA Sequencing Service at VBC-Genomics. Immunodetec-tion (Pierce SuperSignal West Pico chemiluminescent sub-strate) was performed according to the manufacturer's protocols. ICP-MS measurement was performed at ARC-Seiberdorf.

References

1 Kehres DG, Lawyer CH & Maguire ME (1998) The CorA magnesium transporter gene family. *Microb Comp Genomics* **3**, 151–169.

2 Gardner RC (2003) Genes for magnesium transport. *Curr Opin Plant Biol* **6**, 263–267.

3 Kolisek M, Zsurka G, Samaj J, Weghuber J, Schweyen RJ & Schweigel M (2003) Mrs2p is an essential compo-nent of the major electrophoretic Mg^{2+} influx system in mitochondria. *EMBO J* **22**, 1235–1244.

4 Zsurka G, Gregan J & Schweyen RJ (2001) The human mitochondrial Mrs2 protein functionally substitutes for its yeast homologue, a candidate magnesium transpor-ter. *Genomics* **72**, 158–168.

5 Li L, Tutone AF, Drummond RS, Gardner RC & Luan S (2001) A novel family of magnesium transport genes in *Arabidopsis*. *Plant Cell* **13**, 2761–2775.

6 Schock I, Gregan J, Steinhauser S, Schweyen R, Bren-nicke A & Knoop V (2000) A member of a novel *Arabi-dopsis thaliana* gene family of candidate Mg^{2+} ion transporters complements a yeast mitochondrial group II intron-splicing mutant. *Plant J* **24**, 489–501.

7 MacDiarmid CW & Gardner RC (1998) Overexpression of the Saccharomyces cerevisiae magnesium transport system confers resistance to aluminum ion. *J Biol Chem* **273**, 1727–1732.

8 Graschopf A, Stadler JA, Hoellerer MK, Eder S, Sieg-hardt M, Kohlwein SD & Schweyen RJ (2001) The yeast plasma membrane protein Alr1 controls Mg^{2+} homeostasis and is subject to Mg^{2+}-dependent control of its synthesis and degradation. *J Biol Chem* **276**, 16216–16222.

9 Voets T, Nilius B, Hoefs S, van der Kemp AW, Droogmans G, Bindels RJ & Hoenderop JG (2004) TRPM6 forms the Mg^{2+} influx channel involved in

intestinal and renal Mg^{2+} absorption. *J Biol Chem* **279**, 19–25.

10 Schmitz C, Dorovkov MV, Zhao X, Davenport BJ, Ryazanov AG & Perraud AL (2005) The channel kinases TRPM6 and TRPM7 are functionally non-redundant. *J Biol Chem* **280**, 37763–37771.

11 Knoop V, Groth-Malonek M, Gebert M, Eifler K & Weyand K (2005) Transport of magnesium and other divalent cations: evolution of the 2-TM-GxN proteins in the MIT superfamily. *Mol Genet Genomics* **274**, 205–216.

12 Bui DM, Gregan J, Jarosch E, Ragnini A & Schweyen RJ (1999) The bacterial magnesium transporter CorA can functionally substitute for its putative homologue Mrs2p in the yeast inner mitochondrial membrane. *J Biol Chem* **274**, 20438–20443.

13 Warren MA, Kucharski LM, Veenstra A, Shi L, Grulich PF & Maguire ME (2004) The CorA Mg^{2+} transporter is a homotetramer. *J Bacteriol* **186**, 4605–4612.

14 Liu GJ, Martin DK, Gardner RC & Ryan PR (2002) Large Mg(2+)-dependent currents are associated with the increased expression of ALR1 in *Saccharomyces cerevisiae*. *FEMS Microbiol Lett* **213**, 231–237.

15 Gietz RD & Sugino A (1988) New yeast-*Escherichia coli* shuttle vectors constructed with in vitro mutagenized yeast genes lacking six-base pair restriction sites. *Gene* **74**, 527–534.

16 Stagljar I, Korostensky C, Johnsson N & te Heesen S (1998) A genetic system based on split-ubiquitin for the analysis of interactions between membrane proteins *in vivo*. *Proc Natl Acad Sci USA* **95**, 5187–5192.

17 Reinders A, Schulze W, Kuhn C, Barker L, Schulz A, Ward JM & Frommer WB (2002) Protein–protein interactions between sucrose transporters of different affinities colocalized in the same enucleate sieve element. *Plant Cell* **14**, 1567–1577.

18 Szegedy MA & Maguire ME (1999) The CorA Mg(2+) transport protein of *Salmonella typhimurium*. Mutagenesis of conserved residues in the second membrane domain. *J Biol Chem* **274**, 36973–36979.

19 Weghuber J, Dieterich F, Froschauer EM, Svidova S & Schweyen RJ (2006) Mutational analysis of functional domains in Mrs2p, the mitochondrial Mg channel protein of *Saccharomyces cerevisiae*. *FEBS J* **273**, 1198–1209.

20 Lunin VV, Dobrovetsky E, Khutoreskaya G, Zhang R, Joachimiak A, Doyle DA, Bochkarev A, Maguire ME, Edwards AM & Koth CM (2006) Crystal structure of the CorA Mg^{2+} transporter. *Nature* **440**, 833–837.

21 Kern AL, Bonatto D, Dias JF, Yoneama ML, Brendel M & Pegas Henriques JA (2005) The function of Alr1p of *Saccharomyces cerevisiae* in cadmium detoxification: insights from phylogenetic studies and particle-induced X-ray emission. *Biometals* **18**, 31–41.

22 Lee JM & Gardner RC (2006) Residues of the yeast ALR1 protein that are critical for magnesium uptake. *Curr Genet* **49**, 7–20.

23 Sherman F (1991) Getting started with yeast. *Methods Enzymol* **194**, 3–21.

24 Niedenthal RK, Riles L, Johnston M & Hegemann JH (1996) Green fluorescent protein as a marker for gene expression and subcellular localization in budding yeast. *Yeast* **12**, 773–786.

25 Longtine MS, McKenzie A, 3rd Demarini DJ, Shah NG, Wach A Brachat A, Philippsen P & Pringle JR (1998) Additional modules for versatile and economical PCR-based gene deletion and modification in *Saccharomyces cerevisiae*. *Yeast* **14**, 953–961.

26 Ludewig U, Wilken S, Wu B, Jost W, Obrdlik P, El Bakkoury M, Marini AM, Andre B, Hamacher T, Boles E, *et al.* (2003) Homo- and hetero-oligomerization of ammonium transporter-1 NH4 uniporters. *J Biol Chem.* **278**, 45603–45610.

27 Obrdlik P, El-Bakkoury M, Hamacher T, Cappellaro C, Vilarino C, Fleischer C, Ellerbrok H, Kamuzinzi R, Ledent V, Blaudez D, *et al.* (2004) K$^+$ channel interactions detected by a genetic system optimized for systematic studies of membrane protein interactions. *Proc Natl Acad Sci USA* **101**, 12242–12247.

5.2. Publication II

Wachek M., Schweyen R., and Graschopf A.

An internal α-helix and sequence motifs are essential for vesicular transport and turnover of the plasma membrane Mg2+ transporter Alr1p.

Submitted

An internal α-helix and sequence motifs are essential for vesicular transport and turnover of the plasma membrane Mg^{2+} transporter Alr1p

Marcin Wachek[1], Rudolf Schweyen[1], and Anton Graschopf[1*]

1) Max F. Perutz Laboratories, Department of Genetics, University of Vienna, A-1030 Vienna, Austria,

* corresponding author: Anton Graschopf, Department of Genetics, University of Vienna, A-1030 Vienna, Dr. Bohr-Gasse, Austria, Tel. +43-1-4277-74538; Fax. +43-1-4277-9546; EMail: anton.graschopf@univie.ac.at

Running Title: Alr1p signal for secretory pathway

Keywords: ER-to-Golgi transport, α-helical signal sequence, Alr1p protein recycling, mutational analysis

ABSTRACT

Fungal Alr1 proteins differ from other members of the CorA-superfamily of magnesium transporters by a long N-terminal extension. We speculate that this sequence may be important for Alr1p translocation to the plasma membrane or its rapid removal from this membrane followed by vacuolar degradation in the presence of high Mg^{2+} concentrations. Deletions in the Alr1p N-terminus revealed motifs essential for translocation of the protein to the plasma membrane, its stability and degradation. Translocation is dependent on an α-helix, spanning amino acids E293 to L312 with some primary sequence conservation and a well conserved motif shortly upstream. Deletion or mutation of the α-helix, impeded anterograde protein translocation to the plasma membrane and proteins missing or modified in this particular sequence accumulated in punctuated structures, putatively of the ER-to-Golgi transport, and were rapidly degraded via the proteasome. Addition of this α-helical region to GFP made this protein enter punctuated structure, putatively of the secretory pathway. Truncation of sequences N-terminal to the putative secretory pathway signal strongly impaired Mg^{2+}-dependent Alr1p phosphorylation and stability, but did not fully prevent their translocation to the plasma membrane. We regard the conserved α-helical region in Alr1 proteins as a unique signal sequence for ER-to-Golgi transport.

INTRODUCTION

Alternating environmental conditions permanently force cells to adapt membranes to assure a controlled uptake of nutrients, influx and efflux of ions and other substrates. The coaction of secretory and endocytic pathways allows the selective trafficking of channels, transporters, receptor proteins and sensors to different cellular compartments, providing a balanced number of proteins at their appropriate positions.

Before a protein is released to other compartments, several ER quality control (QC) mechanisms proof its native conformation. The coaction of the unfolded protein response, activating retention and retrieval mechanisms, in concert with ER associated degradation have been implicated in selecting and sorting misfolded proteins for degradation (Brodsky and McCracken, 1999; Ferreira *et al.*, 2002; Jarosch *et al.*, 2002). ER export is mediated by vesicles (Schekman and Orci, 1996). Coat protein complex I (COPI) and COPII are believed to confer anterograde and retrograde transport of protein between the ER and the trans Golgi network (TGN) (Schekman and Orci, 1996; Stephens *et al.*, 2000). In addition, export signals or motifs are described, promoting export of native proteins from the ER (Ma *et al.*, 2001; Stockklausner *et al.*, 2001; Ma and Jan, 2002). ER retention an retrieval signals of many membrane-spanning proteins have been described previously to be constituted by short primary sequence motifs in intracellular regions at or near the C-terminus (Barlowe, 2003). These motifs may be bipartite, governing ER export and transport to the Golgi and beyond (Farhan *et al.*, 2004; Farhan *et al.*, 2008a). The GABA transporter 1 (SLC6A1) has been reported to have two adjacent N-terminal motifs, one for ER release and another one for export from the ER-Golgi intermediate compartment (ERGIC) (Farhan *et al.*, 2008b). Several more protein trafficking pathways are known from the late Golgi to the vacuole.

Protein Alr1p constitutes the major magnesium uptake system in the plasma membrane of the yeast *Saccharomyces cerevisiae* (MacDiarmid and Gardner, 1998; Graschopf *et al.*, 2001). Like a large number of plasma membrane transporters and channels, e.g. Itr1p, Smf1p, Zrt1p (Lai *et al.*, 1995; Liu and Culotta, 1999; Gitan and Eide, 2000), Alr1p levels are subject to tight posttranslational control. Removal of Alr1p from the plasma membrane starts at elevated Mg^{2+} concentrations that trigger substrate phosphorylation and specific endocytosis, followed by internalization and transport to the vacuole for subsequent

degradation. This process of Alr1p turnover is highly specific to Mg^{2+} (Graschopf *et al.*, 2001).

Proteins closely related to Alr1p are found in all fungal genomes sequenced and in some protozoal genomes. Alr1 proteins belong to the CorA superfamily of Mg^{2+} transporters, which are ubiquitous in archaea and bacteria. Most eukaryotic genomes contain another CorA-related protein subfamily called Mrs2 which form Mg^{2+} channels of mitochondria and which in plants also reside in other membranes (Li *et al.*, 2001; Gardner, 2003; Kolisek *et al.*, 2003; Schindl *et al.*, 2007; Piskacek *et al.*, 2008). A common feature of the CorA-related proteins is a conserved Gly-Met-Asn motif at the end of a transmembrane domain near the C-terminus. The crystal structure of the CorA protein of *Thermatoga maritima* revealed the presence of two transmembrane domains (TMD) of which the N-terminal one forms a cation pore in a homo-pentameric CorA-complex. A short C-terminal and a long N-terminal stretch both are oriented towards the bacterial cytoplasm (Eshaghi *et al.*, 2006; Lunin, 2006; Maguire, 2006). Split ubiquitin assays and cross-linking experiments (Wachek *et al.*, 2006), indicated that yeast Alr1p, like CorA and Mrs2 proteins, contains two membrane spanning domains and that both, the N- and the C-terminal sequences protrude into the cytoplasm. Secondary structure features in sequences N-terminal to the TMDs further underline homology between bacterial CorA and eukaryotic Mrs2 and Alr1 proteins (Lunin, 2006). Unique among Alr1 proteins are additional nearly 300 residues long sequences of low complexity N-terminal to the CorA-homology regions. Deletion of as much as 240 N-terminal residues of this unique sequence in yeast did not abolish Mg^{2+} transport (Lee and Gardner, 2006).

In this report, we investigated possible roles of the unique N-terminal sequences of the yeast Alr1p. Truncations in this sequence interfered with Alr1p translocation to the plasma membrane and, dependent on the partial sequences deleted, led to Alr1p entrapment in vesicles and to rapid degradation independent of the environmental Mg^{2+} concentration. A critical region towards the end of the sequence unique to Alr1 proteins is shown to decide whether Alr1p is translocated to the plasma membrane. Features of this sequence are an α-helical stretch surrounded by moderately conserved sequence motifs in Alr1-type proteins.

Strains, plasmids and growth conditions

Escherichia coli strain DH10b (Invitrogen, Paisley, UK) was cultivated at 37 °C in Luria-Bertani medium supplemented with 150 µg·mL^{-1} ampicillin when appropriate. Yeast strains were grown at 28 °C in YPD medium (1% yeast extract, 2% peptone, 2% dextrose), standard SD medium (0.67% yeast nitrogen base, 2% glucose, and amino acids), or synthetic SD medium (Sherman, 1991), supplemented with Mg^{2+} when indicated. The following yeast strains were used JS74A (*ALR1, ALR2*), AG012 (*alr1Δ, alr2Δ*) (Wachek *et al.*, 2006), BY4742 (Brachmann *et al.*, 1998) and BY*pep12Δ* [EUROSCARF]. For subcloning, plasmids YEp351HA (Bui *et al.*, 1999), YIplac204, YCplac22 (Gietz and Sugino, 1988) pUG34 and pUG23 (Niedenthal *et al.*, 1996) were used.

Plasmid constructions

Plasmid YEpM351HA was generated by subcloning a 449 bp *Sac*I/*Sal*I fragment of plasmid pUG23, containing the p_{Met25}, into the *Sac*I/*Sal*I opened vector YEp351-HA. The different *ALR1*-constructs (Fig. 1), amplified via PCR using YEpALR1-HA (Graschopf *et al.*, 2001) as a template and the used primers are listed in Table 1, supplementary data. The resulting PCR fragments were cleaved with *Spe*I and *Sal*I and ligated into the *Spe*I / *Sal*I opened plasmid YEpM351-HA. The various p_{Met25}-ALR1-HA constructs were further subcloned as *Sac*I / *Hin*DIII fragments into the *Sac*I / *Hin*DIII opened vector YIplac204 creating YIpMALR1-constructs (cf. Table 1A, supplementary data).

To create ALR1-GFP fusion constructs, gene sequences as cloned into YEpM351-HA were subcloned as *Sac*I / *Bam*HI fragments into the GFP-fusion vector pUG23, creating thereby plasmids pUG23ALR1, pUG23ALR1-n128, pUG23ALR1-n155, pUG23ALR1-n204, pUG23ALR1-n277, pUG23ALR1-n485, pUG23ALR1-M9, pUG23ALR1-M11, pUG23ALR1-P1M11, and pUG23ALR1-P3M11.

For preparation of "module deletions", a two-step PCR amplification procedure was performed. First, both sequences flanking the deletion were amplified using primers listed in Table 1B (supplementary data; Modules), introducing thereby *Eco*RI restriction sites. Then 5´ and 3´ components of each *ALR1* module were digested with *Eco*RI, ligated and used as a template for the second PCR reaction using flanking primers. The resulting PCR products were digested with enzymes *Rsr*II / *Cla*I and subcloned into plasmid

YCp22ALR1-HA, deleted for the original *Rsr*II / *Cla*I fragment (1565 bp), thereby creating plasmids YCp22ALR M1, - M2, - M3, - M5, - M6, - M7, - M8, - M9, - M1-9, - M11, - M12 and - M13 (Fig. 1 and Table 1B, supplementary data). To obtain GFP-tagged *ALR1* constructs, identical *Rsr*II / *Cla*I fragments were used to exchange the original fragment in plasmid pUG23ALR1GFP (Table 1, supplementary data). A scheme of all constructs used is given in Figure 1.

Amino acid substitutions in modules M9 and M11 were produced similarly to the module deletions flanking and mutagenic primers listed in Table 1B (supplementary data), except that the mutated overlapping sequence was used as a megaprimer before the second round of PCR was started.

Plasmid pUG34M11 was created by cloning of a 96bp PCR fragment, synthesized with primers m9f-BamHI and m12rEco+Stop (Table 1B, supplementary data), into pUG34GFP opened with enzymes *Bam*HI / *Eco*RI.

Analysis of cellular free Mg^{2+} content

Cellular free Mg^{2+} was measured spectrophotometrically by the use of Eriochrome Blue as described in Wachek et *al*., 2006.

Protein preparation and western blotting analysis

Cells with plasmids bearing wild type and *NH$_2$*-terminal mutants of Alr1 protein under native or methionine promoter were grown to saturation in synthetic liquid SD medium containing 100 mM Mg^{2+} to support equal growth of all constructs. Over night cultures were washed 3-times with ddH$_2$O and incubated in medium supplemented with 25 μM Mg^{2+} for 3.5 hours. Appropriate aliquots were simultaneously incubated with 0, 1, 10 and 100 mM Mg^{2+} and 100 μg·mL^{-1} cycloheximide (CHX) to stop further translation. For protein preparation, cells were harvested after the given time-points, washed twice in ice-cold 1 mM EDTA to complex cations and once in HPLC-grade water to remove EDTA. Total protein extracts were prepared by lysis in 2N NaOH and 1.25% β-mercaptoethanol for 10 minutes. Proteins were precipitated with trichloroacetic acid (25% final concentration) for at least 60 minutes. Precipitated proteins were washed with acetone and dissolved by boiling in 5% SDS for 5 minutes. Protein concentrations were measured using the Bio-Rad DC Protein Assay Kit according to the manufacturer's protocol. Equal amounts of proteins were separated on 8% or 10% SDS-polyacrylamide gels, blotted and

incubated with an anti-HA (Bui *et al.*, 1999) and rabbit anti-Hxk1p (Biotrend, Köln, Germany). As a secondary antibody either horseradish peroxidase-conjugated goat anti-mouse IgG or horseradish peroxidase-conjugated goat anti-rabbit IgG (Promega, Mannheim, Germany) was used. For immunodetection SuperSignal West Pico and SuperSignal Femto Maximum Sensitivity chemiluminescent substrates from Pierce were used. The membranes were exposed to AGFA CRONEX 5 X-Ray medical film and developed with AGFA Curix 60 Developer.

Fluorescence microscopy

To prepare cells for microscopical examination, cells were grown in Mg^{2+}-depleted medium for at least 3 hours. The subcellular localization and distribution of the protein was either determined after preincubation in medium limited for Mg^{2+} or when subsequently exposed to high external Mg^{2+}. GFP fluorescence was analyzed with a Zeiss Axioplan UV microscope (Carl Zeiss, Oberkochen, Germany) using the METAVUE Software (Universal Imaging Corp., Downington, PA). For FM4-64 staining of the yeast vacuole, the lipophilic dye was added to a final concentration of 30 µg/µl to the cell suspension and pulse labeled for 30 minutes. GFP and FM4-46 fluorescence were visualized together after an appropriate chase.

RESULTS

The NH$_2$-terminal domain of Alr1p has a minor influence on Mg^{2+} uptake

Conserved features of CorA-related proteins are two adjacent transmembrane domains (TM1, TM2) near the C-terminus and a GMN motif at the end of TM1 (Bui *et al.*, 1999; Knoop *et al.*, 2005). The short sequence connecting TM1, the pore forming domain, and TM2 only appears to be on the outside of the membrane (Wachek *et al.*, 2006). N-terminal to TM1 follows a series of conserved α-helices and β-sheets (Lunin, 2006). Additional sequences of various lengths may follow at the very N-terminus. These sequences are particularly long in proteins of the Alr1 subfamily of CorA-related proteins, which constitute the major Mg^{2+} transporter in the plasma membrane of lower eukaryotes (MacDiarmid and Gardner, 1998; Graschopf *et al.*, 2001). Recently, Lee and Gardner (Lee and Gardner, 2006) published that deletions up to 239 aa at the N-terminus of Alr1p, do not abolish Mg^{2+}-uptake.

Interested in the vesicular transport, stability and endocytosis of the Alr1 protein, we constructed several N-terminally truncated *ALR1* alleles, to investigate their effect on the protein fate (cf. Table 3, supplementary data). As novel start codons, internal methionine codons were used, except for mutant *alr1-n204*, where Leu$_{204}$ was converted to Met$_{204}$ (Figure 1). The resulting constructs, cloned into YIplac204 (ALR1HA-wt, alr1-n128, alr1-n155, alr1-n204, alr1-n277 and alr1-n485, expressed under the met promoter (cf. Table 1A, supplementary data) were integrated into strain AG012 (*alr1Δ, alr2Δ*) (Wachek *et al.*, 2006) and tested for their ability to suppress its Mg^{2+} dependent growth phenotype. Before and throughout the experiment, constant growth of cells carrying the different *ALR1* alleles was maintained in media containing 50 mM Mg^{2+}. Reduction of the Mg^{2+} content to 1.5 mM, 100 μM, and 25 μM revealed wild-type growth rates for cells carrying alleles *alr1-n128*, *alr1-n155* and *alr1-n204*. Clones expressing alleles *alr1-n277* and *alr1-n485* supported only poor or no growth in these media, respectively (Figure 2A). Expression of truncated proteins was confirmed by immunoblotting equal amounts of total protein by the use of a HA-antibody (Figure 2B).

Intracellular free Mg^{2+} contents were determined by the use of Eriochrome Blue as a fluorescence indicator (Figure 2C). All constructs except allele *alr1-n485* and the *alr1Δ alr2Δ* mutant strain showed comparable Mg^{2+} contents at both, limiting (30 μM) and high

(50 mM) Mg^{2+} growth conditions. AG012 (*alr1Δ alr2Δ*) and AG012 expressing isomer *alr1-n485* showed Mg^{2+} contents about 5 times lower than those of wild-type in media with low Mg^{2+} supplementation while their contents were only moderately reduced when grown in media with high Mg^{2+} supplementation. Surprisingly, the Mg^{2+} content of cells expressing *alr1-n277* showed no reduction compared to the wild type protein, although their growth rate was severely reduced in medium limited for Mg^{2+}. This observation strongly indicates that the N-terminal 277 aa of Alr1p are dispensable for cellular Mg^{2+} import in *Saccharomyces cerevisiae*, but not for normal growth. This suggested that the absence of the very N-terminus of Alr1p disturbed some other function than Mg^{2+} homeostasis.

The NH$_2$-terminus of Alr1p bears motifs to control Alr1p stability

Retention of Alr1p depends on the Mg^{2+} concentration in the medium. Increasing Mg^{2+} contents induce Alr1p phosphorylation, endocytosis and delivery to the vacuole for degradation (Graschopf *et al.*, 2001; Wachek *et al.*, 2006). To determine protein stability of the N-terminally truncated Alr1 proteins, wild-type and mutant cells were grown in media supplemented with 50 mM Mg^{2+} to support homogenous growth of all cells. To avoid Mg^{2+} dependent protein degradation of Alr1p prior to the assay, the cells were washed and further cultivated in methionine-free SD medium containing 25 μM Mg^{2+}. Alr1p synthesis was thus allowed to proceed for 3.5 hours. Then cells were transferred to SD media with 0, 1, 10 or 100 mM Mg^{2+} and 100 μg·mL^{-1} cycloheximide, preventing further protein synthesis. Aliquots of the samples were withdrawn after 0, 30, 90 and 180 minutes and proteins were extracted, separated on SDS-polyacrylamide gel and immunoblotted to observe the fate of Alr1p.

Results obtained for Alr1p wild-type protein (Figure 3A) are comparable with our previous studies (Graschopf *et al.*, 2001; Wachek *et al.*, 2006). At limiting Mg^{2+} concentration (nominally Mg^{2+} free, actually about 25 μM), Alr1p was stable for 180 min. After exposure to increasing Mg^{2+} concentrations (1, 10 or 100 mM), variants with slightly lower mobility due to hyperphosphorylation (Wachek *et al.*, 2006) appeared within 30 to 90 min, and the protein was completely degraded within 180 min. Compared to wild-type Alr1p, the degradation patterns of the truncated Alr1 isomers were all affected, but to different degrees (Figure 3A). Whereas the mobility shift and subsequent degradation of isomer

Alr1-n128 were only slightly reduced, mobility shifts of proteins Alr1-n155 and Alr1-n204 were much less pronounced and their degradation was significantly reduced. Isomer Alr1-n277 showed no mobility shift and its stability remained unaffected throughout the experiment. This correlates with the fact that Alr277p lacked 11 of 13 potential phosphorylation sites of full length Alr1p (http://www.expasy.org/uniprot/Q08269). Its apparent absence from the plasma membrane and its high stability is at variance with the above mentioned findings of residual complementation of the *alr1Δ* phenotype and restoration of intracellular Mg^{2+} levels by overexpression of Alr1-n277, which both indicate that this isomer has at least residual Mg^{2+} transport capacity. Like Alr1-n277 isomer Alr1-n485 showed no mobility shift, but in contrast a strongly increased general protein turnover, leading to a rapid, but Mg^{2+} independent degradation of this protein (Figure 3A). Taken together, deletions in the N-terminal domain of Alr1p lower or abolish hyperphosphorylation-dependent mobility shifts and Mg^{2+}-induced vacuolar degradation.

Subcellular localization of Alr1p and truncated Alr1p alleles

In order to observe subcellular locations of wild-type and mutant Alr1 proteins C-terminally GFP-tagged fusion genes under transcriptional control of the p_{Met25} were expressed in strain BY4742 and the fluorescence was monitored by DIC/UV microscopy (Figure 3B). The relative intensities and distribution of the tagged proteins were calculated by the use of ImageQuant software. Average values of at least 8 individual cells are given in Figure 3C.

Incubation of cells at limiting Mg^{2+} concentrations (0.01 mM) in the medium for 3 h, triggered about 50% of the wild-type Alr1p to the plasma membrane, shown as a bright rim structure at the cell surface and a weak fluorescence in cellular compartments (Figures 3B, panels b, c, d and 3C). Subsequent addition of 100 mM Mg^{2+} for 3 h led to a complete degradation of Alr1p (Figure 3B, panel e). At identical conditions, truncated isoforms Alr1-n128, Alr1-n155 and Alr1-n204 were partially found at the plasma membrane (about 22%, 17% and 14%, respectively), but most of the protein accumulated at cytoplasmic compartments and, as revealed from colocalization with the FM4-64 fluorescent lipophilic dye, in the vacuolar and prevacuolar compartments (Figure 3B, panels b, c, d). Considerable fluorescence could still be detected when cells were treated with 100 mM Mg^{2+} (panel e), which is consistent with immunoblotting data (Figure 3A) and points to

reduced Mg^{2+}-dependent turnover of these proteins. Interestingly, high Mg^{2+} appeared to favour location of Alr1-n204 in the plasma membrane. Alr1-n277p and Alr1-n485 accumulated in punctuated spots in the cytoplasm and the presence in the plasma membrane was below detection level. Yet Alr1-n277p supported growth at low Mg^{2+} conditions and maintained normal intracellular Mg^{2+} levels, suggesting that a small part of the protein made its way to the plasma membrane. While Alr1-n277p showed some colocalization with vacuoles, Alr1-n485p clearly was excluded from this compartment. Taken together, N-terminal deletions alter subcellular localization of Alr1p, favouring its accumulation in cytoplasmic compartments and lower its turn-over via vesicle transport and vacuolar degradation.

Cluster of short amino acid segment deletions affecting Alr1 protein functionality

To narrow down sequences or motifs possibly important for cellular trafficking and processing of Alr1p, intragenic deletions (modules comprising about 15 to 30 aa) were generated (Figure 1). All mutant Alr1 proteins deleted for module 1 to 13 were C-terminally HA-tagged and expressed under control of the endogenous *ALR1* promoter in a centromeric plasmid in strain AG012 (*alr1Δalr2Δ*). To observe effects of these deletions, wild-type and mutant cells were first cultured in selective medium with high Mg^{2+} concentration to allow for homogenous growth and then washed free of magnesium before series of 10-fold dilutions were dropped onto medium with indicated Mg^{2+} concentrations. Deletion of amino acids in modules M1 to M8, M12 and M13 had no significant effect on growth (data not shown). Interestingly, Alr1 mutants deleted for modules M9 (E271 to F291) and M11 (D292 to Q318) or M1-9 (Q99 to F291), could not complement the magnesium deficient growth phenotype of *alr1Δ* cells on low Mg^{2+} containing media (Figure 4A). In addition, we detected a rapid turnover of Alr1p deleted for M9 and M11, which was independent of the addition of Mg^{2+} (Figure 4B). In case of deletion isomer M1-9 we failed to detect any Alr1 protein. While deletion of the successive module M12 had no significant effect on the Mg^{2+}-deficient growth phenotype, it also caused Mg^{2+} independent Alr1p degradation, but to a somewhat lower extent, compared to deletions M9 and M11. On the other hand, deletion of module M3 resulted in slightly increased Alr1p stability compared to the full length Alr1p (Figure 4B). All other constructs were expressed and processed similar to full length Alr1p (data not shown).

To investigate if the activity of Alr1, deleted for modules, correlated with their subcellular localization, the different *ALR1* alleles were fused to GFP (green fluorescent protein) under control of p_{MET25}. Cells were incubated prior to microscopic analysis for at least 3 h in Mg^{2+} limited medium. As expected, all tested proteins except Alr1ΔM9, Alr1ΔM1-9, and Alr1ΔM11 were localized at the plasma membrane. These three non-functional isomers were found as punctuated spots in the cells, but excluded from the vacuole, very much like it was observed for the truncated molecules Alr1-n485 and partially for Alr1-n277 (Figure 4C). Taken together, phenotypes of N-terminal deletions (Figure 3) and of module deletions are highly consistent and indicative of a region of Alr1p from aa 270 to 320 with particular importance for proper localization, vacuolar targeting and function as a Mg^{2+} transporter of the plasma membrane.

Inspection of Alr1p sequences from various ascomycete fungi revealed a highly conserved motif EEDVCFP followed by an α-helical stretch which also exhibited some sequence conservation (Table 1). These conserved elements occur in nearly all Alr1 related proteins of Ascomycetes in a region preceding the CorA homology. To investigate a possible influence of these elements in Alr1p translocation, we substituted in wild-type Alr1p via PCR mediated mutagenesis aa $_{273}DVCFP_{277}$ by GGGEF, E_{271}-E_{272} by KK and E_{295}-E_{296} by KK (named Alr1-G3M9, Alr1-KKM9 and Alr1-KKM11, respectively). To disrupt the α-helical structure covered by module M11, the amino acid L_{294} and amino acids Y_{297}, F_{300}, and A_{303} were substituted by prolines, (named Alr1-P1M11 and Alr1-P3M11, respectively). All constructs were expressed in strain AG012 and tested for growth on Mg^{2+} limiting conditions (Figure 5A). The expression of constructs *alr1-G3M9*, *alr1-KKM9* and *alr1-KKM11* in AG012 affected the growth ability only slightly when compared to the expression of *ALR1*-wt, although the mutations created a drastic change in the local polarity of the protein. Analyses of these constructs fused to GFP were comparable to those found with the wild-type protein (data not shown). In contrast, the destabilization of the α-helical stretch by the insertion of prolines in constructs *alr1-P1M11* and *alr1-P3M11* completely impeded growth of AG012 cells in standard medium. Even upon addition of 100 mM Mg^{2+} to the growth medium, cell growth remained slightly retarded. As expected, GFP fusions of these proteins were not delivered to the plasma membrane but found as punctuated spots in the cytoplasm as observed with proteins Alr1-n485, Alr1ΔM9, Alr1ΔM1-9, and Alr1ΔM11 (Figures 5B and 4C). These

data indicate that this α-helical stretch is essential for protein-protein interactions, necessary to allow correct translocation of the protein to the plasma membrane.

In order to see if the M11 module alone (27 aa, essentially consisting of the α-helical element) would affect protein localization, we fused this module with GFP and compared the cellular location of GFP only (empty-GFP) and the M11-GFP fusion protein (Figure 5C). Interestingly, the fusion protein M11-GFP was targeted to small intracellular vesicles, while GFP without module M11 was diffusely distributed in the cytoplasm (Figure 5C). This suggests that the M11 module constitutes an element with vesicle targeting information. Yet without its flanking regions it targets the fusion protein to small intracellular vesicles similar to the complete Alr1p with disturbed α-helical structure.

Inhibition of prevacuolar fusion enhances plasma membrane location of some Alr1p variants

The yeast SNARE protein Pep12p is a multifunctional syntaxin that is required for the biosynthetic, endocytic and retrograde traffic into the prevacuolar compartment (Becherer *et al.*, 1996; Bryant and Stevens, 1998; Gerrard *et al.*, 2000; Prescianotto-Baschong and Riezman, 2002; Blanchette *et al.*, 2004). To investigate the potential influence of Pep12p on the Alr1p sorting pathway, we examined the topology of GFP-tagged wild-type Alr1p and its NH_2-terminally mutated isomers expressed in the mutant strain BY4742 *pep12Δ* (Figure 6A).

Abundance of full length wild-type Alr1p at the plasma membrane was high both at low and high Mg^{2+} concentrations in growth media. Mutant Alr1 proteins Alr1-n155, -n204, -n277 at low Mg^{2+} conditions were somewhat more abundant than in *PEP12* background. Ratios between Alr1p abundance in plasma membrane and cytoplasmic vesicular structures decreased with the length of the deletion essentially as in *PEP12* background. Interestingly, at 10 mM Mg^{2+} in growth media all of these proteins were abundantly present in the plasma membrane in the absence of Pep12p. Only Alr1-n485 protein distribution was unchanged in *PEP12* and in *pep12Δ* backgrounds. Internally deleted Alr1ΔM1 to -ΔM3, -ΔM5 to -ΔM8, -ΔM12 and -ΔM13 proteins were somewhat less abundant in the plasma membrane than wild-type Alr1p, but stayed unchanged upon addition of 10 mM Mg^{2+} (Figure 6B and not shown). Alr1ΔM9, -ΔM1-9 and -ΔM11 proteins at low Mg^{2+} were somewhat less abundant in *pep12Δ* than in *PEP12* background

but in both conditions mostly present in cytoplasmic vesicles. In *pep12Δ* cells at high Mg^{2+} these proteins were hardly detectable. As a consensus from these data we find that i) the absence of *PEP12* favors the plasma membrane location of wild-type Alr1p and of mutant proteins with mild effects on Mg^{2+} transport and cell growth, ii) Alr1 proteins with partial or total deletion of sequences from aa 270 to 318, with the VCFP motif followed by an α-helical stretch, lacked Mg^{2+}-dependent protein modification. These proteins tend to accumulate in cytoplasmic particles; its plasma membrane location was not favored by *pep12Δ* and mutant cells showed no significant growth at low Mg^{2+}. iii) These mutant proteins were rapidly degraded even at low Mg^{2+}, but both in *PEP12* and *pep12Δ* background and this apparently not through a vacuolar pathway. This behavior and their location in cytoplasmic particles suggest that they were mislocalised and subject to proteasomal degradation. Alr1-n277 protein showed a mixed behavior, showing accumulation in cytoplasmic particles but also some insertion into the plasma membrane, which was favored by *pep12Δ*, and residual growth on low Mg^{2+}.

DISCUSSION

The CorA protein superfamily of Mg^{2+} transporters consists of the CorA proteins in bacteria and archaea, the Alr1 in plasma membranes of fungi and the Mrs2 proteins in most eukaryotic mitochondria (Mrs2) (Knoop *et al.*, 2005). Matching their sequences to the crystal structure for the *Thermotoga maritima* CorA (*Tm*CorA) (Lunin, 2006; Maguire, 2006) revealed that the eukaryotic subfamilies frequently have N- and C-terminal extensions not present on their prokaryotic counterparts. Proteins of the Alr1 subfamily, present in most sequenced genomes of fungi and some protozoa, have a particularly long N-terminus, which has no counterpart in CorA or Mrs2 and to which no specific function could be assigned yet. We speculated that this part of Alr1p might be important for the vesicular transport of Alr1p to the plasma membrane, i.e. it may exert functions which are neither required in bacteria, archaea nor in mitochondria.

Sequence analyses and *in silico* structure analyses of the N-terminal moiety of Alr1p revealed a rather unstructured and disordered protein pattern. To narrow down regions of interest and circumvent an extensive damage of the whole protein, we designed "deletion-modules", small intragenic deletions comprising only 15 to 30 amino acids of the Alr1p N-terminus. The deletion of modules M1 to M8 and M12 to M13, covering internal amino acids from Q99 to T270 and K319 to K367, respectively, neither affected the localization and the Mg^{2+} transport function of the protein, nor significantly influenced the stability of these Alr1p isomers. However, deletion of modules M9 and M11, ranging from E271 to F291 and D292 to Q318, respectively, seriously disturbed vesicular transport and stability of Alr1p. The sequence from D290 to S311 exhibits a high probability to form a stable alpha helical structure recognizable in a wide range of Alr1 proteins (cf. Table 1). It shows some sequence conservation and is preceded by another sequence of considerable conservation. Mutational changes of the local polarity of the Alr1 protein by substitution of negatively charged amino acids by lysine residues within the helix or in the preceding motif did not significantly affect the anterograde pathway of the protein to the plasma membrane, protein stability and degradation. However, insertion of one or several prolines in the helix led to a complete collapse of Alr1p translocation.

N-terminal Alr1p deletion isomers which retained these M9 and M11 modules unchanged reached the plasma membrane, showed Mg^{2+}-dependent phosphorylation and appeared in prevacuolar and vacuolar compartments, and thus behaved similar to wild-type Alr1p

which we previously have shown to be vacuolarly degraded (Graschopf *et al.*, 2001). Also, their presence in the plasma membrane was stimulated in the absence of Pep12p, a multifunctional syntaxin that is required for endocytic and retrograde traffic into the prevacuolar compartment. Accordingly, these isomers reached the endosomal recycling compartment. In contrast, Alr1p isomers with mutations or deletions affecting modules M9 and M11 (Alr1ΔM9, -ΔM11, Alr1-P1M11, -Alr1-P3M11, Alr1-n485, Alr1ΔM1-9) accumulated in punctuated spots in the cytoplasm, their degradation was independent of the presence or absence of Mg^{2+} and of Pep12p and they were not seen in prevacuolar or vacuolar compartments. They are likely to be subject to proteasomal degradation. Therefore we assume that the punctuated spots in these mutants signify an arrest in ER-to-Golgi transport and that sequences in M9/M11 modules constitute an essential transport signal.

The M9/11 transport signal in Alr1p identified here is unique in that it exists of an α-helix starting with a moderately conserved sequence motif (M11: GIDFDELEEF) and is preceded by another motif (M9: EEDVCFP) which is particularly well conserved among Alr1 proteins. Although these motifs are well conserved, multiple mutations introduced in one or the other had no major effect on transport of Alr1p to the plasma membrane. Only deletion of M9 (aa 271 to aa 291) or deletion of M11 (aa 292 to aa 318) as well as proline insertion into the α-helix in M11 had dramatic effects. Possibly there is some redundancy of sequence motifs helping to guide Alr1p beyond the Golgi, explaining why mutation of one or the other conserved motif was without major effects. M9/11 is predicted to be exposed on the surface of the Alr1 protein (R. Konrat, pers. comm.), possibly to display the conserved sequence motifs, and the conserved M11 α-helix is likely to be important for this positioning of the conserved motifs. This is reminiscent of ER export motifs located in membrane-proximal C-termini (Dong and Wu, 2006) or in an internal loop between two transmembrane domains (Zhang *et al.*, 2008). Secondary structure domains generally may help to expose sequence motifs for their interaction with binding partners, e.g. COPII components in case of ER export signals.

The role of the M11 sequence in directing Alr1p through the secretory pathway is supported by our finding that its fusion to GFP led to an accumulation of GFP in punctuated structures similar to those observed with Alr1-M11 isomers of Alr1p. Apparently, the M11 motif was able to direct GFP into the secretory pathway, but it was

not sufficient to direct it through this pathway into final compartments like endosome or vacuole.

Consistent with data published by Lee and Gardner (Lee and Gardner, 2006), we found that truncations up to about 204 amino acids at the N-terminus of Alr1p are dispensable to achieve sufficient magnesium uptake in *S. cerevisiae*, as shown by growth analyses and measurements of the internal free magnesium. Yet, Mg^{2+}-dependent protein modification by hyper-phosphorylation, protein turnover and subcellular location of these proteins were altered. With increasing N-terminal deletions Alr1p accumulated mostly in prevacuolar and vacuolar compartments and small amounts only reached the plasma membrane. Endocytic and vacuolar pathways converge at a prevacuolar/late endosomal compartment (Raymond *et al.*, 1992; Schimmoller and Riezman, 1993; Vida *et al.*, 1993). Accordingly, Alr1p may reach these compartments from different sides (cf. Figure 1, supplementary data). Alr1p phosphorylation is thought to occur at the membrane (Graschopf *et al.*, 2001). Accordingly, the small membrane resident fraction of the N-terminal deletion isomers would be expected to be modified. Increasing prevacuolar /vacuolar accumulation with longer N-terminal deletions (up to aa 277) indicates that the N-terminus also contains information for their translocation from post-Golgi to the plasma membrane. But our data did not allow recognizing any specific sequence stretch to be responsible for post-Golgi transport. Signals for this step may be widespread over larger parts of the N-terminus of Alr1p.

Interestingly, upon ablation of Pep12p those mutant Alr1 proteins predominantly localized to the plasma membrane, just like wild-type Alr1p. This shift to the plasma membrane was equally observed with mutant protein Alr1-n277 although it had a part of the M9 motif (EEDVCFP) deleted. Pep12p localizes to the late endosome (LE) and is involved in multiple fusion events e.g. between the LE and the vacuole, but also of vesicles originating from the early endosome (EE) or the late Golgi (Bryant and Stevens, 1998; Gerrard *et al.*, 2000; Prescianotto-Baschong and Riezman, 2002). In its absence fusion of EE-derived vesicles with the LE /prevacuolar complex (PVC) are hampered, but protein recycling from the EE to the plasma membrane appears not to be affected (Becherer *et al.*, 1996; Holthuis *et al.*, 1998; Gerrard *et al.*, 2000). Our data showing an increased presence of Alr1p in a *pep12Δ* mutant in presence of Mg^{2+} suggest that all isomers with deletions up to 277 aa made their way beyond the Golgi compartment into the EE and at least a fraction of them could take part in the recycling between EE and plasma membrane (cf. Figure 1,

supplementary data). Endocytic recycling also has been suggested to participate in the trafficking of other yeast membrane proteins, like the chitin synthetase Chs3p, the vesicle-associated membrane protein receptor Snc1p, the yeast a-factor receptor Ste3p and the zinc transporter Zrt1 (Chuang and Schekman, 1996; Chen and Davis, 2000; Lewis *et al.*, 2000).

ACKNOWLEDGEMENTS

REFERENCES

Barlowe, C. (2003). Signals for COPII-dependent export from the ER: what's the ticket out? Trends Cell Biol *13*, 295-300.

Becherer, K.A., Rieder, S.E., Emr, S.D., and Jones, E.W. (1996). Novel syntaxin homologue, Pep12p, required for the sorting of lumenal hydrolases to the lysosome-like vacuole in yeast. Mol Biol Cell *7*, 579-594.

Blanchette, J.M., Abazeed, M.E., and Fuller, R.S. (2004). Cell-free reconstitution of transport from the trans-golgi network to the late endosome/prevacuolar compartment. J Biol Chem *279*, 48767-48773.

Brachmann, C.B., Davies, A., Cost, G.J., Caputo, E., Li, J., Hieter, P., and Boeke, J.D. (1998). Designer deletion strains derived from Saccharomyces cerevisiae S288C: a useful set of strains and plasmids for PCR-mediated gene disruption and other applications. Yeast *14*, 115-132.

Brodsky, J.L., and McCracken, A.A. (1999). ER protein quality control and proteasome-mediated protein degradation. Semin Cell Dev Biol *10*, 507-513.

Bryant, N.J., and Stevens, T.H. (1998). Vacuole biogenesis in Saccharomyces cerevisiae: protein transport pathways to the yeast vacuole. Microbiol Mol Biol Rev *62*, 230-247.

Bui, D.M., Gregan, J., Jarosch, E., Ragnini, A., and Schweyen, R.J. (1999). The bacterial magnesium transporter CorA can functionally substitute for its putative homologue Mrs2p in the yeast inner mitochondrial membrane. J Biol Chem *274*, 20438-20443.

Chen, L., and Davis, N.G. (2000). Recycling of the yeast a-factor receptor. J Cell Biol *151*, 731-738.

Chuang, J.S., and Schekman, R.W. (1996). Differential trafficking and timed localization of two chitin synthase proteins, Chs2p and Chs3p. J Cell Biol *135*, 597-610.

Dong, C., and Wu, G. (2006). Regulation of anterograde transport of alpha2-adrenergic receptors by the N termini at multiple intracellular compartments. J Biol Chem *281*, 38543-38554.

Eshaghi, S., Niegowski, D., Kohl, A., Martinez Molina, D., Lesley, S.A., and Nordlund, P. (2006). Crystal structure of a divalent metal ion transporter CorA at 2.9 angstrom resolution. Science *313*, 354-357.

Farhan, H., Korkhov, V.M., Paulitschke, V., Dorostkar, M.M., Scholze, P., Kudlacek, O., Freissmuth, M., and Sitte, H.H. (2004). Two discontinuous segments in the carboxyl

terminus are required for membrane targeting of the rat gamma-aminobutyric acid transporter-1 (GAT1). J Biol Chem *279*, 28553-28563.

Farhan, H., Reiterer, V., Kriz, A., Hauri, H.P., Pavelka, M., Sitte, H.H., and Freissmuth, M. (2008a). Signal-dependent export of GABA transporter 1 from the ER-Golgi intermediate compartment is specified by a C-terminal motif. J Cell Sci *121*, 753-761.

Farhan, H., Weiss, M., Tani, K., Kaufman, R.J., and Hauri, H.P. (2008b). Adaptation of endoplasmic reticulum exit sites to acute and chronic increases in cargo load. EMBO J *27*, 2043-2054.

Ferreira, T., Mason, A.B., Pypaert, M., Allen, K.E., and Slayman, C.W. (2002). Quality control in the yeast secretory pathway: a misfolded PMA1 H+-ATPase reveals two checkpoints. J Biol Chem *277*, 21027-21040.

Gardner, R.C. (2003). Genes for magnesium transport. Curr Opin Plant Biol *6*, 263-267.

Gerrard, S.R., Levi, B.P., and Stevens, T.H. (2000). Pep12p is a Multifunctional Yeast Syntaxin that Controls Entry of Biosynthetic, Endocytic and Retrograde Traffic into the Prevacuolar Compartment doi:10.1034/j.1600-0854.2000.010308.x. Traffic *1*, 259-269.

Gietz, R.D., and Sugino, A. (1988). New yeast-Escherichia coli shuttle vectors constructed with in vitro mutagenized yeast genes lacking six-base pair restriction sites. Gene *74*, 527-534.

Gitan, R.S., and Eide, D.J. (2000). Zinc-regulated ubiquitin conjugation signals endocytosis of the yeast ZRT1 zinc transporter. Biochem J *346 Pt 2*, 329-336.

Graschopf, A., Stadler, J.A., Hoellerer, M.K., Eder, S., Sieghardt, M., Kohlwein, S.D., and Schweyen, R.J. (2001). The yeast plasma membrane protein Alr1 controls Mg^{2+} homeostasis and is subject to Mg^{2+}-dependent control of its synthesis and degradation. J Biol Chem *276*, 16216-16222.

Holthuis, J.C., Nichols, B.J., Dhruvakumar, S., and Pelham, H.R. (1998). Two syntaxin homologues in the TGN/endosomal system of yeast. Embo J *17*, 113-126.

Jarosch, E., Geiss-Friedlander, R., Meusser, B., Walter, J., and Sommer, T. (2002). Protein dislocation from the endoplasmic reticulum--pulling out the suspect. Traffic *3*, 530-536.

Knoop, V., Groth-Malonek, M., Gebert, M., Eifler, K., and Weyand, K. (2005). Transport of magnesium and other divalent cations: evolution of the 2-TM-GxN proteins in the MIT superfamily. Mol Genet Genomics *274*, 205-216.

Kolisek, M., Zsurka, G., Samaj, J., Weghuber, J., Schweyen, R.J., and Schweigel, M. (2003). Mrs2p is an essential component of the major electrophoretic Mg2+ influx system in mitochondria. Embo J *22*, 1235-1244.

Lai, K., Bolognese, C.P., Swift, S., and McGraw, P. (1995). Regulation of inositol transport in Saccharomyces cerevisiae involves inositol-induced changes in permease stability and endocytic degradation in the vacuole. J Biol Chem *270*, 2525-2534.

Lee, J.M., and Gardner, R.C. (2006). Residues of the yeast ALR1 protein that are critical for magnesium uptake. Curr Genet *49*, 7-20.

Lewis, M.J., Nichols, B.J., Prescianotto-Baschong, C., Riezman, H., and Pelham, H.R. (2000). Specific retrieval of the exocytic SNARE Snc1p from early yeast endosomes. Mol Biol Cell *11*, 23-38.

Li, L., Tutone, A.F., Drummond, R.S., Gardner, R.C., and Luan, S. (2001). A novel family of magnesium transport genes in Arabidopsis. Plant Cell *13*, 2761-2775.

Liu, X.F., and Culotta, V.C. (1999). Post-translation control of Nramp metal transport in yeast. Role of metal ions and the BSD2 gene. J Biol Chem *274*, 4863-4868.

Lunin, V.V., Dobrovetsky, E., Khutoreskaya, G., Zhang, R., Joachimiak, A., Bochkarev, A., Maguire, M.E., Edwards, A.M., Koth, C.M. (2006). Crystal structure of the CorA Mg2+ transporter. to be published.

Ma, D., and Jan, L.Y. (2002). ER transport signals and trafficking of potassium channels and receptors. Curr Opin Neurobiol *12*, 287-292.

Ma, D., Zerangue, N., Lin, Y.F., Collins, A., Yu, M., Jan, Y.N., and Jan, L.Y. (2001). Role of ER export signals in controlling surface potassium channel numbers. Science *291*, 316-319.

MacDiarmid, C.W., and Gardner, R.C. (1998). Overexpression of the Saccharomyces cerevisiae magnesium transport system confers resistance to aluminum ion. J Biol Chem *273*, 1727-1732.

Maguire, M.E. (2006). The structure of CorA: a Mg(2+)-selective channel. Curr Opin Struct Biol *16*, 432-438.

Niedenthal, R.K., Riles, L., Johnston, M., and Hegemann, J.H. (1996). Green fluorescent protein as a marker for gene expression and subcellular localization in budding yeast. Yeast *12*, 773-786.

Piskacek, M., Zotova, L., Zsurka, G., and Schweyen, R.J. (2008). Conditional knock-down of hMRS2 results in loss of mitochondrial Mg(2+) uptake and cell death. J Cell Mol Med.

Prescianotto-Baschong, C., and Riezman, H. (2002). Ordering of compartments in the yeast endocytic pathway. Traffic *3*, 37-49.

Raymond, C.K., Howald-Stevenson, I., Vater, C.A., and Stevens, T.H. (1992). Morphological classification of the yeast vacuolar protein sorting mutants: evidence for a prevacuolar compartment in class E vps mutants. Mol Biol Cell *3*, 1389-1402.

Schekman, R., and Orci, L. (1996). Coat proteins and vesicle budding. Science *271*, 1526-1533.

Schimmoller, F., and Riezman, H. (1993). Involvement of Ypt7p, a small GTPase, in traffic from late endosome to the vacuole in yeast. J Cell Sci *106 (Pt 3)*, 823-830.

Schindl, R., Weghuber, J., Romanin, C., and Schweyen, R.J. (2007). Mrs2p forms a high conductance mg2+ selective channel in mitochondria. Biophys J *93*, 3872-3883.

Sherman, F. (1991). Getting started with yeast. Methods Enzymol *194*, 3-21.

Stephens, D.J., Lin-Marq, N., Pagano, A., Pepperkok, R., and Paccaud, J.P. (2000). COPI-coated ER-to-Golgi transport complexes segregate from COPII in close proximity to ER exit sites. J Cell Sci *113 (Pt 12)*, 2177-2185.

Stockklausner, C., Ludwig, J., Ruppersberg, J.P., and Klocker, N. (2001). A sequence motif responsible for ER export and surface expression of Kir2.0 inward rectifier K(+) channels. FEBS Lett *493*, 129-133.

Vida, T.A., Huyer, G., and Emr, S.D. (1993). Yeast vacuolar proenzymes are sorted in the late Golgi complex and transported to the vacuole via a prevacuolar endosome-like compartment. J Cell Biol *121*, 1245-1256.

Wachek, M., Aichinger, M.C., Stadler, J.A., Schweyen, R.J., and Graschopf, A. (2006). Oligomerization of the Mg2+-transport proteins Alr1p and Alr2p in yeast plasma membrane. Febs J *273*, 4236-4249.

Zhang, Z.N., Li, Q., Liu, C., Wang, H.B., Wang, Q., and Bao, L. (2008). The voltage-gated Na+ channel Nav1.8 contains an ER-retention/retrieval signal antagonized by the {beta}3 subunit. J Cell Sci *121*, 3243-3252.

Table 1: Comparison of Alr1-homolog sequences of various ascomycete fungi

```
TrEMBL      Sequence motives

Q08269      SQASRDSQETEEDVCFPMPPQLHTRVNGIDFDELEEYAQFANAEKSQFLASLQVPNE
Q6CP63      SQVSHLSQETEEDVCFPIQKREHTRINGIDFDELEEFTAQEKAINNSHLYSHPAVT
Q5AJW3      SHASRSSQETEEDVCFPMVGD-HIRVNGIDFDEIDEFIREEREEAYLQKQMIAK
Q6BL48      SHASRSSQETEEDVCFPMLRE-HVRVKGIDFDEIEEFIRDEKENEMHLKEEQQ
O13657      SQVDENTRVVEEDVCFPMQEESHVNK-GIDFDELDNFAEEELQKQRQNTDHFRSRQYS
Q6FVI5      SQASRESQETEEDVCFPMPPQLHSRVNGIDFDELEEFAEQVNEQKKLCEISLSAQKSG
Q6CAS6      DTGSQVSMDHDDDVCLPVEEGSG----GIDFEEIDDYVQQQRRGSNATRTGTALNKE
Q75AU1      SNASRESQETEEDVCFPMQQPEHTRINGIDFDELEEFAQESLRANLTMNINVGVSKGD
A5DLQ4      SHASRSSQETEEDVCFPM-LREHIRVKGIDFDEIEEFIKEEREEEEFMRQQQTL
A7UWR3      TASLATNKSAEEDVCFPLQDDHRDDNLHIDFHYLETFIKAENEARQSARRPSAIRVFP
A7E403      AKSLATNKSAEEDVCFPLQDDHRDDNLHIDFHYLETFIKAENEARQSARRPSAIRVFP
Q2H687      TASLATNKSAEEDVCFPLQDEQRGDHLYIDFDYLENFIQSENEARQAARRPEV
A4RM30      VSSLSTNKSAEEDVCFPLQDDHRDDNLHIDFHYLETFIKAENEARQS
Q0UGL1      IEVSSANSSAEEDVCFPVTEDPGKTTR-FDYEELEEFIAEPQTKTLIGQEL
A6R075      TVDPRTGLNDDADVCFPTYDESGKTS-IIDFEELEEFVALSRRKSQTVPR
```

Putative α-helical stretches are underlined. Conserved amino acids are shown in bold letters. (Accession numbers (TrEMBL) and species: Q08269, Saccharomyces cerevisiae; Q6CP63, Kluyveromyces lactis; Q5AJW3, Candida albicans; Q6BL48, Debaromyces hansenii; O13657, Schizosaccharomyces pombe; Q6FVI5, Candida glabrata; Q6CAS6, Yarrowia lipolytica; Q75AU1, Ashbya gossypii; A5DLQ4, Pichia guilliermondii; A7UQR3, Neurospora crassa; A7E403, Sclerotina sclerotiorum; Q2H687, Chaetomium globosum; A4RM30, Magnaporte grisea; QOUGL1, Phaeosphaeria nodorum; A6RO75, Ajellomyces capsulatus)

Figure 1. Schematic map of Alr1p constructs**.** The positions of novel start codons (-128, -155, -204, -277, and -485) of *ALR1*-isomers are indicated below the grey bar representing Alr1p. Transmembrane domains (TMDs) are given as black boxes close to the C-terminus. Positions of amino acids deleted in modules M1 to M13 are consecutively numbered in open bars. The region comprising the complete set of deletion modules is indicated as dotted lines. The amino acid sequence enclosed by modules M9 and M11 and relevant substitutions are shown in dotted boxes.

Figure 2. Effects of N-terminal Alr1p deletions on Mg^{2+} dependent growth. (A) Gene *ALR1* and all truncated alleles, *alr1-n128, alr1-n155, alr1-n204, alr1-n277, alr1-n485*, integrated into strain AG012 (*alr1Δ, alr2Δ*) via the yeast YIplac204 vector, were tested for their ability to restore growth of an *alr1Δ alr2Δ* strain. Before growth analysis, cells were precultured at 28 °C in medium supplemented with 50 mM Mg^{2+} to support homogenous growth of all cells. Cells were washed and diluted at equal D_{600} levels, and growth analyses were carried out by measuring the D_{600} in selective medium containing the following Mg^{2+} concentrations: 0.025, 0.1, 1.5 and 50 mM. Generation times (in hours) of cultures are given in the table. (B) Protein expression levels of different *ALR1* clones: To confirm expression of truncated Alr1 proteins (tagged with a 3 x HA-epitope), similar amounts of total protein extracts were analysed by Western blotting and immunodetection. Detection of Hxk1p served as an internal loading control. (C) Measurement of the intracellular free Mg^{2+} contents: N-terminally truncated *ALR1* alleles were expressed in strain AG012, and the free Mg^{2+} content of enzymatically opened cells was measured using Eriochrome Blue as an indicator. Before preparation for the measurement (see Experimental procedures), the cells were incubated in medium supplemented with 30 μM (low) or 50 mM (high) Mg^{2+}.

Figure 3. Mg^{2+} specific degradation of Alr1p strongly depends on the N-terminal sequence. (A) Deletion of N-terminal parts of Alr1p interfered with its stability: AG012 cells carrying chromosomally integrated YIpALR1HA wild type and truncated mutant alleles *alr1-n128, alr1-n155, alr1-n204, alr1-n277* and *alr1-n485* were grown in synthetic SD medium containing 100 mM Mg^{2+}. To allow Alr1p accumulation in the plasma membrane, cells were washed free of Mg^{2+} and incubated in medium supplemented with

$25\,\mu M$ Mg^{2+}, $3.5\,h$ prior to simultaneous treatment of aliquots with $100\,\mu g \cdot mL^{-1}$ cycloheximide (CHX) and 0, 1, 10 or 100 mM Mg^{2+}. After 0, 30, 90 and 180 min of incubation, total cell extracts were prepared and equal amounts of protein were immunoblotted for HA-tagged Alr1p and hexokinase (Hxk1p), used as a loading control. (B) Subcellular distribution of Alr1p and N-terminally truncated isoforms: GFP-tagged Alr1p and its mutated variants (Alr1-n128, Alr1-n155, Alr1-n204, Alr1-n277 and Alr1-n485) were expressed in BY4742 wt strain and detected by fluorescence microscopy. After overnight cultivation in standard, Mg^{2+} replete medium, cells were incubated for further 3 hours in low magnesium-containing medium (10 μM Mg^{2+}, panels a-d) and medium with 100 mM Mg^{2+} (panel e). Before fluorescence microscopical analysis, cells were treated with dye FM4-64, specific for endosomal and vacuolar membranes. Differential phase contrast (a), GFP-fluorescence (b and e), FM4-64 vacuolar dye (c), and merged images (d). (C) Analysis of protein content of plasma membrane bound Alr1p and intracellular fraction. An average value of at least 8 individual cells for each Alr1p truncation has been given in the figure. The fluorescence ratio was calculated using ImageQuant software.

Figure 4. Short intragenic sequence deletions affect Alr1p function. (A) Complementation of *alr1Δ* null mutant growth defect by Alr1p deleted for "modules". AG012 cells, transformed with low copy plasmids bearing wild type and Alr1p deleted for modules M9, M1-9 and M11, were grown in selective medium containing high Mg^{2+} concentration, washed free of Mg^{2+} with water, and diluted to equal D_{600} values. Serial dilutions were dropped onto selective medium plates with Mg^{2+} concentrations as indicated. Growth was recorded after 3 days at 28 °C. (B) Protein turnover of Alr1p deleted for modules creating significant variances to native Alr1p. To support equal growth, all cells expressing deletion mutants of *ALR1* were cultivated in selective media supplemented with 100 mM Mg^{2+}. Prior to protein extraction, cells were washed 3 times with media lacking magnesium and further incubated in medium containing 25 μM Mg^{2+} for 3.5 h. Then aliquots were simultaneously exposed to $100\,\mu g \cdot mL^{-1}$ of cycloheximide (CHX) and 0, 1, 10 or 100 mM Mg^{2+}. After 0, 30, 90 and 180 min of incubation, total cell extracts were prepared and equal amounts of protein were immunoblotted for HA-tagged Alr1p and hexokinase (Hxk1p), used as a loading control. (C) C-terminally GFP tagged mutant Alr1 isomers (modules M3, M9, M1-9, M11 and M12), expressed in AG012 are shown. Before
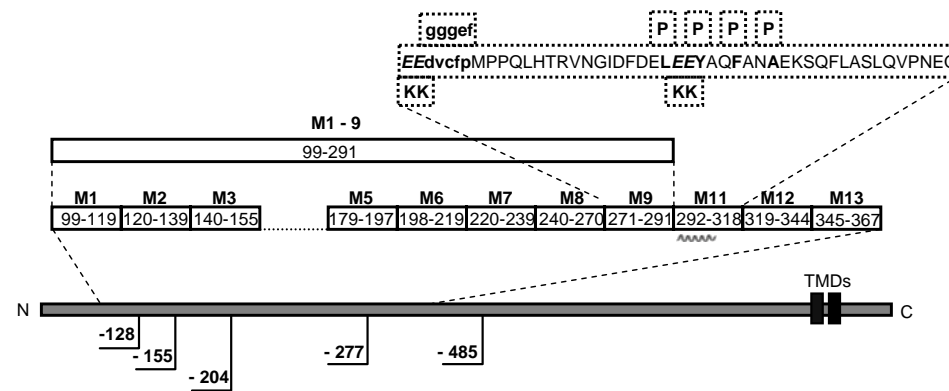
fluorescence microscopical analysis, cells were incubated in low magnesium containing media for 3 h.
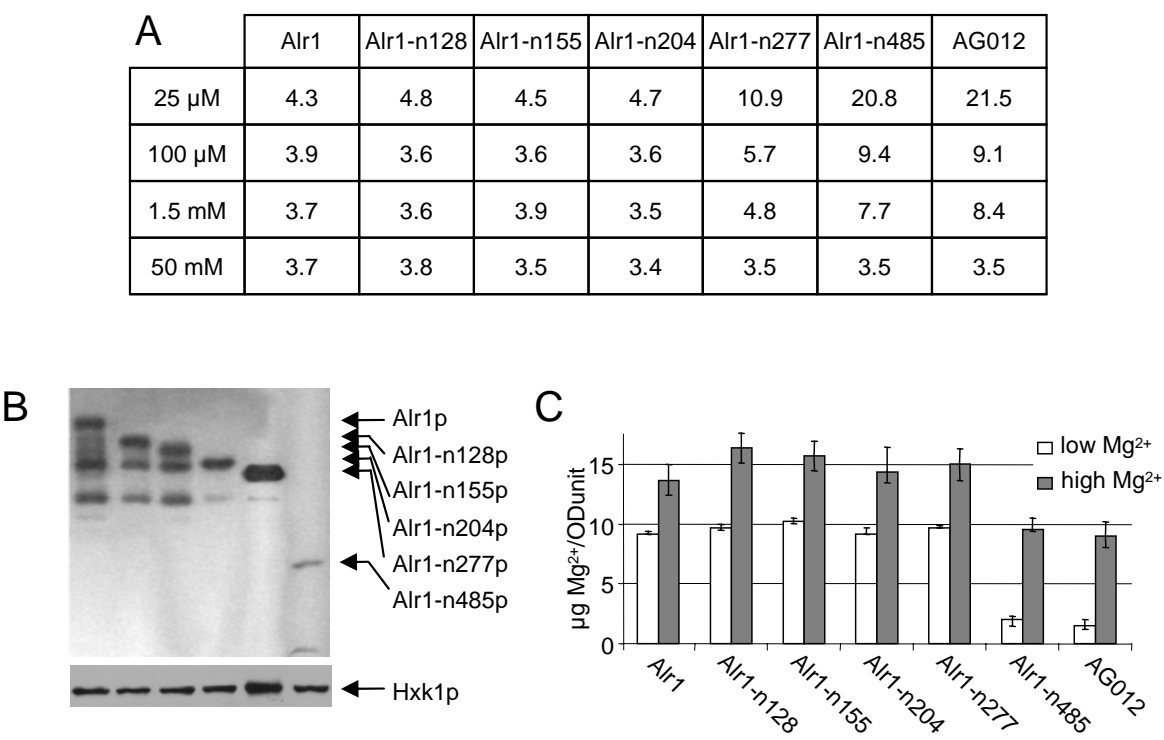
Figure 5. The helix in module M11 is crucial for Alr1p translocation to the plasma membrane. (A) Strain AG012 was transformed with the integrative vector YIplac204 carrying *ALR1* and alleles mutated in modules M9 and M11 (see Table 2, supplementary data). Cells, precultured in SD-medium supplemented with 100 mM Mg^{2+}, were washed and further incubated in SD-medium containing Mg^{2+} as indicated in the figure and growth was monitored by measurement of the D_{600}; *ALR1* (♦), *alr1-G3M9* (◊), *alr1-KKM9* (▲), *alr1-KKM11* (Δ), *alr1-P1M11* (■), *alr1-P3M11* (□). (B) Alleles *alr1-P1M11* and *alr1-P3M11*, modified in module M11, were C-terminally tagged with GFP and analyzed via fluorescence microscopy. (C) Module M11, comprising 27 aa, was fused to the GFP-epitope, expressed in strain BY4742 and analyzed by fluorescence microscopy.

Figure 6. Lack of Pep12p differently affects membrane location and degradation of Alr1p isomers. Cells, precultured in SD-medium supplemented with 10 mM Mg^{2+}, were washed and further incubated in SD-medium containing 10 µM or 10 mM Mg^{2+} for 3h and examined by differential interference contrast (*panel DIC*) and fluorescence microscopy with a filter specific for GFP (*panel GFP*). (A) Cells of strain BY *pep12Δ* expressing GFP-tagged wild-type Alr1p or N-terminally truncated isomers incubated with 0.01 mM (a) and 10 mM Mg^{2+} (b). (B) Cells of strain BY *pep12Δ* expressing GFP-tagged wild-type Alr1p or Alr1p isomers deleted for internal modules incubated with 10 mM Mg^{2+}.
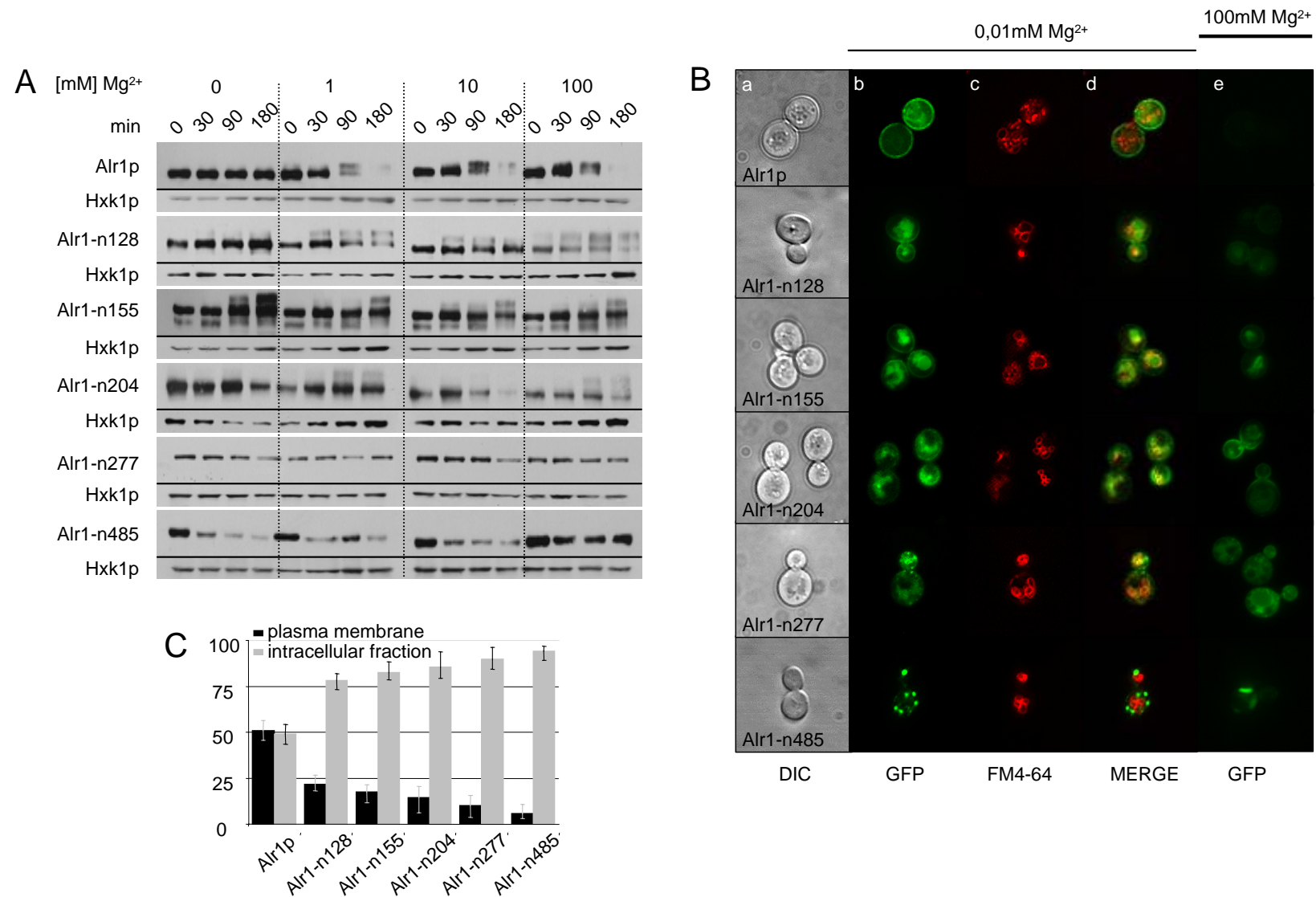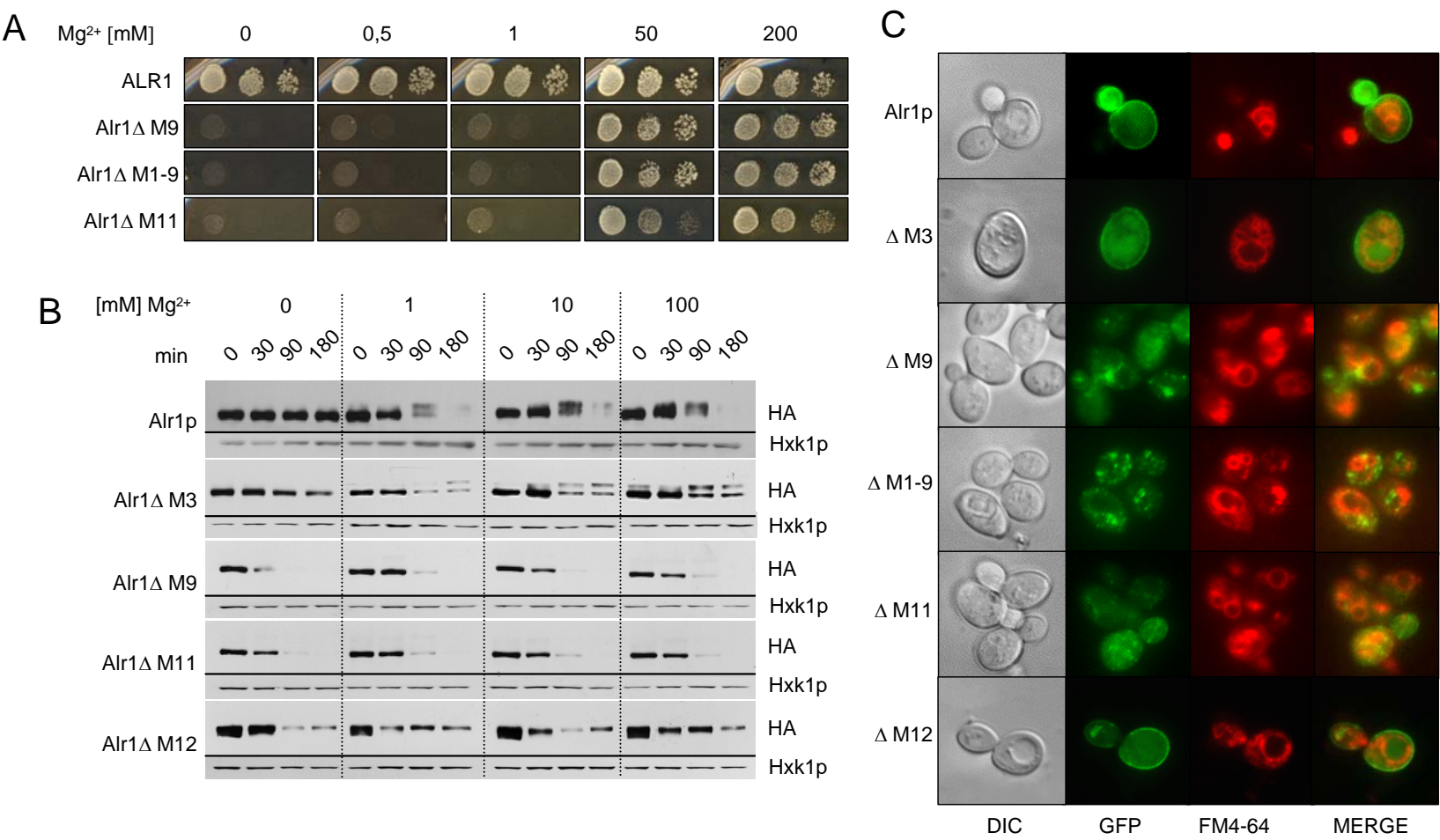
Figure 1. Schematic map of Alr1p constructs

**Figure 2.** Effects of N-terminal Alr1p deletions on Mg^{2+} dependent growth

A

	Alr1	Alr1-n128	Alr1-n155	Alr1-n204	Alr1-n277	Alr1-n485	AG012
25 µM	4.3	4.8	4.5	4.7	10.9	20.8	21.5
100 µM	3.9	3.6	3.6	3.6	5.7	9.4	9.1
1.5 mM	3.7	3.6	3.9	3.5	4.8	7.7	8.4
50 mM	3.7	3.8	3.5	3.4	3.5	3.5	3.5

Figure 3. Mg^{2+} specific degradation of Alr1p strongly depends on the N-terminal sequence.

Figure 4. Short intragenic sequence deletions affect Alr1p function

A

25 µM Mg

100 µM Mg

25 mM Mg

2 mM Mg

100 mM Mg

B

Alr1-P1M11

Alr1-P3M11

DIC   GFP

C

M11-GFP

empty-GFP

DIC   GFP   MERGE

Figure 5. The helix in module M11 is crucial for Alr1p translocation to the plasma membrane
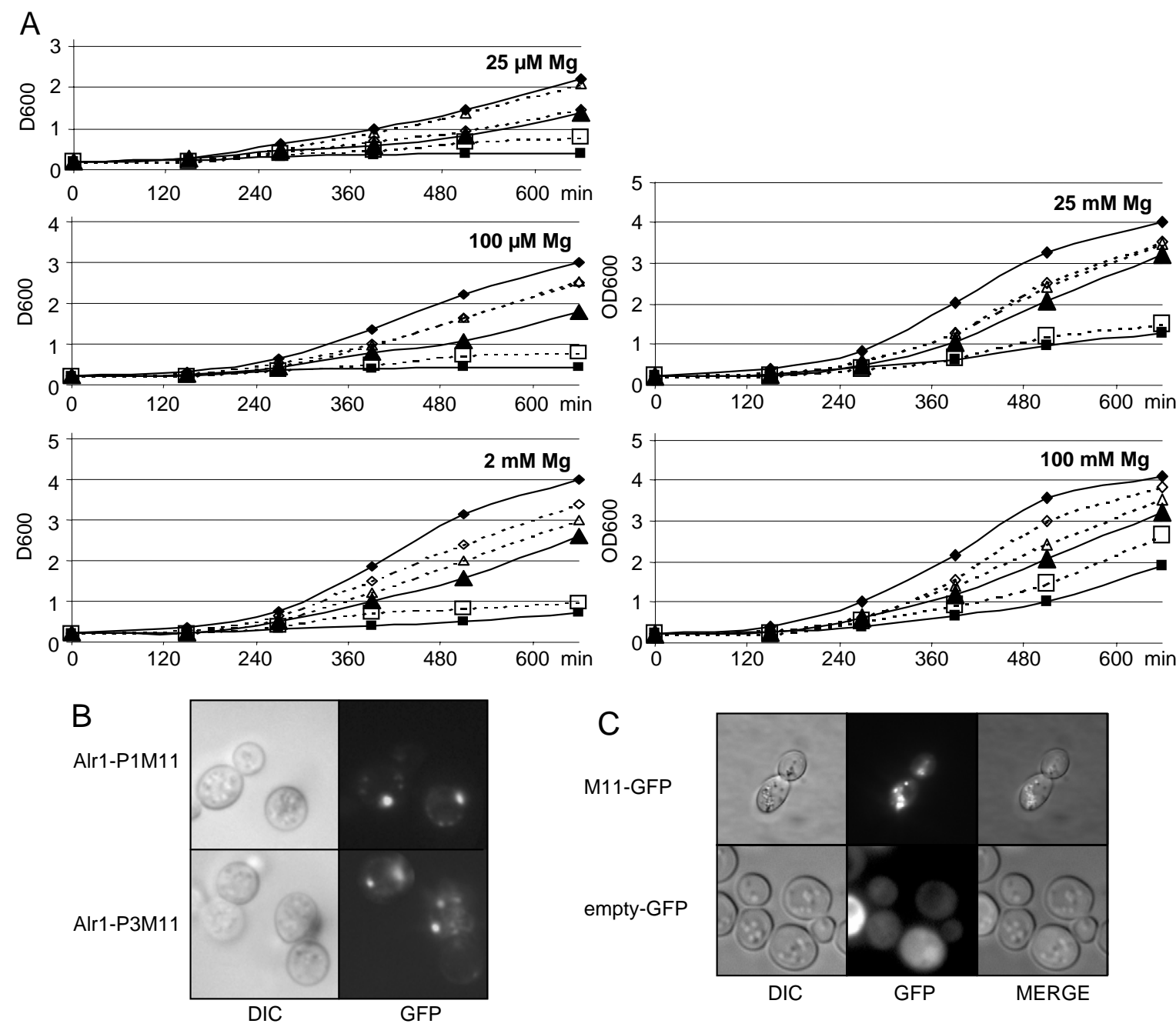
Figure 6. Lack of Pep12p differently affects membrane location and degradation of Alr1p isomers.
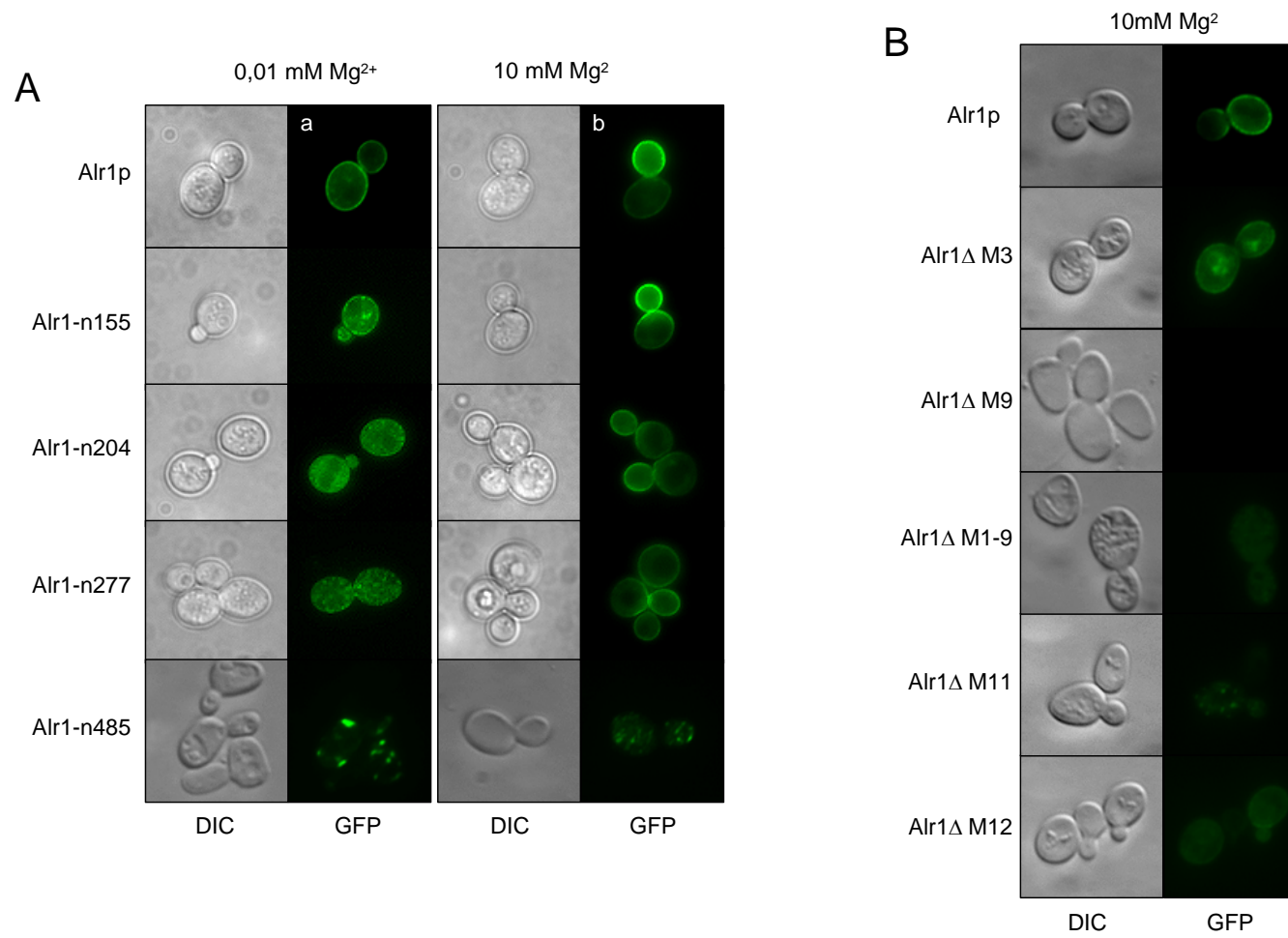
SUPPLEMENTARY DATA

Figure 1.

A model for Pep12p interference with Alr1p protein secretory and endocytic pathways in wild-type (A) and *pep12Δ* mutant yeast cells (B). Standard transfer routes of Alr1p are shown in solid arrows. Dashed arrows indicate alternative pathways of Alr1p as a consequence of *pep12Δ* defects in retrograde traffic into the prevacuolar compartment (A) Wild type Alr1p enter the secretory pathway from endoplasmic reticulum (ER) to trans Golgi network (TGN) and further to the plasma membrane (PM), either directly from TGN or via early endosome (EE). Its mutant isomers retaining modules M9 and M11 also can reach PM, but a fraction of non-native Alr1p, particularly with larger N-terminal deletions, was not qualified for transport to PM and diverted from TGN to pre vacuolar complex (PVC) and the vacuole (2). Most severely affected Alr1p isomers, i.e. Alr1n-485 truncation and M9, M1-9, and M11 modules, failed to appear in PVC and vacuole, and are likely directed to endoplasmic reticulum associated degradation (ERAD before reaching TGN (1). Addition of Mg2+ to the wild type cells induces ubiquitination of Alr1p at the PM followed by endocytosis. (2) Internalized protein moves through the EE and reaches the PVC; constitutive recycling back to the PM is not excluded (3). Finally, Alr1p is sorted to the vacuole for degradation. This last step is highly dependent on Pep12p, which controls retrograde traffic into the prevacuolar compartment (4). (B) In *pep12Δ* cells, transport to PM of wild-type Alr1p is unimpaired. Mutant Alr1p isomers with deletions not including M9 and M11 modules also reach PM at least partially. In *pep12Δ* cells their entering into PVC is blocked and therefore they stay in the EE to PM retrieving process, even in presence of high Mg2+. Alr1p isomers Alr1n-485, M9, M1-9 and M11, which do not reach TGN, are subject to ERAD and independent of *PEP12* presence or absence (1) (for more details see text).

Supplementary data: **Figure 1**. A model for Pep12p interference with Alr1p protein secretory and endocytic pathways in wild-type (A) and *pep12Δ* mutant yeast cells (B).
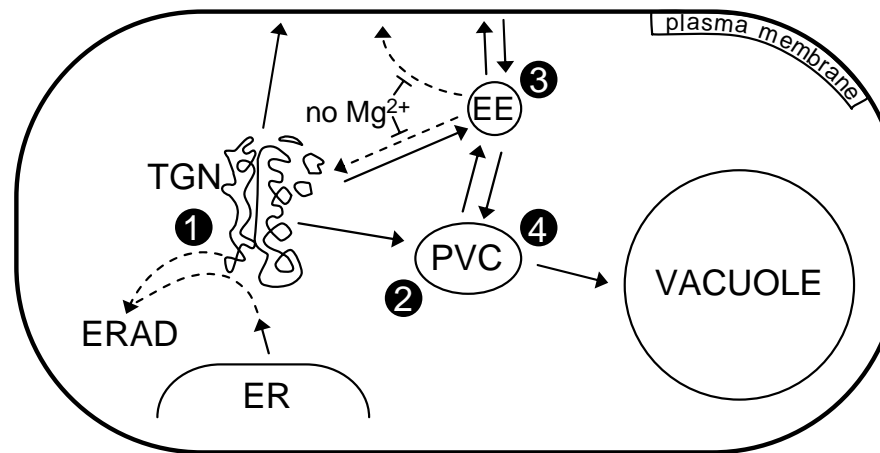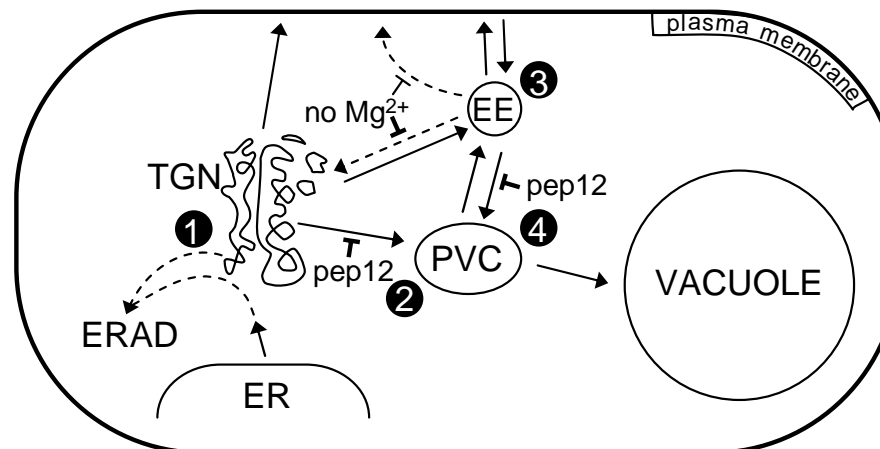
Table 1. Plasmids and oligonucleotides used for N-terminal modifications in *ALR1*

Plasmids	primer	sequence
(A) N´-terminal truncations	N´-terminal truncations	
YIpMALR1HA-wt	ALR1HA-WT_f	5´-AAAGCG**ACTAGT**CATTTTACCATG-3´
	ALR1HA-WT_r	5´-AAA**GTCGAC**TGTCGTAGCGGC-3´
YIpMalr-n128	ALR1HA-n128_f	5´-AATGTGGGAAGCGTA**ACTAGT**AGG-3´
	ALR1HA-n128_r	5´-AAA**GTCGAC**TGTCGTAGCGGC-3´
YIpMalr-n155	ALR1HA-n155_f	5´-TTTTCCAG**ACTAGT**CCACTCCATG-3´
	ALR1HA-n155_r	5´-AAA**GTCGAC**TGTCGTAGCGGC-3´
YIpMalr-n204	ALR1HA-n204_f	5´-TTGATAC**ACTAGT**CAAG<u>ATG</u>GCTAAACC-3´
	ALR1HA-n204_r	5´-AAA**GTCGAC**TGTCGTAGCGGC-3´
YIpMalr-n277	ALR1HA-n277_f	5´-AAGAAGAT**ACTAGT**TTCCCTATG-3´
	ALR1HA-n277_r	5´-AAA**GTCGAC**TGTCGTAGCGGC-3´
YIpMalr-n485	ALR1HA-n485_f	5´-TTGACTGC**ACTAGT**TATCAGAATG-3´
	ALR1HA-n485_r	5´-AAA**GTCGAC**TGTCGTAGCGGC-3´
(B) Modules	Modules	
YCp22ALR1HA	WT-(p:mU3f)	5´-CAAACTAGTTGGCTAACACGATG-3´
	WT-(p:mU4r)	5´-ATCTTCGATTGCATCTGC-3´
YCp22ALR1HA M1	M1-5´ p:m1r	5´-CCTG<u>GAATTC</u>ATCTTCAAATCC-3´
	M1-3´ p:m1f	5´-TAACT<u>GAATTC</u>GCGAGG-3´
YCp22ALR1HA M2	M2-5´ p:m2r	5´-TCGC<u>GAATTC</u>AGTTAAAATGG-3´
	M2-3´ p:m2f	5´-ATGT<u>GGAATTC</u>AATATACAC-3´
YCp22ALR1HA M3	M3-5´ p:m3r	5´-TATT<u>GAATTC</u>CACATAAAGC-3´
	M3-3´ p:m3f	5´-TTCTACT<u>GAATTC</u>TCAGG-3´
YCp22ALR1HA M5	M5-5´ p:m5r	5´-TTCGT<u>GAATTC</u>ACTTGC-3´
	M5-3´ p:m5f	5´-ACAC<u>GAATTC</u>AAATCTG-3´
YCp22ALR1HA M6	M6-5´ p:m6r	5´-ATTT<u>GAATTC</u>GTGTGG-3´
	M6-3´ p:m6f	5´-ATCT<u>GAATTC</u>TCATCTATCAATCC-3´
YCp22ALR1HA M7	M7-5´ p:m7r	5´-ATGA<u>GAATTC</u>AGATGTGG-3´
	M7-3´ p:m7f	5´-GGAT<u>GAATTC</u>GATGATACATTGG-3´
YCp22ALR1HA M8	M8-5´ p:m8r	5´-TATCATC<u>GAATTC</u>ATCCG-3´
	M8-3´ p:m8f	5´-TCAG<u>AATTC</u>GAAGAAGATG-3´
YCp22ALR1HA M9	M9-5´ p:m9r	5´-TCTTC<u>GAATTC</u>TTGAGAATCTCTCG-3´
	M9-3´ p:m9f	5´-TATA<u>GAATTC</u>GATGAACTGG-3´
YCp22ALR1HA M1-9	M1-9-5´ p:m1r	5´-CCTG<u>GAATTC</u>ATCTTCAAATCC-3´
	M1-9-3´ p:m9f	5´-TATA<u>GAATTC</u>GATGAACTGG-3´
YCp22ALR1HA M11	M11-5´ p:m11r	5´-TTCATC<u>GAATTC</u>TATACC-3´
	M11-3´ p:m11f	5´-TGCCCAAC<u>GAATTC</u>AAGTACAGTAACG-3´
YCp22ALR1HA M12	M12-5´ p:m12r	5´-TACTT<u>GAATTC</u>GTTGG-3´
	M12-3´ p:m12f	5´-TGCCCTA<u>GAATTC</u>ACACC-3´
YCp22ALR1HA M13	M13-5´ p:m13r	5´-TTGGTGT<u>GAATTC</u>TAGG-3´
	M13-3´ p:m13f	5´-AAGAAG<u>GAATTC</u>GAGC-3´
YCp22ALRG3M9	Gx3M9-r	5´-GGCAT<u>GAATTC</u>ACCACCACCTTCTTCCGTCTCTTGAG-3´
	Gx3M9-f	5´-GGTGGTGGT<u>GAATTC</u>ATGCCACCACAATTGC-3´
YCp22ALRKKM9	KKM9-r	5´-AACATCCTTCTTCGTCTCTTGAGAATCTCTCG -3´
	KKM9-f	5´-AAGAGACGAAGAAGGATGTTTGTTTCCC-3´
YCp22ALRKKM11	KKM11-r	5´-TGAGCGTACTTCTTCAGTTCATCGAAATCTATACC-3´
	KKM11-f	5´-GAACTGAAGAAGTACGCTCAGTTTGC-3´
YCp22ALRP1M11	P1M11-r	5´-TACTCTTCAGGTTCATCGAAATCTATACC-3´
	P1M11-f	5´-TTCGATGAACCTGAAGAGTACGCTCAG-3´
YCp22ALRP3M11	P3M11-r	5´-TTCTCAGGGTTTGCAGGCTGAGCAGGCTCTTCCAGTTC-3´
	P3M11-f	5´-GAAGAGCCTGCTCAGCCTGCAAACCCTGAGAAGAGTC-3´
universal for. primer	p:mU1f	5´-AAAGCGACTAGTCATTTTACCATG-3´
universal rev. primer	p:mU2r	5´-ATCAACGTCATTGTCTTACG-3´
pUG34M11	m9f-BamHI	5´-TATA<u>GGATCC</u>GATGAACTGG-3´
	m12rEco+STOP	5´-TACTGTACTT<u>GAATCC</u>TTAGGGCACTTGC-3´

The cleavage sites for *Spe*I and *Sal*I are indicated in bold letters. The introduction of an ATG instead of a CTG in construct *alr1-n204* is marked as underlined. Digestion site for *EcoR*I enzyme (underlined) was introduced in primers for 5´ and 3´ module segments to enable ligation of the respective *ALR1* fragments. The ligation product was used as a template in a second step of PCR amplification.

Table 2. Position and sequence of modified residues in Alr1p modules.

Module	Length (aa)	Position	Removed or substituted residues
WT	859	no	no
M1	838	99 - 119	QGMDETVAHHQLRASAILTSN
M2	839	120 - 139	ARPSRLAHSMPHQRQLYVES
M3	836	140 - 162	NIHTPPKDVGVKRDYTMSSSTAS
M5	840	179 - 197	TKVRKSSLVSPVLEIPHES
M6	837	198 - 219	KSDTHSKLAKPKKRTYSTTSAH
M7	839	220 - 239	SSINPAVLLTKSTSQKSDAD
M8	828	240 - 270	DDTLERKPVRMNTRASFDSDVSQASRDSQET
M9	838	271 - 291	EEDVCFPMPPQLHTRVNGIDF
M1-9	682	99 - 291	deletion of M1 to M9
M11	832	292 - 318	DELEEYAQFANAEKSQFLASLQVPNEQ
M12	833	319 - 344	KYSNVSQDIGFTSSTSTSGSSAALKY
M13	836	345 - 367	TPRVSQTGEKSESTNETEIHEKK
G3M9	859	273 - 277	$D_{273}G$, $V_{274}G$, $C_{275}G$, $F_{276}E$, $P_{277}F$
KKM9	859	271 - 272	$E_{271}K$, $E_{272}K$
KKM11	859	295 - 296	$E_{295}K$, $E_{296}K$
P1M11	859	294	$L_{294}P$
P3M11	859	297, 300, 303	$Y_{297}P$, $F_{300}P$, $A_{303}P$

Table 3. Summary of phenotypical modifications generated by mutations in the N-terminal domain of Alr1p

| Isoforms | presence of | | $alr1\Delta$ | Alr1 turnover | | Alr1 topology | | | | | | Alr1 topology | | | |
| | VCFP | α-helix | growth on low Mg^{2+} | high Mg^{2+} | | low Mg^{2+} | | | high Mg^{2+} | | | low Mg^{2+} | | high Mg^{2+} | |
				modif.	degrad.	P	C	V	P	C	V	P	C	P	C
Alr1p	yes	yes	+++	+++	+++	+++	+	+	-	-	-	+++	+	+++	-
alr1-n128	yes	yes	+++	+++	++	++	+	++	-	+	+	nd	nd	nd	nd
M1, 2, 5, 6, 13	yes	yes	+++	+++	+++	+++	+	+	-	-	-	+++	+	+++	-
alr1-n155	yes	yes	+++	++	+	++	+	++	+	+	++	++	++p	+++	-
M3Δ140-162	yes	yes	+++	+++	+++	+++	++	++	-	-	+	++	++	++	++
alr1-n204	yes	yes	+++	+	+	+	++	++	+	+	+	++	++p	+++	-
M7Δ220-239	yes	yes	+++	+++	+++	++	+	++	-	-	-	++	+	+++	-
M8Δ240-270	yes	yes	+++	+++	+++	++	+	++	-	-	-	++	+	+++	-
M12Δ319-344	yes	yes	+++	+++	+++	+++	+	+	-	+	+	+++	+	+	+
alr1-n277	no	yes	+	-	-	+	++p	-	+	++	++	+	++p	+++	-
alr1-n485	no	no	-	-	+++*	-	++p	-	-	++	-	-	++p	-	++p
M9 Δ271-291	no	yes	-	-	+++*	-	++p	-	-	++p	-	-	++p	-	-
M1-9Δ99-291	no	no	-	-	+++*	-	++p	-	-	++p	-	-	++p	-	+
M11Δ292-318	yes	no	-	-	+++*	-	++p	-	-	++p	-	-	++p	-	+p
G3M9	no	yes	+++	nd	nd	++	+	+	-	+	+	nd	nd	nd	nd
KKM9	yes	yes	++	nd	nd	++	+	+	-	+	+	nd	nd	nd	nd
KKM11	yes	yes	+++	nd	nd	++	+	+	-	+	+	nd	nd	nd	nd
P1M11	yes	no	-	nd	nd	-	+p	-	-	+p	-	nd	nd	nd	nd
P3M11	yes	no	-	nd	nd	-	+p	-	-	+p	-	nd	nd	nd	nd

(*) - rapid degradation independent of Mg^{2+}; (p) - punctuated fluorescence; (P) - plasma membrane; (C) - cytoplasmic fraction; (V) - vacuolar fraction; classification of growth, protein modification or degradation and localization: (+++) - strong; (++) - medium; (+) - weak; (-) - no; (nd) - not defined.

6. DISCUSSION

The yeast *Saccharomyces cerevisiae* has proved to be an ideal experimental model organism. The convenience of its biology together with technical advantages, as the manifold applications and methods of molecular genetics, resulted in the importance of *Saccharomyces cerevisiae* in studies elucidating innumerous cellular functions and pathways, *e.g.* cell cycle, organelle biogenesis, signalling pathways and many other cell functions including transport mechanisms (Botstein & Fink, 1988). In my thesis, yeast was taken as the preferential research system to address the functional characterization of Alr proteins, which are essential for the Mg^{2+} homeostasis in *Saccharomyces cerevisiae*. The *ALR* genes were identified for the first time due to their ability to confer Al^{3+} resistance when overexpressed by MacDiarmid and Gardner (MacDiarmid & Gardner, 1998). The *Sc*Alr proteins belong to the large superfamily of 2-TM-GxN type transporters forming likely membrane potential-driven ion-selective channels in their cognate membranes to control Mg^{2+} homeostasis. This family is widely distributed throughout the prokaryotic and eukaryotic world, including the bacterial CorA-like proteins, the fungal Alr1-like homologues, and the Mrs2-like proteins, found from yeast to human. The typical features of this protein family are the formation of 2 TMD´s with the highly conserved GMN signature at the end of the first TM and a relatively short C-terminus. The fungal representatives of this family developed a long, largely unstructured N-terminus, which is missing in the bacterial CorA-subfamily. (Knoop et al, 2005). Generally, all members of the CorA-Mrs2-Alr1 family of divalent metal ion transporters reveal low sequence homology with respect to the prototypical CorA protein. Despite such sequence divergence Alr1p and Alr2p proteins apparently show homology to this family, as supported by our data collected in this work.

At present the knowledge of the molecular fundament of Mg^{2+} homeostasis is still poorly defined, though many components of the Mg^{2+} transport network are investigated. Although extensive data for the existence of various regulated Mg^{2+} transporters (Odblom & Handy, 1999; Quamme & Rabkin, 1990; Schweigel et al, 2006; Schweigel et al, 2000), only two plasma-membrane localized proteins have been identified at the molecular level, namely, TRPM6 and TRPM7, which are ion channels of the melastatin-related transient receptor potential family, and Mrs2p, a channel located in the inner mitochondrial membrane (Chubanov et al, 2005; Kolisek et al, 2003; Schmitz et al, 2003). Further

evidences reporting functional propensities of other transporters like bacterial CorA, MgtA/B and MgtE (Romani, 2007; Smith & Maguire, 1998; Smith et al, 1995), yeast vacuolar magnesium utilization protein (VUM1p) (Wood et al, 2002), a plant vacuolar Mg^{2+}/H^{+} exchanger AtMHX (Shaul et al, 1999), and higher eukaryotic solute carrier family 41 (SLC41) (Goytain & Quamme, 2005b; Goytain & Quamme, 2005c; Sahni et al, 2007; Wabakken et al, 2003), the ancient conserved domain protein (ACDP) subtype 2 (Goytain & Quamme, 2005a; Wang et al, 2003), a protein termed magnesium transporter 1 (MagT1) (Goytain & Quamme, 2005d), the protein NIPA1 (Goytain et al, 2007), or PCLN-1 (Simon et al, 1999) have significantly expanded the field of research into cellular Mg^{2+} transport systems. Yet functional analysis of several cell biology aspects of the fungal transport system formed by Alr proteins presented in this work contributes valuably to the understanding of Mg^{2+} homeostasis.

The main conclusions from the study presented here in the first publication are that both, Alr1p and Alr2p are Mg^{2+} transporters, localized in the plasma membrane of *Saccharomyces cerevisiae*, which exist in oligomeric complexes and that the C-terminal domain is essential for the oligomerization of the protein monomers. At the same time, the crystal structure of the CorA protein of *T. maritima* was identified by (Eshaghi et al, 2006; Lunin et al, 2006; Payandeh & Pai, 2006). The published structure confirmed the ability of these proteins to form multimers, generating a channel-like architecture (Eshaghi et al, 2006; Lunin et al, 2006; Payandeh & Pai, 2006). Five monomers of CorA create a homopentameric oligomer with a central ion-conduction pathway made by helix $\alpha 7$, partially building the transmembrane domain TM1, which is surrounded by helix $\alpha 8$, creating the 2nd TMD (as mentioned in the chapter "Introduction"). Channel formation by the oligomerization of multiple monomers was also reported for other transport proteins with two or three TM domains like Ctr3 and hCtr1 as homotrimers (Lee et al, 2002a; Pena et al, 2000), KcsA and KirBac1.1 as homotetramers (Doyle et al, 1998; Kuo et al, 2003) or MscL as homopentamer (Chang et al, 1998). We have provided biochemical and genetic evidences for the physical association between either Alr1 protein monomers, or Alr1p and Alr2p, and Alr2p, indicating that these proteins can exist as homo- and hetero-oligomers. Both, cross-linking analysis, indicating the formation of at least tetramers, and the *in vivo* mating-based split-ubiquitin system resulted in the formation of oligomerization events (Wachek et al, 2006).

Electrophysiological analyses are available for Mrs2 and Alr1p (Liu et al, 2002; Schindl et al, 2007; Weghuber et al, 2006). Results found by these authors substantiate the formation of a high conductance Mg^{2+} channel. Furthermore, Mrs2 protein was found to form higher oligomeric complexes up to pentamers (Kolisek et al, 2003).

The ability of proteins conducting transmembrane fluxes to occur as oligomers is favourable by the dimensional scaffold. Both, amino – and carboxy termini are in the protein connected by several TM-spanning domains that are physiologically juxtaposed to create the amino acid-lined pore, which acts as the physical conduit for the ion passes from one side of the membrane to the other. The accessibility of channel-type transporter for proper substrate ion is subjected to appropriate signals generated by the cell (Dubyak, 2004). Such common arrangement was also reported for bacterial CorA protein by the revelation of crystal structure. The information need for proper channel function is encoded in the protein sequence with both N- and C-terminal ends facing the cytosol, one of which comprise 2 TM helical segments connected by a short periplasmic loop. The C-terminal region seems to be highly sensitive to modifications, what revealed an array of mutational studies in all members of CorA-Mrs2-Alr1 family. The interference with various conserved regions resulted in the isolation of mutants with reduced or improved Mg^{2+} transport capacity. Almost all amino acid substitutions in this central part of the protein, particularly in Y/FGMN signature, resulted in a changed phenotype with negative effects (Lee & Gardner, 2006; Szegedy & Maguire, 1999; Weghuber et al, 2006). The prominent role ascribed to transmembrane domains together with adhesive N- and C-termini of the protein in formation of functional translocation pathway was also highlighted in my recent work. Dominant negative effects were exerted by single mutations localized in each TM affecting presumably the flexibility and the integrity of a predicted hydrophobic core (Kern et al, 2005) and transmembrane domain conformation, respectively (Wachek et al, 2006). The coexpression of mutated Alr1p isomers with native Alr1p exerted a dominant negative effect on Mg^{2+} uptake by Alr1p. Similar reduction in Alr1p activity was also found after simultaneous coexpression with modified Alr2p. This is consistent with the idea that Alr proteins form oligomeric complexes to constitute active metal translocation pathway. The presence of inactive proteins in the oligomer renders them defective by possible influencing of channel architecture. This peculiarity was similarly used to infer an oligomeric structure for EmrE, a 4-TM domains transporter from *E. coli* (Yerushalmi et al, 1996) and ammonia transporters in *S. cerevisiae* (Marini et al,

2000) and in *A. nidulans* (Monahan et al, 2002). The severity of the phenotype associated with the sequence modification reflects the functional importance of intact alpha helical structures in this critical region, as unveiled the CorA crystal structure. Thus, there is worth of assume that like in the case of CorA protein, where Lunin and colleagues proposed asparagine residue from GMN motif as a critical component of pore entrance (Lunin et al, 2006), analogous scenario may take place in other members of CorA family.

Furthermore, the importance of negative charges in the small portion of the protein exposed on the extracellular face of the membrane, comprising a short loop between TMs was underlined. In most CorA-related proteins and in about half of the available Alr1-related sequences of *Ascomycota* the sequence inspection revealed highly conserved glutamic acid or glutamine residues, respectively. Only the exception is the Alr2p with unparalleled presence of positively charged arginine at this conserved position. Our further analysis of Alr2p functionality after R768E mutation confirmed the Alr2 moderated activity as a result of intrinsic charges exchange. Such experiment with inverse substitution was also carried out in Mrs2p, where positively charged lysine was introduced instead of negative glutamic acid residue giving contrary effect; the mutated Mrs2p isomer showed complete loss of Mg^{2+} transport activity (Weghuber et al, 2006). Thus, these observations support the potential relevance of conserved sequence stretches in the protein "surface" for the Mg^{2+} transport capacity linked with selection and electrostatic attraction of the substrate (Lunin et al, 2006; Payandeh & Pai, 2006).

The function of the C-terminal tail of the Alr1 protein was investigated, generating C-terminal truncations. Our experimental data are in agreement with a previous report of Lee and Gardner, showing that deletions of up to 53 amino acids at the C-terminus are dispensable for Mg^{2+} uptake (Lee & Gardner, 2006). In our study, deletions up to 36 residues has been proved to have no effect on protein functionality, whereas the truncation of 63 amino acids, enclosing the complete C-terminal tail, resulted in a significant growth defect and partial mislocalization of the protein. Moreover, truncation of the C-termial portion had a strong influence in the formation of oligomers as has been shown by the use of the split ubiquitin system. Truncations, which include the transmembrane regions, completely have destroyed the protein function. Taken together, the C-terminal part of Alr1p is not essential for the formation of basic sphincter, but most likely is involved in oligomerization and anchoring the protein in the plasma membrane. In contrast to the C-terminus, which is quite homolog for all members of the CorA-superfamily, the N-termini

of CorA, Mrs2 and Alr1 proteins are highly diverse in sequence and length. Sequence analyses and homology searches of the long N-terminal tail, common for the fungal Alr-subfamily, did not result in the detection of defined signals or protein structures.

To investigate putative functions, encoded in this sequence, a set of mutants with amino-terminal truncations was constructed. The investigations focused on the stability of the proteins and on the localization, distribution and translocation of the generated isomers. Previous results prove a magnesium dependent stability of the Alr1 protein. A surplus of magnesium to the growing cells causes hyperphosphorylation of the protein, which probably designates the protein for degradation following the endocytotic pathway, finalized in the yeast vacuole. Interestingly, as has been similarly shown previously by experiments from Lee and Gardner (Lee & Gardner, 2006), the truncation of up to 240 amino acids did not destroy the transport function of the Alr1p and cellular growth as well as magnesium uptake were not affected. But, by determination of the protein stability of the generated isomers, we observed a significant variation in protein modification *e.g.* phosphorylation and stability, in context with the treatment with magnesium. The rate of protein degradation decreased directly with the shortage of the N-terminus. This probably reflects the loss of putative modification sites in the N-terminal domain, required as a signal to enter the endocytotic degradation pathway. Furthermore, not only the modification decreased, also the stability of these isomers increased over the observed treatment with magnesium. In context with our observations, using GFP-tagged proteins, the enhanced stability of the protein isomers was caused by inhibition of steps in the endocytotic degradation pathway, required for vacuolar degradation. The isomeric Alr1 proteins seemed to be entrapped in early (EE) or late endosomal (LE) vesicles, and excluded from degradation.

According to the work from Lee and Gardner (Lee & Gardner, 2006), truncation of the N-terminal 240 residues of Alr1p did not result in loss of the Mg^{2+}-transport function of Alr1p. However, the deletion of 277 residues in Alr1-n277 and 485 residues in Alr1-n485 clearly influenced the transport capacity of Alr1p. Cells expressing Alr1-n277 showed slow growth at low Mg^{2+} conditions, whereas growth of cells expressing Alr1-n485 was not distinguishable from cells deleted for *ALR1*. Nevertheless, these two proteins were found to be completely different in their behaviour. Alr1-n277 caused high protein stability, whereas Alr1-n485 was degraded in a Mg^{2+} independent manner, most probably via the proteosome.

Avoiding the comprehensive damage of the whole Alr1p protein structure and to better define probable functional regions, mutants with serial deletion modules encompassing up to 30 amino acids were designed. This set of deletions confirmed the importance of N-terminal region ranging between residues 277 to 320 for proper Alr1p protein processing and cellular location. The deletion of modules M1 to M8 and M12 to M13, covering internal amino acids from Q99 to T270 and K319 to K367, respectively, neither affected the localization and the Mg^{2+} transport function of the protein, nor significantly influenced the stability of these Alr1p isomers. However, deletion of modules M9 and M11, ranging from E271 to F291 and D292 to Q318, respectively, seriously disturbed vesicular transport and stability of Alr1p. The sequence from D290 to S311 exhibits a high probability to form a stable alpha helical structure recognizable in a wide range of Alr1 proteins. It shows some sequence conservation and is preceded by another sequence of considerable conservation. Mutational changes of the local polarity of the Alr1 protein by substitution of negatively charged amino acids by lysine residues within the helix or in the preceding motif did not significantly affect the anterograde pathway of the protein to the plasma membrane, protein stability and degradation. However, insertion of one or several prolines in the helix led to a complete collapse of Alr1p translocation.

N-terminal Alr1p deletion isomers which retained these M9 and M11 modules unchanged reached the plasma membrane, showed Mg^{2+}-dependent phosphorylation and appeared in prevacuolar and vacuolar compartments, and thus behaved similar to wild-type Alr1p which we previously have shown to be vacuolarly degraded (Graschopf et al, 2001). Also, their presence in the plasma membrane was stimulated in the absence of Pep12p, a multifunctional syntaxin that is required for endocytic and retrograde traffic into the prevacuolar compartment. Accordingly, these isomers reached the endosomal recycling compartment. In contrast, Alr1p isomers with mutations or deletions affecting modules M9 and M11 (Alr1ΔM9, -ΔM11, Alr1-P1M11, -Alr1-P3M11, Alr1-n485, Alr1ΔM1-9,) accumulated in punctuated spots in the cytoplasm, their degradation is independent of the presence or absence of Mg^{2+} and of Pep12p and they were not seen in prevacuolar or vacuolar compartments. They are likely to be subject to proteasomal degradation. Therefore we assume that the punctuated spots in these mutants signify an arrest in ER-to-Golgi transport and that sequences in M9/M11 modules constitute a transport signal.

Beside ER protein quality control constituting the first selection barrier for newly synthesized proteins (Bonifacino & Lippincott-Schwartz, 1991), there is growing evidence

for a post-endoplasmic reticulum quality control mechanism functioning at the Golgi level (Chang & Fink, 1995; Hsu et al, 1991; Jenness et al, 1997; Li et al, 1999; Luo & Chang, 2000; Minami et al, 1987). Like the ER, the Golgi complex may also make conformational-based sorting decisions leading to disposal of selected proteins protecting the cell from damage caused by deployment of non-native proteins in the secretory pathway (Arvan et al, 2002). Such defective proteins are routed most often via the endosomal system for degradation. This occurs in the vacuole, which most prominent role is the degradation of macromolecules, apart from function in the storage of metabolites and the regulation of ion homeostasis in the cytosol (Klionsky et al, 1990).

Transport from late Golgi to the vacuole in yeast proceeds via an intermediate endosome-like compartment (Vida et al, 1993). This process is controlled by Pep12p (Becherer et al, 1996; Prescianotto-Baschong & Riezman, 2002) along with other vacuolar protein sorting (VPS) proteins. Pep12p is a multifunctional syntaxin that is required for biosynthetic, endocytic and retrograde trafficking into the prevacuolar compartment (Becherer et al, 1996; Blanchette et al, 2004; Bryant et al, 1998; Gerrard et al, 2000; Prescianotto-Baschong & Riezman, 2002).

This t-SNARE protein was used to track the trafficking behaviour of plasma membrane protein Alr1p in the endosomal system. We showed that deletion of Pep12 protein important for control of *trans*-Golgi to the late endosome route did not interfere with the traffic of Alr1p to the plasma membrane under conditions stabilizing Alr1p. In *pep12Δ* cells exposed to external conditions promoting Alr1p inactivation, a fraction of Alr1p wild-type was rescued from vacuolar degradation and delivered to the cell surface. It is consistent with previous reports where showed that inactivation of traffic step between Golgi apparatus and PVC results in cargo mislocalization to the plasma membrane instead of to the vacuole.

Furthermore, additional support comes from studies with N-terminal mutated isomers of Alr1p. In *pep12Δ* mutants exposed to high Mg^{2+} concentration, Alr1p expressed from almost all amino-truncated *ALR1* variants was localized merely at the cell surface, whereas cells cultivated without Mg^{2+} revealed Alr1p distribution similar to that of wild-type cells. In contrast, alr1-n485 mutant version of Alr1 protein together with M9, M1-9 and M11 Alr1p modules behave quite differently showing exclusively internal dot-like fluorescence in wild-type yeast cells. These mutant proteins were trapped into intracellular vesicles corresponding presumably to the post-Golgi or endocytic structures, but unlikely above

described Alr1p variants did not co-localize with vacuolar lumen. Despite of inactivation of major converging point for secretory and endocytic pathways – PVC/LE – treatment with high Mg^{2+} concentration promoted decline of fluorescence intensity of these Alr1p chimeras corresponding to the protein degradation. This was also observed when translation inhibitor cycloheximide (CHX) was used to stop the constitutive protein expression controlled by the strong methionine promotor. Interestingly, in *PEP12* deleted cells only wild-type Alr1p and two Alr1p modules M3 and M12 showed cell surface staining in cycloheximide presence similar to that of wild-type yeast cells. All other N-terminal truncations revealed loss of surface-localized fluorescent signal and a concomitant appearance of an intracellular puncta staining.

Why the presence of cycloheximide does exert such striking and varied changes in some amino-terminal Alr1p mutants? As was shown, cycloheximide contributes to the ubiquitin state of the cell. Treatment with this chemical compound highly depletes cellular levels of ubiquitin, what by turn may indirectly lead to perturbation of some aspects of cellular physiology like targeting, degradation, trafficking, etc. (Hanna et al, 2003). According to the model where deubiquitination results in protein stabilization, plasma membrane proteins should either stay at the cell surface all the time during exposition to factors triggering its degradation or be retrieved back to the cell surface from degradative pathway as a consequence of ubiquitination loss as was shown for some plasma membrane proteins (see text below). This is in contradiction with results obtained for most of Alr1p mutants. Only for fully expressed Alr1 protein was observed protein stability consistent with this model, whereas remaining mutants exhibited dispersion puncta staining into the cell interior indicatinig unaffected internalization process, but impaired moving back to the cell surface when given that Alr1p recycle between early endocytic compartments and the plasma membrane. On the other hand, treatment with cycloheximide results in a strong induction of *UBI4*, a major stress-inducible ubiquitin gene (Finley et al, 1987). This compensatory response might reflect a mechanism designed to restore ubiquitin levels. However, in the presence of strong translational inhibition, this response is insufficient to maintain ubiquitin status. Together, accumulation of N-terminal Alr1p mutants in early endocytic structures is tightly coupled with ubiquitination machinery. Cells exposed to cycloheximide change the cellular ubiquitin status, what may by turn account for a defective retrieval pathway from early endosome. Another possibility might be the implication of alternative ubiquitination types in internalization steps of mutant Alr1p

compared with wild-type. As a result of partial sequence deletion in connection with deprivation of potential ubiquitination sites Alr1p mutants employed compensatory ubiquitination mechanisms to provide efficient targeting for endocytosis followed by degradation. However, although such modification is enough to ensure sorting to the early endosome prevents efficiently recycling back to the plasma membrane. After targeting to the early endosome Alr1p truncations might end up further in the tubular extension of EE what occurs by default unless proteins are specifically retained in the vacuolar part of the sorting endosome. The tubules pinch off and develop into recycling endosome. According to this model, mutants which acquired such a specific signal after ubiquitination will be retained in the vacuolar part of the sorting endosome, whereas wild-type Alr1p that modification does not interfere with this process will be distributed into the tubules and thus funneled into the recycling pathway. It is thought that sorting into the recycling pathway is not a signal-mediated process, but instead occurs by default (Maxfield & McGraw, 2004), thus N-terminal Alr1p mutants might be freely sorted into both subcompartments of sorting endosome but only wild-type Alr1p is able to recycle back to the cell surface in *pep12Δ* cells. The following model is largely based on information gathered from mammalian cells about sorting events in the early endocytic pathway (Gruenberg & Stenmark, 2004; Maxfield & McGraw, 2004).

Based on our results, we assume that degradation of wild-type Alr1p and its N-terminal mutants with some exceptions occurs in both, biosynthetic and endocytotic pathways, via the prevacuolar compartment. Blockage of vesicles fusion at this LE level leads to accumulation of endosomal intermediates what in turn enhances protein recycling after sufficient vesicles saturation. In mutants defective in this t-SNARE protein, the endocytic pathway is impaired in fusion of early endosome-derived vesicles with the late endosome/prevacuolar compartment, but protein recycling from the early endosome to the plasma membrane appears not to have interference (Becherer et al, 1996; Gerrard et al, 2000; Holthuis et al, 1998). Although cells were exposed to high Mg^{2+} favouring Alr1p internalization followed by vacuolar degradation, strong fluorescent signal at the plasma membrane was still observed. This could be an indication of an equilibrium in which ongoing internalization is balanced by the recycling return of Alr1p back to the cell surface. Endocytic recycling also has been suggested for, as participating in the trafficking of other yeast membrane proteins, the chitin synthetase Chs3p, the vesicle-associated membrane protein (VAMP)-like vesicle soluble NSF attachment protein receptor Snc1p or

the yeast a-factor receptor Ste3p (Chen & Davis, 2000; Chuang & Schekman, 1996; Lewis et al, 2000).

However, not all Alr1p mutants used in our study revealed such phenotype. Some mutated Alr1p variants, in particular alr1-n485, M9, M1-9 and M11 were successfully degraded in *pep12Δ* mutant cells. Taken together, Alr1 proteins expressed from alr1-n485, M9, M1-9 and M11 isomers are subjected to distinct mechanism controlling protein degradation in comparison to Alr1p wild-type and other mutants. It might be possibly endoplasmic reticulum associated degradation (ERAD) that, unlike degradation process in the vacuole, does not require functional action of Pep12p and transition via prevacuolar compartment. Although mutated at N-terminus, various Alr1p mutants are differentially recognized for degradation at distinct cellular locales. A part of amino-terminal Alr1p truncations entirely escape ER associated quality control mechanism and after apparently normal targeting to the cell surface are able to sustain cell viability. However, residency of such proteins that avoid both ER and Golgi quality control mechanisms is transient as they are rapidly endocytosed and degraded by vacuolar/lysosomal proteases (Fayadat & Kopito, 2003; Ferreira et al, 2002). Besides, these Alr1p mutants show also truncation size-dependent secretion defect and direct sorting to the degradative pathway indicated by intracellular puncta staining coincident with the vacuole. Unlikely, location of alr1-n485 together with M9, M1-9 and M11 Alr1p variants is restricted only to the cell interior. In spite of more dispersed staining compared with alr1-n485 M9, M1-9 and M11 are also unsuitable substrates for the vacuolar degradation. This notion might be supported also by efficient degradation in *pep12Δ* cells under high Mg^{2+} or by no co-localization of accumulated intracellular fraction with the vacuole in wild-type cells. Export from ER followed by missorting to any post-ER compartments has not to mean escape from protein selection machinery operating on this level. Under certain circumstances, ERAD substrates will use the distal Golgi checkpoint. Recent evidences indicate that the ERAD pathway is composed of multiple routes. Vashist and Ng (Vashist & Ng, 2004) proposed that endoplasmic reticulum associated degradation system in yeast consists of two surveillance mechanisms converging at the proteosomal degradation step – ERAD-L (ERAD-Luminal) and ERAD-C (ERAD-Cytosolic) that monitor the folded state of lumenal domains (soluble and membrane proteins) or cytosolic domains (membrane proteins), respectively. In contrast to ERAD-C pathway, degradation of ERAD-L substrates reveals apparent requirement for ER-to-Golgi transport. Thus, the specific fluorescence signal of alr1-n485,

M9, M10 and M11 mutants corresponding probably to the Golgi or other ER- associated compartments (ERAC) (Huyer et al, 2004) could reflect correlation with the ERAD pathway they are subjected to. Such proteosomal degradation was shown for some transmembrane proteins *e.g.* ATP-binding cassette (ABC) transporter Ste6p and plasma membrane H^+-ATPase Pma1p or plasma membrane ABC multidrug transporter Pdr6p and vacuolar hydrolase CPY, with a cytoplasmic and luminal lesions, respectively (reviewed, (Pety de Thozee & Ghislain, 2006)).

It was shown that exocytic cargo is, in fact, transported by at least two routes (Harsay & Bretscher, 1995). Late-acting *sec* and *snc* mutants, that are deficient in Golgi to PM transport, accumulate two distinct types of SVs. One type is of higher density (HDSV) and contains the soluble secreted enzymes invertase and acid phosphatase, as well as the bulk of exoglucanase activity, while the other is of low density (LDSV) and contains a plasma membrane H^+-ATPase activity among its cargo (David et al, 1998; Harsay & Bretscher, 1995). The existence of multiple exocytic pathways allow for the controlled segregation and secretion, of proteins that need proteolytic processing prior to the secretion from those secreted directly from Golgi, by HDSV and LDSV pathways, respectively. In contrast to the dynamin and clathrin independent HDSV route, LDSV branch to the cell surface is the default path when the Golgi to PVC route is blocked (*i.e.* in *vps* mutants like *vps1, chc1, vps4*). Interestingly, the mutation in *PEP12* gene also completely blocks HDSV biogenesis, while no significant block in exocytosis via LDSV route has been observed. It would seem likely that HDSV-destined cargo is sorted to the PVC prior being packaged into HDSVs (Gurunathan et al, 2002). Inactivation of Golgi to PVC traffic by *PEP12* deletion favour the shift of cargo to LDSV bringing about alternative uncontrollable way of secretion for proteins destined to prevacuolar compartment or further to the vacuole. Hence, the possible explanation for redistribution of N-terminal truncated Alr1p variants to the cell surface in *pep12Δ* cells is that these alr1-n128, alr1-n155, alr1-n204 and alr1-n277 Alr1p mutants make a most of impaired sorting into the vesicles destined to the late endosome and instead are transferred to the plasma membrane by default flow in LDSVs.

The yeast endocytic pathway is complicated because there are apparently multiple routes that can be taken to reach the vacuole. The evidences come from the analysis of targeting information on proteins that traverse the pathway (Lewis et al, 2000), but also from consistent findings that mutants affecting the pathway do not usually completely block delivery of endocytic content to the vacuole. The results obtained in our work beside

reported for other proteins bear witness to importance of Pep12p on the background of other SNARE proteins in intracellular trafficking. Therefore, deletion of *PEP12* gene result in severe phenotype causing endocytic and vacuolar protein sorting pathway disarrangement and cargo redirection to other compartments. Such observed effect of Pep12p inactivation is not specific only for this class D *vps* mutant. A variety of other mutants belonging to this *VPS* class genes as well as other that block endosomal transport to the vacuole have a tendency to secretion or to an accumulation of the transported substrates at the plasma membrane (Li et al, 1999; Luo & Chang, 1997; Piper et al, 1995). Of the 146 genes identified in a genetic screen for mutants affecting more or less protein sorting to the vacuole (Bonangelino et al, 2002) 70 are classified as a *VPS* genes. This group of *vps* mutants has been divided into six classes (A-F) based on several criteria, including the morphology of the mutant vacuoles (Banta et al, 1988; Raymond et al, 1992) and deletion of any gene belonging to these sections highly impairs vacuolar hydrolases sorting to the vacuole. In the result, it comes to the greatly increased secretion of carboxypeptidase (CPY) (Nothwehr et al, 1995; Robinson et al, 1988; Rothman et al, 1989; Rothman et al, 1990; Rothman & Stevens, 1986) as well as proteinase A (PrA) and aminopeptidase Y (Cooper & Stevens, 1996; Jorgensen et al, 1999; Marcusson et al, 1994). Among the proteins with altered peculiar distribution resulting from block of intracellular sorting are either the Kex2p, mating pheromone α-factor processing enzyme, the A-ALP, chimeric protein consisting of the cytosolic domain of dipeptidyl aminopeptidase A fused to the transmembrane and lumenal domains of alkaline phosphatase, and the Vps10p, vacuolar hydrolases sorting receptor (Deloche & Schekman, 2002; Nothwehr et al, 1995; Wilsbach & Payne, 1993). This suggests that enhanced secretion, protein recycling back to the plasma membrane or alternative transport to the vacuole through bypassing of endocytic compartments via cell surface is a general feature of majority genes contributing to protein trafficking from the yeast late Golgi to the vacuole.

A hypothetical model of multiple degradation pathways for wild-type Alr1p and its mutated N-terminal variants in wild-type yeast cells and *pep12Δ* mutants is shown in Figure 6.1.
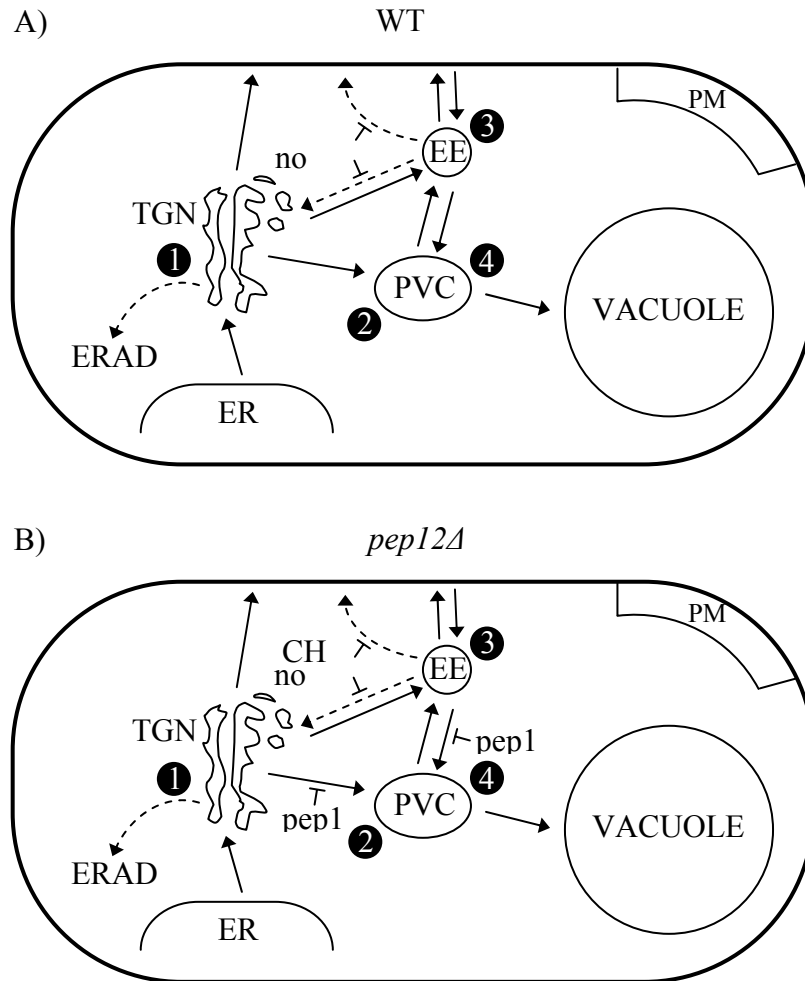
Fig. 6.1. A model for Pep12p interference with Alr1p protein exocytosis and endocytosis in wild-type (A) and *pep12Δ* mutant yeast cells (B). Biosynthetic and degradative itinerary of Alr1p and its N-terminal mutants in support of typical intracellular network is depicted by black arrows. Dashed arrows indicate possible scenario of Alr1p as a consequence of PVC function inactivation. **(A)** Secretory vesicles with Alr1p cargo derived from ER undergo docking with the Golgi. Wild-type Alr1p is further directed to its final destination – PM, but the exact sorting event is not known and occurs possibly directly from TGN or via EE. The LE is excluded because studies with *PEP12* gene deletion showed no interference with Alr1p exocytosis. Most severe N-terminal Alr1p mutants, *i.e.* alr1n-485 truncation and M9, M10, and M11 modules are recognized as misfolded proteins by quality control machinery operating at the ER or post-ER level and retrieved back by retrograde transport from the Golgi stacks for subsequent inactivation in proteosome (1). Meanwhile, after ER escaping, a fraction of non-native Alr1p mutants not qualified for transport to PM diverted biosynthetic pathway to join proteins from endocytic route in PVC *en route* to the vacuole (2). Addition of Mg^{2+} to the wild-type cells induces ubiquitination of Alr1p at the PM followed by endocytosis. The internalized protein moves through the EE and reaches the PVC; constitutive recycling back to the PM is not excluded (3). Finally, Alr1p is sorted to the vacuole for degradation. This last step is highly dependent on

Pep12p, which was shown to localize to the PVC (4). **(B)** In *pep12Δ* mutant cells, secretion mechanism of Alr1p and its mild N-terminal isomers seems to be also unimpaired. Furthermore, degradation of alr1n-485, M9, M10 and M11 mutants by ERAD system proceeds intact (1). In contrast, impairment of LE function and subsequent inactivation of main converge station for biosynthetic and endocytic pathways makes impossible vacuolar degradation. This results by turn in enhanced redirection to the plasma membrane (2). Malfunction of prevacuolar compartment has also consequences in later stage of protein downregulation in high Mg^{2+} environment. Magnesium surplus was enough to trigger substrate specific protein internalization followed by transport to EE and further in LE direction (3), but deletion of Pep12p that controls all possible traffic at the late endosome level, caused enhanced retrieval of native Alr1p and its alr-n128, alr-n155, alr-n204 and alr-n277 mutants from vacuolar degradation and missorting to the plasma membrane (4). Cell surface stabilization of Alr1p by continuous embedding in the plasma membrane is also not excluded. Moreover, CHX treatment of cells expressing N-terminal Alr1p mutants might result in protein distribution changes compared with wild-type Alr1p, where strong cell surface signal was still detected (for more details see text).

7. REFERENCES

al-Ghamdi SM, Cameron EC, Sutton RA (1994) Magnesium deficiency: pathophysiologic and clinical overview. *Am J Kidney Dis* **24**(5)**:** 737-752

Alberts B, Johnson A, Lewis J, Raff M, Roberts K, Walter P (2002) Molecular biology of the cell. 4th edn. .

Amerik AY, Hochstrasser M (2004) Mechanism and function of deubiquitinating enzymes. *Biochimica et biophysica acta* **1695**(1-3)**:** 189-207

Appenzeller-Herzog C, Hauri HP (2006) The ER-Golgi intermediate compartment (ERGIC): in search of its identity and function. *Journal of cell science* **119**(Pt 11)**:** 2173-2183

Aridor M, Bannykh SI, Rowe T, Balch WE (1995) Sequential coupling between COPII and COPI vesicle coats in endoplasmic reticulum to Golgi transport. *The Journal of cell biology* **131**(4)**:** 875-893

Arvan P, Zhao X, Ramos-Castaneda J, Chang A (2002) Secretory pathway quality control operating in Golgi, plasmalemmal, and endosomal systems. *Traffic (Copenhagen, Denmark)* **3**(11)**:** 771-780

Ashby MC, Tepikin AV (2001) ER calcium and the functions of intracellular organelles. *Seminars in cell & developmental biology* **12**(1)**:** 11-17

Babst M (2005) A protein's final ESCRT. *Traffic (Copenhagen, Denmark)* **6**(1)**:** 2-9

Babst M, Katzmann DJ, Estepa-Sabal EJ, Meerloo T, Emr SD (2002a) Escrt-III: an endosome-associated heterooligomeric protein complex required for mvb sorting. *Developmental cell* **3**(2)**:** 271-282

Babst M, Katzmann DJ, Snyder WB, Wendland B, Emr SD (2002b) Endosome-associated complex, ESCRT-II, recruits transport machinery for protein sorting at the multivesicular body. *Developmental cell* **3**(2)**:** 283-289

Bagnat M, Chang A, Simons K (2001) Plasma membrane proton ATPase Pma1p requires raft association for surface delivery in yeast. *Molecular biology of the cell* **12**(12)**:** 4129-4138

Bagnat M, Keranen S, Shevchenko A, Shevchenko A, Simons K (2000) Lipid rafts function in biosynthetic delivery of proteins to the cell surface in yeast. *Proceedings of the National Academy of Sciences of the United States of America* **97**(7)**:** 3254-3259

Bannykh SI, Rowe T, Balch WE (1996) The organization of endoplasmic reticulum export complexes. *The Journal of cell biology* **135**(1)**:** 19-35

Banta LM, Robinson JS, Klionsky DJ, Emr SD (1988) Organelle assembly in yeast: characterization of yeast mutants defective in vacuolar biogenesis and protein sorting. *The Journal of cell biology* **107**(4)**:** 1369-1383

Barlowe C (1997) Coupled ER to Golgi transport reconstituted with purified cytosolic proteins. *The Journal of cell biology* **139**(5)**:** 1097-1108

Barrowman J, Sacher M, Ferro-Novick S (2000) TRAPP stably associates with the Golgi and is required for vesicle docking. *The EMBO journal* **19**(5)**:** 862-869

Becherer KA, Rieder SE, Emr SD, Jones EW (1996) Novel syntaxin homologue, Pep12p, required for the sorting of lumenal hydrolases to the lysosome-like vacuole in yeast. *Molecular biology of the cell* **7**(4)**:** 579-594

Beck T, Schmidt A, Hall MN (1999) Starvation induces vacuolar targeting and degradation of the tryptophan permease in yeast. *The Journal of cell biology* **146**(6)**:** 1227-1238

Behnia R, Munro S (2005) Organelle identity and the signposts for membrane traffic. *Nature* **438**(7068)**:** 597-604

Bennett MK, Scheller RH (1993) The molecular machinery for secretion is conserved from yeast to neurons. *Proceedings of the National Academy of Sciences of the United States of America* **90**(7)**:** 2559-2563

Benting JH, Rietveld AG, Simons K (1999) N-Glycans mediate the apical sorting of a GPI-anchored, raft-associated protein in Madin-Darby canine kidney cells. *The Journal of cell biology* **146**(2)**:** 313-320

Black CB, Huang HW, Cowan JA (1994) Biological coordination chemistry of magnesium, sodium, and potassium ions. Protein and nucleotide binding sites. *Coordination Chemistry Rev* **135**(136)**:** 165-202

Black MW, Pelham HR (2000) A selective transport route from Golgi to late endosomes that requires the yeast GGA proteins. *The Journal of cell biology* **151**(3)**:** 587-600

Blanchette JM, Abazeed ME, Fuller RS (2004) Cell-free reconstitution of transport from the trans-golgi network to the late endosome/prevacuolar compartment. *The Journal of biological chemistry* **279**(47)**:** 48767-48773

Blondel MO, Morvan J, Dupre S, Urban-Grimal D, Haguenauer-Tsapis R, Volland C (2004) Direct sorting of the yeast uracil permease to the endosomal system is controlled by uracil binding and Rsp5p-dependent ubiquitylation. *Molecular biology of the cell* **15**(2)**:** 883-895

Bock JB, Matern HT, Peden AA, Scheller RH (2001) A genomic perspective on membrane compartment organization. *Nature* **409**(6822)**:** 839-841

Bonangelino CJ, Chavez EM, Bonifacino JS (2002) Genomic screen for vacuolar protein sorting genes in Saccharomyces cerevisiae. *Molecular biology of the cell* **13**(7)**:** 2486-2501

Bonifacino JS, Glick BS (2004) The mechanisms of vesicle budding and fusion. *Cell* **116**(2)**:** 153-166

Bonifacino JS, Lippincott-Schwartz J (1991) Degradation of proteins within the endoplasmic reticulum. *Current opinion in cell biology* **3**(4)**:** 592-600

Bonifacino JS, Traub LM (2003) Signals for sorting of transmembrane proteins to endosomes and lysosomes. *Annual review of biochemistry* **72:** 395-447

Bootman MD, Collins TJ, Peppiatt CM, Prothero LS, MacKenzie L, De Smet P, Travers M, Tovey SC, Seo JT, Berridge MJ, Ciccolini F, Lipp P (2001) Calcium signalling-an overview. *Seminars in cell & developmental biology* **12**(1)**:** 3-10

Botstein D, Fink GR (1988) Yeast: an experimental organism for modern biology. *Science* **240**(4858)**:** 1439-1443

Brown DA, London E (1998) Functions of lipid rafts in biological membranes. *Annual review of cell and developmental biology* **14:** 111-136

Brown EM, MacLeod RJ (2001) Extracellular calcium sensing and extracellular calcium signaling. *Physiological reviews* **81**(1)**:** 239-297

Bryant NJ, Piper RC, Weisman LS, Stevens TH (1998) Retrograde traffic out of the yeast vacuole to the TGN occurs via the prevacuolar/endosomal compartment. *The Journal of cell biology* **142**(3)**:** 651-663

Bryant NJ, Stevens TH (1998) Vacuole biogenesis in Saccharomyces cerevisiae: protein transport pathways to the yeast vacuole. *Microbiol Mol Biol Rev* **62**(1)**:** 230-247

Bui DM, Gregan J, Jarosch E, Ragnini A, Schweyen RJ (1999) The bacterial magnesium transporter CorA can functionally substitute for its putative homologue Mrs2p in the yeast inner mitochondrial membrane. *The Journal of biological chemistry* **274**(29)**:** 20438-20443

Burd CG, Babst M, Emr SD (1998) Novel pathways, membrane coats and PI kinase regulation in yeast lysosomal trafficking. *Seminars in cell & developmental biology* **9**(5)**:** 527-533

Burri L, Lithgow T (2004) A complete set of SNAREs in yeast. *Traffic (Copenhagen, Denmark)* **5**(1)**:** 45-52

Cai H, Yu S, Menon S, Cai Y, Lazarova D, Fu C, Reinisch K, Hay JC, Ferro-Novick S (2007) TRAPPI tethers COPII vesicles by binding the coat subunit Sec23. *Nature* **445**(7130)**:** 941-944

Chang A, Fink GR (1995) Targeting of the yeast plasma membrane [H+]ATPase: a novel gene AST1 prevents mislocalization of mutant ATPase to the vacuole. *The Journal of cell biology* **128**(1-2)**:** 39-49

Chang G, Spencer RH, Lee AT, Barclay MT, Rees DC (1998) Structure of the MscL homolog from Mycobacterium tuberculosis: a gated mechanosensitive ion channel. *Science* **282**(5397)**:** 2220-2226

Chen CY, Graham TR (1998) An arf1Delta synthetic lethal screen identifies a new clathrin heavy chain conditional allele that perturbs vacuolar protein transport in Saccharomyces cerevisiae. *Genetics* **150**(2)**:** 577-589

Chen L, Davis NG (2000) Recycling of the yeast a-factor receptor. *The Journal of cell biology* **151**(3)**:** 731-738

Chen YA, Scheller RH (2001) SNARE-mediated membrane fusion. *Nat Rev Mol Cell Biol* **2**(2)**:** 98-106

Chuang JS, Schekman RW (1996) Differential trafficking and timed localization of two chitin synthase proteins, Chs2p and Chs3p. *The Journal of cell biology* **135**(3)**:** 597-610

Chubanov V, Gudermann T, Schlingmann KP (2005) Essential role for TRPM6 in epithelial magnesium transport and body magnesium homeostasis. *Pflugers Arch* **451**(1)**:** 228-234

Cole DE, Quamme GA (2000) Inherited disorders of renal magnesium handling. *J Am Soc Nephrol* **11**(10)**:** 1937-1947

Collins KM, Thorngren NL, Fratti RA, Wickner WT (2005) Sec17p and HOPS, in distinct SNARE complexes, mediate SNARE complex disruption or assembly for fusion. *The EMBO journal* **24**(10)**:** 1775-1786

Conibear E, Cleck JN, Stevens TH (2003) Vps51p mediates the association of the GARP (Vps52/53/54) complex with the late Golgi t-SNARE Tlg1p. *Molecular biology of the cell* **14**(4)**:** 1610-1623

Conibear E, Stevens TH (1998) Multiple sorting pathways between the late Golgi and the vacuole in yeast. *Biochimica et biophysica acta* **1404**(1-2)**:** 211-230

Conibear E, Stevens TH (2000) Vps52p, Vps53p, and Vps54p form a novel multisubunit complex required for protein sorting at the yeast late Golgi. *Molecular biology of the cell* **11**(1)**:** 305-323

Conner SD, Schmid SL (2003) Regulated portals of entry into the cell. *Nature* **422**(6927)**:** 37-44

Cooper AA, Stevens TH (1996) Vps10p cycles between the late-Golgi and prevacuolar compartments in its function as the sorting receptor for multiple yeast vacuolar hydrolases. *The Journal of cell biology* **133**(3)**:** 529-541

Costaguta G, Stefan CJ, Bensen ES, Emr SD, Payne GS (2001) Yeast Gga coat proteins function with clathrin in Golgi to endosome transport. *Molecular biology of the cell* **12**(6)**:** 1885-1896

Cowan JA (1995) Introduction to the biological chemistryof magnesium. In: Cowan, J.A. ed, The Biological Chemistry of Magnesium. VCH, New York.

Cowles CR, Odorizzi G, Payne GS, Emr SD (1997a) The AP-3 adaptor complex is essential for cargo-selective transport to the yeast vacuole. *Cell* **91**(1)**:** 109-118

Cowles CR, Snyder WB, Burd CG, Emr SD (1997b) Novel Golgi to vacuole delivery pathway in yeast: identification of a sorting determinant and required transport component. *The EMBO journal* **16**(10)**:** 2769-2782

David D, Sundarababu S, Gerst JE (1998) Involvement of long chain fatty acid elongation in the trafficking of secretory vesicles in yeast. *The Journal of cell biology* **143**(5)**:** 1167-1182

de Rouffignac C, Quamme G (1994) Renal magnesium handling and its hormonal control. *Physiological reviews* **74**(2)**:** 305-322

Deloche O, Schekman RW (2002) Vps10p cycles between the TGN and the late endosome via the plasma membrane in clathrin mutants. *Molecular biology of the cell* **13**(12)**:** 4296-4307

Doyle DA, Morais Cabral J, Pfuetzner RA, Kuo A, Gulbis JM, Cohen SL, Chait BT, MacKinnon R (1998) The structure of the potassium channel: molecular basis of K+ conduction and selectivity. *Science* **280**(5360)**:** 69-77

Drummond RSM, Tutone A, Li YC, Gardner RC (2006) A putative magnesium transporter AtMRS2-11 is localized to the plant chloroplast envelope membrane system. *Plant Science* **170**(1)**:** 78-89

Dubyak GR (2004) Ion homeostasis, channels, and transporters: an update on cellular mechanisms. *Adv Physiol Educ* **28**(1-4)**:** 143-154

Dunn R, Hicke L (2001) Domains of the Rsp5 ubiquitin-protein ligase required for receptor-mediated and fluid-phase endocytosis. *Molecular biology of the cell* **12**(2)**:** 421-435

Ehrlich M, Boll W, Van Oijen A, Hariharan R, Chandran K, Nibert ML, Kirchhausen T (2004) Endocytosis by random initiation and stabilization of clathrin-coated pits. *Cell* **118**(5)**:** 591-605

Eshaghi S, Niegowski D, Kohl A, Martinez Molina D, Lesley SA, Nordlund P (2006) Crystal structure of a divalent metal ion transporter CorA at 2.9 angstrom resolution. *Science* **313**(5785)**:** 354-357

Fang S, Weissman AM (2004) A field guide to ubiquitylation. *Cell Mol Life Sci* **61**(13)**:** 1546-1561

Fasshauer D (2003) Structural insights into the SNARE mechanism. *Biochimica et biophysica acta* **1641**(2-3)**:** 87-97

Fasshauer D, Sutton RB, Brunger AT, Jahn R (1998) Conserved structural features of the synaptic fusion complex: SNARE proteins reclassified as Q- and R-SNAREs. *Proceedings of the National Academy of Sciences of the United States of America* **95**(26)**:** 15781-15786

Fatholahi M, LaNoue K, Romani A, Scarpa A (2000) Relationship between total and free cellular Mg(2+) during metabolic stimulation of rat cardiac myocytes and perfused hearts. *Arch Biochem Biophys* **374**(2)**:** 395-401

Fayadat L, Kopito RR (2003) Recognition of a single transmembrane degron by sequential quality control checkpoints. *Molecular biology of the cell* **14**(3)**:** 1268-1278

Ferreira T, Mason AB, Pypaert M, Allen KE, Slayman CW (2002) Quality control in the yeast secretory pathway: a misfolded PMA1 H+-ATPase reveals two checkpoints. *The Journal of biological chemistry* **277**(23)**:** 21027-21040

Ferro-Novick S, Jahn R (1994) Vesicle fusion from yeast to man. *Nature* **370**(6486)**:** 191-193

Fetchko M, Stagljar I (2004) Application of the split-ubiquitin membrane yeast two-hybrid system to investigate membrane protein interactions. *Methods* **32**(4)**:** 349-362

Finley D, Ozkaynak E, Varshavsky A (1987) The yeast polyubiquitin gene is essential for resistance to high temperatures, starvation, and other stresses. *Cell* **48**(6)**:** 1035-1046

Froschauer EM, Kolisek M, Dieterich F, Schweigel M, Schweyen RJ (2004) Fluorescence measurements of free [Mg2+] by use of mag-fura 2 in Salmonella enterica. *FEMS microbiology letters* **237**(1)**:** 49-55

Gajewska B, Kaminska J, Jesionowska A, Martin NC, Hopper AK, Zoladek T (2001) WW domains of Rsp5p define different functions: determination of roles in fluid phase and uracil permease endocytosis in Saccharomyces cerevisiae. *Genetics* **157**(1)**:** 91-101

Galan JM, Haguenauer-Tsapis R (1997) Ubiquitin lys63 is involved in ubiquitination of a yeast plasma membrane protein. *The EMBO journal* **16**(19)**:** 5847-5854

Gerrard SR, Levi BP, Stevens TH (2000) Pep12p is a multifunctional yeast syntaxin that controls entry of biosynthetic, endocytic and retrograde traffic into the prevacuolar compartment. *Traffic (Copenhagen, Denmark)* **1**(3)**:** 259-269

Gerst JE (1999) SNAREs and SNARE regulators in membrane fusion and exocytosis. *Cell Mol Life Sci* **55**(5)**:** 707-734

Gillingham AK, Munro S (2003) Long coiled-coil proteins and membrane traffic. *Biochimica et biophysica acta* **1641**(2-3)**:** 71-85

Gitan RS, Eide DJ (2000) Zinc-regulated ubiquitin conjugation signals endocytosis of the yeast ZRT1 zinc transporter. *Biochem J* **346 Pt 2:** 329-336

Gitan RS, Luo H, Rodgers J, Broderius M, Eide D (1998) Zinc-induced inactivation of the yeast ZRT1 zinc transporter occurs through endocytosis and vacuolar degradation. *The Journal of biological chemistry* **273**(44)**:** 28617-28624

Gonzalez-Gaitan M, Jackle H (1997) Role of Drosophila alpha-adaptin in presynaptic vesicle recycling. *Cell* **88**(6)**:** 767-776

Goytain A, Hines RM, El-Husseini A, Quamme GA (2007) NIPA1(SPG6), the basis for autosomal dominant form of hereditary spastic paraplegia, encodes a functional Mg2+ transporter. *The Journal of biological chemistry* **282**(11)**:** 8060-8068

Goytain A, Quamme GA (2005a) Functional characterization of ACDP2 (ancient conserved domain protein), a divalent metal transporter. *Physiol Genomics* **22**(3)**:** 382-389

Goytain A, Quamme GA (2005b) Functional characterization of human SLC41A1, a Mg2+ transporter with similarity to prokaryotic MgtE Mg2+ transporters. *Physiol Genomics* **21**(3)**:** 337-342

Goytain A, Quamme GA (2005c) Functional characterization of the mouse [corrected] solute carrier, SLC41A2. *Biochem Biophys Res Commun* **330**(3)**:** 701-705

Goytain A, Quamme GA (2005d) Identification and characterization of a novel mammalian Mg2+ transporter with channel-like properties. *BMC Genomics* **6**(1)**:** 48

Graschopf A, Stadler JA, Hoellerer MK, Eder S, Sieghardt M, Kohlwein SD, Schweyen RJ (2001) The yeast plasma membrane protein Alr1 controls Mg2+ homeostasis and is subject to Mg2+-dependent control of its synthesis and degradation. *The Journal of biological chemistry* **276**(19)**:** 16216-16222

Gregan J, Bui DM, Pillich R, Fink M, Zsurka G, Schweyen RJ (2001a) The mitochondrial inner membrane protein Lpe10p, a homologue of Mrs2p, is essential for magnesium homeostasis and group II intron splicing in yeast. *Mol Gen Genet* **264**(6)**:** 773-781

Gregan J, Kolisek M, Schweyen RJ (2001b) Mitochondrial Mg(2+) homeostasis is critical for group II intron splicing in vivo. *Genes Dev* **15**(17)**:** 2229-2237

Grenson M (1992) Molecular aspects of transport proteins. *Elsevier Science Publishers B V, Amsterdam***:** 219-245

Grosshans BL, Ortiz D, Novick P (2006) Rabs and their effectors: achieving specificity in membrane traffic. *Proceedings of the National Academy of Sciences of the United States of America* **103**(32)**:** 11821-11827

Grubbs RD (1990) Hormonal regulation of magnesium homeostasis in cultured mammalian cells. *in: Sigel, H, Sigel, A (Eds), Metal Ions in Biological Systems, Marcel Dekker, New York***:** 177-192

Gruenberg J (2001) The endocytic pathway: a mosaic of domains. *Nat Rev Mol Cell Biol* **2**(10)**:** 721-730

Gruenberg J, Stenmark H (2004) The biogenesis of multivesicular endosomes. *Nat Rev Mol Cell Biol* **5**(4)**:** 317-323

Gu F, Crump CM, Thomas G (2001) Trans-Golgi network sorting. *Cell Mol Life Sci* **58**(8)**:** 1067-1084

Guenther T (1990) Membrane trasport of magnesium. *in: Sigel, H, Sigel, A (Eds), Metal Ions in Biological Systems, Marcel Dekker, New York***:** 215-225

Gupta R, Kus B, Fladd C, Wasmuth J, Tonikian R, Sidhu S, Krogan NJ, Parkinson J, Rotin D (2007) Ubiquitination screen using protein microarrays for comprehensive identification of Rsp5 substrates in yeast. *Mol Syst Biol* **3:** 116

Gurunathan S, David D, Gerst JE (2002) Dynamin and clathrin are required for the biogenesis of a distinct class of secretory vesicles in yeast. *The EMBO journal* **21**(4)**:** 602-614

Gut A, Kappeler F, Hyka N, Balda MS, Hauri HP, Matter K (1998) Carbohydrate-mediated Golgi to cell surface transport and apical targeting of membrane proteins. *The EMBO journal* **17**(7)**:** 1919-1929

Haglund K, Dikic I (2005) Ubiquitylation and cell signaling. *The EMBO journal* **24**(19)**:** 3353-3359

Haguenauer-Tsapis R, André B (2004) Membrane trafficking of yeast transporters: mechanisms and physiological control of downregulation. *Topics in Current Genetics* **9:** 273-322

Hammond AT, Glick BS (2000) Dynamics of transitional endoplasmic reticulum sites in vertebrate cells. *Molecular biology of the cell* **11**(9)**:** 3013-3030

Hanna J, Leggett DS, Finley D (2003) Ubiquitin depletion as a key mediator of toxicity by translational inhibitors. *Molecular and cellular biology* **23**(24)**:** 9251-9261

Harris SL, Waters MG (1996) Localisation of yeast early Golgi mannosyltransferase, Och1p, involves retrograde transport. . *The Journal of cell biology* **132**(6)**:** 985-998

Harsay E, Bretscher A (1995) Parallel secretory pathways to the cell surface in yeast. *The Journal of cell biology* **131**(2)**:** 297-310

Harsay E, Schekman R (2002) A subset of yeast vacuolar protein sorting mutants is blocked in one branch of the exocytic pathway. *The Journal of cell biology* **156**(2)**:** 271-285

Hartl FU (1996) Molecular chaperones in cellular protein folding. *Nature* **381**(6583)**:** 571-579

Hartwig A (2001) Role of magnesium in genomic stability. *Mutat Res* **475**(1-2)**:** 113-121

Harty RN, Brown ME, Wang G, Huibregtse J, Hayes FP (2000) A PPxY motif within the VP40 protein of Ebola virus interacts physically and functionally with a ubiquitin ligase: implications for filovirus budding. *Proceedings of the National Academy of Sciences of the United States of America* **97**(25)**:** 13871-13876

Hattori M, Tanaka Y, Fukai S, Ishitani R, Nureki O (2007) Crystal structure of the MgtE Mg2+ transporter. *Nature* **448**(7157)**:** 1072-1075

Hauri H, Appenzeller C, Kuhn F, Nufer O (2000) Lectins and traffic in the secretory pathway. *FEBS Lett* **476**(1-2)**:** 32-37

Hay JC, Scheller RH (1997) SNAREs and NSF in targeted membrane fusion. *Current opinion in cell biology* **9**(4)**:** 505-512

Hein C, Andre B (1997) A C-terminal di-leucine motif and nearby sequences are required for NH4(+)-induced inactivation and degradation of the general amino acid permease, Gap1p, of Saccharomyces cerevisiae. *Mol Microbiol* **24**(3)**:** 607-616

Helliwell SB, Losko S, Kaiser CA (2001) Components of a ubiquitin ligase complex specify polyubiquitination and intracellular trafficking of the general amino acid permease. *The Journal of cell biology* **153**(4)**:** 649-662

Hershko A, Ciechanover A (1998) The ubiquitin system. *Annual review of biochemistry* **67:** 425-479

Hettema EH, Valdez-Taubas J, Pelham HR (2004) Bsd2 binds the ubiquitin ligase Rsp5 and mediates the ubiquitination of transmembrane proteins. *The EMBO journal* **23**(6)**:** 1279-1288

Hicke L (2001) Protein regulation by monoubiquitin. *Nat Rev Mol Cell Biol* **2**(3)**:** 195-201

Hicke L, Dunn R (2003) Regulation of membrane protein transport by ubiquitin and ubiquitin-binding proteins. *Annual review of cell and developmental biology* **19:** 141-172

Hmiel SP, Snavely MD, Miller CG, Maguire ME (1986) Magnesium transport in Salmonella typhimurium: characterization of magnesium influx and cloning of a transport gene. *J Bacteriol* **168**(3)**:** 1444-1450

Hochstrasser M (1996) Ubiquitin-dependent protein degradation. *Annu Rev Genet* **30:** 405-439

Hochstrasser M (2000) Evolution and function of ubiquitin-like protein-conjugation systems. *Nature cell biology* **2**(8)**:** E153-157

Holthuis JC, Nichols BJ, Pelham HR (1998) The syntaxin Tlg1p mediates trafficking of chitin synthase III to polarized growth sites in yeast. *Molecular biology of the cell* **9**(12)**:** 3383-3397

Hong W (2005) SNAREs and traffic. *Biochimica et biophysica acta* **1744**(3)**:** 493-517

Horak J, Wolf DH (2001) Glucose-induced monoubiquitination of the Saccharomyces cerevisiae galactose transporter is sufficient to signal its internalization. *J Bacteriol* **183**(10)**:** 3083-3088

Hou J, Paul DL, Goodenough DA (2005) Paracellin-1 and the modulation of ion selectivity of tight junctions. *Journal of cell science* **118**(Pt 21)**:** 5109-5118

Howard JP, Hutton JL, Olson JM, Payne GS (2002) Sla1p serves as the targeting signal recognition factor for NPFX(1,2)D-mediated endocytosis. *The Journal of cell biology* **157**(2)**:** 315-326

Hsu VW, Yuan LC, Nuchtern JG, Lippincott-Schwartz J, Hammerling GJ, Klausner RD (1991) A recycling pathway between the endoplasmic reticulum and the Golgi apparatus for retention of unassembled MHC class I molecules. *Nature* **352**(6334)**:** 441-444

Huibregtse JM, Scheffner M, Beaudenon S, Howley PM (1995) A family of proteins structurally and functionally related to the E6-AP ubiquitin-protein ligase. *Proceedings of the National Academy of Sciences of the United States of America* **92**(7)**:** 2563-2567

Huyer G, Longsworth GL, Mason DL, Mallampalli MP, McCaffery JM, Wright RL, Michaelis S (2004) A striking quality control subcompartment in Saccharomyces cerevisiae: the endoplasmic reticulum-associated compartment. *Molecular biology of the cell* **15**(2)**:** 908-921

Jahn R, Lang T, Sudhof TC (2003) Membrane fusion. *Cell* **112**(4)**:** 519-533

Jenness DD, Li Y, Tipper C, Spatrick P (1997) Elimination of defective alpha-factor pheromone receptors. *Molecular and cellular biology* **17**(11)**:** 6236-6245

Jentsch S, Pyrowolakis G (2000) Ubiquitin and its kin: how close are the family ties? *Trends Cell Biol* **10**(8)**:** 335-342

Joazeiro CA, Weissman AM (2000) RING finger proteins: mediators of ubiquitin ligase activity. *Cell* **102**(5)**:** 549-552

Johnsson N, Varshavsky A (1994) Split ubiquitin as a sensor of protein interactions in vivo. *Proceedings of the National Academy of Sciences of the United States of America* **91**(22)**:** 10340-10344

Jorgensen MU, Emr SD, Winther JR (1999) Ligand recognition and domain structure of Vps10p, a vacuolar protein sorting receptor in Saccharomyces cerevisiae. *Eur J Biochem* **260**(2)**:** 461-469

Kamikura DM, Cooper JA (2003) Lipoprotein receptors and a disabled family cytoplasmic adaptor protein regulate EGL-17/FGF export in C. elegans. *Genes Dev* **17**(22)**:** 2798-2811

Kaminska J, Gajewska B, Hopper AK, Zoladek T (2002) Rsp5p, a new link between the actin cytoskeleton and endocytosis in the yeast Saccharomyces cerevisiae. *Molecular and cellular biology* **22**(20)**:** 6946-6948

Katzmann DJ, Babst M, Emr SD (2001) Ubiquitin-dependent sorting into the multivesicular body pathway requires the function of a conserved endosomal protein sorting complex, ESCRT-I. *Cell* **106**(2)**:** 145-155

Katzmann DJ, Sarkar S, Chu T, Audhya A, Emr SD (2004) Multivesicular body sorting: ubiquitin ligase Rsp5 is required for the modification and sorting of carboxypeptidase S. *Molecular biology of the cell* **15**(2)**:** 468-480

Kehres DG, Lawyer CH, Maguire ME (1998) The CorA magnesium transporter gene family. *Microb Comp Genomics* **3**(3)**:** 151-169

Kehres DG, Maguire ME (2002) Structure, properties and regulation of magnesium transport proteins. *Biometals* **15**(3)**:** 261-270

Kelm KB, Huyer G, Huang JC, Michaelis S (2004) The internalization of yeast Ste6p follows an ordered series of events involving phosphorylation, ubiquitination, recognition and endocytosis. *Traffic (Copenhagen, Denmark)* **5**(3)**:** 165-180

Kern AL, Bonatto D, Dias JF, Yoneama ML, Brendel M, Pegas Henriques JA (2005) The function of Alr1p of Saccharomyces cerevisiae in cadmium detoxification: insights from phylogenetic studies and particle-induced X-ray emission. *Biometals* **18**(1)**:** 31-41

Kerscher O, Felberbaum R, Hochstrasser M (2006) Modification of proteins by ubiquitin and ubiquitin-like proteins. *Annual review of cell and developmental biology* **22:** 159-180

Kirchhausen T (2000) Clathrin. *Annual review of biochemistry* **69:** 699-727

Kleizen B, Braakman I (2004) Protein folding and quality control in the endoplasmic reticulum. *Current opinion in cell biology* **16**(4)**:** 343-349

Klionsky DJ, Herman PK, Emr SD (1990) The fungal vacuole: composition, function, and biogenesis. *Microbiol Rev* **54**(3)**:** 266-292

Klumperman J (2000) Transport between ER and Golgi. *Current opinion in cell biology* **12**(4)**:** 445-449

Klumperman J, Schweizer A, Clausen H, Tang BL, Hong W, Oorschot V, Hauri HP (1998) The recycling pathway of protein ERGIC-53 and dynamics of the ER-Golgi intermediate compartment. *Journal of cell science* **111 (Pt 22):** 3411-3425

Knoop V, Groth-Malonek M, Gebert M, Eifler K, Weyand K (2005) Transport of magnesium and other divalent cations: evolution of the 2-TM-GxN proteins in the MIT superfamily. *Mol Genet Genomics* **274**(3)**:** 205-216

Kolisek M, Zsurka G, Samaj J, Weghuber J, Schweyen RJ, Schweigel M (2003) Mrs2p is an essential component of the major electrophoretic Mg2+ influx system in mitochondria. *The EMBO journal* **22**(6)**:** 1235-1244

Koll H, Schmidt C, Wiesenberger G, Schmelzer C (1987) Three nuclear genes suppress a yeast mitochondrial splice defect when present in high copy number. *Curr Genet* **12**(7)**:** 503-509

Krampe S, Stamm O, Hollenberg CP, Boles E (1998) Catabolite inactivation of the high-affinity hexose transporters Hxt6 and Hxt7 of Saccharomyces cerevisiae occurs in the vacuole after internalization by endocytosis. *FEBS Lett* **441**(3)**:** 343-347

Kuhlbrandt W (2004) Biology, structure and mechanism of P-type ATPases. *Nat Rev Mol Cell Biol* **5**(4)**:** 282-295

Kuo A, Gulbis JM, Antcliff JF, Rahman T, Lowe ED, Zimmer J, Cuthbertson J, Ashcroft FM, Ezaki T, Doyle DA (2003) Crystal structure of the potassium channel KirBac1.1 in the closed state. *Science* **300**(5627)**:** 1922-1926

Kyte J, Doolittle RF (1982) A simple method for displaying the hydropathic character of a protein. *J Mol Biol* **157**(1)**:** 105-132

Lauwers E, Andre B (2006) Association of yeast transporters with detergent-resistant membranes correlates with their cell-surface location. *Traffic (Copenhagen, Denmark)* **7**(8)**:** 1045-1059

Lee J, Pena MM, Nose Y, Thiele DJ (2002a) Biochemical characterization of the human copper transporter Ctr1. *The Journal of biological chemistry* **277**(6)**:** 4380-4387

Lee JM, Gardner RC (2006) Residues of the yeast ALR1 protein that are critical for magnesium uptake. *Curr Genet* **49**(1)**:** 7-20

Lee MC, Hamamoto S, Schekman R (2002b) Ceramide biosynthesis is required for the formation of the oligomeric H+-ATPase Pma1p in the yeast endoplasmic reticulum. *The Journal of biological chemistry* **277**(25)**:** 22395-22401

Lee MC, Miller EA, Goldberg J, Orci L, Schekman R (2004) Bi-directional protein transport between the ER and Golgi. *Annual review of cell and developmental biology* **20:** 87-123

Levine TP, Wiggins CA, Munro S (2000) Inositol phosphorylceramide synthase is located in the Golgi apparatus of Saccharomyces cerevisiae. *Molecular biology of the cell* **11**(7)**:** 2267-2281

Lewis MJ, Nichols BJ, Prescianotto-Baschong C, Riezman H, Pelham HR (2000) Specific retrieval of the exocytic SNARE Snc1p from early yeast endosomes. *Molecular biology of the cell* **11**(1)**:** 23-38

Li Y, Kane T, Tipper C, Spatrick P, Jenness DD (1999) Yeast mutants affecting possible quality control of plasma membrane proteins. *Molecular and cellular biology* **19**(5)**:** 3588-3599

Lindsten K, de Vrij FM, Verhoef LG, Fischer DF, van Leeuwen FW, Hol EM, Masucci MG, Dantuma NP (2002) Mutant ubiquitin found in neurodegenerative disorders is a

ubiquitin fusion degradation substrate that blocks proteasomal degradation. *The Journal of cell biology* **157**(3)**:** 417-427

Liu GJ, Martin DK, Gardner RC, Ryan PR (2002) Large Mg(2+)-dependent currents are associated with the increased expression of ALR1 in Saccharomyces cerevisiae. *FEMS microbiology letters* **213**(2)**:** 231-237

Lucero P, Lagunas R (1997) Catabolite inactivation of the yeast maltose transporter requires ubiquitin-ligase npi1/rsp5 and ubiquitin-hydrolase npi2/doa4. *FEMS microbiology letters* **147**(2)**:** 273-277

Lunin VV, Dobrovetsky E, Khutoreskaya G, Zhang R, Joachimiak A, Doyle DA, Bochkarev A, Maguire ME, Edwards AM, Koth CM (2006) Crystal structure of the CorA Mg2+ transporter. *Nature* **440**(7085)**:** 833-837

Luo W, Chang A (1997) Novel genes involved in endosomal traffic in yeast revealed by suppression of a targeting-defective plasma membrane ATPase mutant. *The Journal of cell biology* **138**(4)**:** 731-746

Luo W, Chang A (2000) An endosome-to-plasma membrane pathway involved in trafficking of a mutant plasma membrane ATPase in yeast. *Molecular biology of the cell* **11**(2)**:** 579-592

Lusk JE, Kennedy EP (1969) Magneisum transport in Escherichia coli. *The Journal of biological chemistry* **244**(6)**:** 1653-1655

MacDiarmid CW, Gardner RC (1998) Overexpression of the Saccharomyces cerevisiae magnesium transport system confers resistance to aluminum ion. *The Journal of biological chemistry* **273**(3)**:** 1727-1732

Maguire ME (2006) Magnesium transporters: properties, regulation and structure. *Front Biosci* **11:** 3149-3163

Maguire ME, Cowan JA (2002) Magnesium chemistry and biochemistry. *Biometals* **15**(3)**:** 203-210

Mahadev RK, Di Pietro SM, Olson JM, Piao HL, Payne GS, Overduin M (2007) Structure of Sla1p homology domain 1 and interaction with the NPFxD endocytic internalization motif. *The EMBO journal* **26**(7)**:** 1963-1971

Marcusson EG, Horazdovsky BF, Cereghino JL, Gharakhanian E, Emr SD (1994) The sorting receptor for yeast vacuolar carboxypeptidase Y is encoded by the VPS10 gene. *Cell* **77**(4)**:** 579-586

Marini AM, Springael JY, Frommer WB, Andre B (2000) Cross-talk between ammonium transporters in yeast and interference by the soybean SAT1 protein. *Mol Microbiol* **35**(2)**:** 378-385

Matejckova-Forejtova A, Kinclova O, Sychrova H (1999) Degradation of Candida albicans Can1 permease expressed in Saccharomyces cerevisiae. *FEMS microbiology letters* **176**(1)**:** 257-262

Matlack KE, Misselwitz B, Plath K, Rapoport TA (1999) BiP acts as a molecular ratchet during posttranslational transport of prepro-alpha factor across the ER membrane. *Cell* **97**(5)**:** 553-564

Matter K, Mellman I (1994) Mechanisms of cell polarity: sorting and transport in epithelial cells. *Current opinion in cell biology* **6**(4)**:** 545-554

Maxfield FR, McGraw TE (2004) Endocytic recycling. *Nat Rev Mol Cell Biol* **5**(2)**:** 121-132

McCarthy JT, Kumar R (1999) Divalent Cation Metabolism: Magnesium. *In: Schrier, RW Atlas of Diseases of the Kidney Disorders of Water, Electrolytes, and Acid-Base* 4.1-4.12

McNew JA, Parlati F, Fukuda R, Johnston RJ, Paz K, Paumet F, Sollner TH, Rothman JE (2000) Compartmental specificity of cellular membrane fusion encoded in SNARE proteins. *Nature* **407**(6801)**:** 153-159

Medintz I, Jiang H, Michels CA (1998) The role of ubiquitin conjugation in glucose-induced proteolysis of Saccharomyces maltose permease. *The Journal of biological chemistry* **273**(51)**:** 34454-34462

Minami Y, Weissman AM, Samelson LE, Klausner RD (1987) Building a multichain receptor: synthesis, degradation, and assembly of the T-cell antigen receptor. *Proceedings of the National Academy of Sciences of the United States of America* **84**(9)**:** 2688-2692

Mitsunari T, Nakatsu F, Shioda N, Love PE, Grinberg A, Bonifacino JS, Ohno H (2005) Clathrin adaptor AP-2 is essential for early embryonal development. *Molecular and cellular biology* **25**(21)**:** 9318-9323

Monahan BJ, Unkles SE, Tsing IT, Kinghorn JR, Hynes MJ, Davis MA (2002) Mutation and functional analysis of the Aspergillus nidulans ammonium permease MeaA and evidence for interaction with itself and MepA. *Fungal Genet Biol* **36**(1)**:** 35-46

Moncrief MB, Maguire ME (1999) Magnesium transport in prokaryotes. *J Biol Inorg Chem* **4**(5)**:** 523-527

Morozova N, Liang Y, Tokarev AA, Chen SH, Cox R, Andrejic J, Lipatova Z, Sciorra VA, Emr SD, Segev N (2006) TRAPPII subunits are required for the specificity switch of a Ypt-Rab GEF. *Nature cell biology* **8**(11)**:** 1263-1269

Morvan J, Froissard M, Haguenauer-Tsapis R, Urban-Grimal D (2004) The ubiquitin ligase Rsp5p is required for modification and sorting of membrane proteins into multivesicular bodies. *Traffic (Copenhagen, Denmark)* **5**(5)**:** 383-392

Mukherjee S, Ghosh RN, Maxfield FR (1997) Endocytosis. *Physiological reviews* **77**(3)**:** 759-803

Mullins C, Bonifacino JS (2001) The molecular machinery for lysosome biogenesis. *Bioessays* **23**(4)**:** 333-343

Munn AL (2001) Molecular requirements for the internalisation step of endocytosis: insights from yeast. *Biochimica et biophysica acta* **1535**(3)**:** 236-257

Munn AL, Riezman H (1994) Endocytosis is required for the growth of vacuolar H(+)-ATPase-defective yeast: identification of six new END genes. *The Journal of cell biology* **127**(2)**:** 373-386

Nadler MJ, Hermosura MC, Inabe K, Perraud AL, Zhu Q, Stokes AJ, Kurosaki T, Kinet JP, Penner R, Scharenberg AM, Fleig A (2001) LTRPC7 is a Mg.ATP-regulated divalent cation channel required for cell viability. *Nature* **411**(6837)**:** 590-595

Nakajima T, Iwasawa K, Hazama H, Asano M, Okuda Y, Omata M (1997) Extracellular Mg2+ inhibits receptor-mediated Ca(2+)-permeable non-selective cation currents in aortic smooth muscle cells. *Eur J Pharmacol* **320**(1)**:** 81-86

Nelson DL, Kennedy EP (1971) Magnesium transport in Escherichia coli. Inhibition by cobaltous ion. *The Journal of biological chemistry* **246**(9)**:** 3042-3049

Nichols BJ, Ungermann C, Pelham HR, Wickner WT, Haas A (1997) Homotypic vacuolar fusion mediated by t- and v-SNAREs. *Nature* **387**(6629)**:** 199-202

Nijman SM, Luna-Vargas MP, Velds A, Brummelkamp TR, Dirac AM, Sixma TK, Bernards R (2005) A genomic and functional inventory of deubiquitinating enzymes. *Cell* **123**(5)**:** 773-786

Nothwehr SF, Conibear E, Stevens TH (1995) Golgi and vacuolar membrane proteins reach the vacuole in vps1 mutant yeast cells via the plasma membrane. *The Journal of cell biology* **129**(1)**:** 35-46

Novick P, Field C, Schekman R (1980) Identification of 23 complementation groups required for post-translational events in the yeast secretory pathway. *Cell* **21**(1)**:** 205-215

Obrdlik P (2004) Manual for the use of mating-based Split ubiquitin system "mbSUS", version B.

Obrdlik P, El-Bakkoury M, Hamacher T, Cappellaro C, Vilarino C, Fleischer C, Ellerbrok H, Kamuzinzi R, Ledent V, Blaudez D, Sanders D, Revuelta JL, Boles E, Andre B, Frommer WB (2004) K+ channel interactions detected by a genetic system optimized for systematic studies of membrane protein interactions. *Proceedings of the National Academy of Sciences of the United States of America* **101**(33)**:** 12242-12247

Odblom MP, Handy RD (1999) A novel DIDS-sensitive, anion-dependent Mg(2+) efflux pathway in rat ventricular myocytes. *Biochem Biophys Res Commun* **264**(2)**:** 334-337

Odorizzi G, Cowles CR, Emr SD (1998) The AP-3 complex: a coat of many colours. *Trends Cell Biol* **8**(7)**:** 282-288

Ohno H (2006) Clathrin-associated adaptor protein complexes. *Journal of cell science* **119**(Pt 18)**:** 3719-3721

Owen DJ, Collins BM, Evans PR (2004) Adaptors for clathrin coats: structure and function. *Annual review of cell and developmental biology* **20:** 153-191

Park MH, Wong BB, Lusk JE (1976) Mutants in three genes affecting transport of magnesium in Escherichia coli: genetics and physiology. *J Bacteriol* **126**(3)**:** 1096-1103

Parlati F, Varlamov O, Paz K, McNew JA, Hurtado D, Sollner TH, Rothman JE (2002) Distinct SNARE complexes mediating membrane fusion in Golgi transport based on combinatorial specificity. *Proceedings of the National Academy of Sciences of the United States of America* **99**(8)**:** 5424-5429

Paumet F, Brugger B, Parlati F, McNew JA, Sollner TH, Rothman JE (2001) A t-SNARE of the endocytic pathway must be activated for fusion. *The Journal of cell biology* **155**(6)**:** 961-968

Payandeh J, Pai EF (2006) A structural basis for Mg2+ homeostasis and the CorA translocation cycle. *The EMBO journal* **25**(16)**:** 3762-3773

Pena MM, Puig S, Thiele DJ (2000) Characterization of the Saccharomyces cerevisiae high affinity copper transporter Ctr3. *The Journal of biological chemistry* **275**(43)**:** 33244-33251

Peng J, Schwartz D, Elias JE, Thoreen CC, Cheng D, Marsischky G, Roelofs J, Finley D, Gygi SP (2003) A proteomics approach to understanding protein ubiquitination. *Nat Biotechnol* **21**(8)**:** 921-926

Peng R, Grabowski R, De Antoni A, Gallwitz D (1999) Specific interaction of the yeast cis-Golgi syntaxin Sed5p and the coat protein complex II component Sec24p of endoplasmic reticulum-derived transport vesicles. *Proceedings of the National Academy of Sciences of the United States of America* **96**(7)**:** 3751-3756

Peplowska K, Markgraf DF, Ostrowicz CW, Bange G, Ungermann C (2007) The CORVET tethering complex interacts with the yeast Rab5 homolog Vps21 and is involved in endo-lysosomal biogenesis. *Developmental cell* **12**(5)**:** 739-750

Pety de Thozee C, Ghislain M (2006) ER-associated degradation of membrane proteins in yeast. *ScientificWorldJournal* **6:** 967-983

Pfeffer SR (1996) Transport vesicle docking: SNAREs and associates. *Annual review of cell and developmental biology* **12:** 441-461

Pfeffer SR (1999) Transport-vesicle targeting: tethers before SNAREs. *Nature cell biology* **1**(1)**:** E17-22

Piao HL, Machado IM, Payne GS (2007) NPFXD-mediated endocytosis is required for polarity and function of a yeast cell wall stress sensor. *Molecular biology of the cell* **18**(1)**:** 57-65

Pickart CM (2001) Mechanisms underlying ubiquitination. *Annual review of biochemistry* **70:** 503-533

Piper RC, Bryant NJ, Stevens TH (1997) The membrane protein alkaline phosphatase is delivered to the vacuole by a route that is distinct from the VPS-dependent pathway. *The Journal of cell biology* **138**(3)**:** 531-545

Piper RC, Cooper AA, Yang H, Stevens TH (1995) VPS27 controls vacuolar and endocytic traffic through a prevacuolar compartment in Saccharomyces cerevisiae. *The Journal of cell biology* **131**(3)**:** 603-617

Poirier MA, Xiao W, Macosko JC, Chan C, Shin YK, Bennett MK (1998) The synaptic SNARE complex is a parallel four-stranded helical bundle. *Nat Struct Biol* **5**(9)**:** 765-769

Pratelli R, Sutter JU, Blatt MR (2004) A new catch in the SNARE. *Trends Plant Sci* **9**(4)**:** 187-195

Prescianotto-Baschong C, Riezman H (2002) Ordering of compartments in the yeast endocytic pathway. *Traffic (Copenhagen, Denmark)* **3**(1)**:** 37-49

Preuss D, Mulholland J, Franzusoff A, Segev N, Botstein D (1992) Characterization of the Saccharomyces Golgi complex through the cell cycle by immunoelectron microscopy. *Molecular biology of the cell* **3**(7)**:** 789-803

Proszynski TJ, Simons K, Bagnat M (2004) O-glycosylation as a sorting determinant for cell surface delivery in yeast. *Molecular biology of the cell* **15**(4)**:** 1533-1543

Puoti A, Desponds C, Conzelmann A (1991) Biosynthesis of mannosylinositolphosphoceramide in Saccharomyces cerevisiae is dependent on genes controlling the flow of secretory vesicles from the endoplasmic reticulum to the Golgi. *The Journal of cell biology* **113**(3)**:** 515-525

Quamme GA (1997) Renal magnesium handling: new insights in understanding old problems. *Kidney Int* **52**(5)**:** 1180-1195

Quamme GA, Rabkin SW (1990) Cytosolic free magnesium in cardiac myocytes: identification of a Mg2+ influx pathway. *Biochem Biophys Res Commun* **167**(3)**:** 1406-1412

Raymond CK, Howald-Stevenson I, Vater CA, Stevens TH (1992) Morphological classification of the yeast vacuolar protein sorting mutants: evidence for a prevacuolar compartment in class E vps mutants. *Molecular biology of the cell* **3**(12)**:** 1389-1402

Rayner JC, Pelham HR (1997) Transmembrane domain-dependent sorting of proteins to the ER and plasma membrane in yeast. *The EMBO journal* **16**(8)**:** 1832-1841

Reggiori F, Black MW, Pelham HR (2000) Polar transmembrane domains target proteins to the interior of the yeast vacuole. *Molecular biology of the cell* **11**(11)**:** 3737-3749

Reggiori F, Wang CW, Stromhaug PE, Shintani T, Klionsky DJ (2003) Vps51 is part of the yeast Vps fifty-three tethering complex essential for retrograde traffic from the early endosome and Cvt vesicle completion. *The Journal of biological chemistry* **278**(7)**:** 5009-5020

Robinson JS, Klionsky DJ, Banta LM, Emr SD (1988) Protein sorting in Saccharomyces cerevisiae: isolation of mutants defective in the delivery and processing of multiple vacuolar hydrolases. *Molecular and cellular biology* **8**(11)**:** 4936-4948

Robinson KS, Lai K, Cannon TA, McGraw P (1996) Inositol transport in Saccharomyces cerevisiae is regulated by transcriptional and degradative endocytic mechanisms during the growth cycle that are distinct from inositol-induced regulation. *Molecular biology of the cell* **7**(1)**:** 81-89

Robinson MS (2004) Adaptable adaptors for coated vesicles. *Trends Cell Biol* **14**(4)**:** 167-174

Romani A (2007) Regulation of magnesium homeostasis and transport in mammalian cells *Archives of Biochemistry and Biophysics* **458**(1)**:** 90-102

Romani A, Marfella C, Scarpa A (1993) Cell magnesium transport and homeostasis: role of intracellular compartments. *Miner Electrolyte Metab* **19**(4-5)**:** 282-289

Romani A, Scarpa A (1992) Regulation of cell magnesium. *Arch Biochem Biophys* **298**(1)**:** 1-12

Rothman JE (1996) The protein machinery of vesicle budding and fusion. *Protein Sci* **5**(2)**:** 185-194

Rothman JE, Orci L (1996) Budding vesicles in living cells. *Sci Am* **274**(3)**:** 70-75

Rothman JE, Warren G (1994) Implications of the SNARE hypothesis for intracellular membrane topology and dynamics. *Curr Biol* **4**(3)**:** 220-233

Rothman JH, Howald I, Stevens TH (1989) Characterization of genes required for protein sorting and vacuolar function in the yeast Saccharomyces cerevisiae. *The EMBO journal* **8**(7)**:** 2057-2065

Rothman JH, Raymond CK, Gilbert T, O'Hara PJ, Stevens TH (1990) A putative GTP binding protein homologous to interferon-inducible Mx proteins performs an essential function in yeast protein sorting. *Cell* **61**(6)**:** 1063-1074

Rothman JH, Stevens TH (1986) Protein sorting in yeast: mutants defective in vacuole biogenesis mislocalize vacuolar proteins into the late secretory pathway. *Cell* **47**(6)**:** 1041-1051

Rougier JS, van Bemmelen MX, Bruce MC, Jespersen T, Gavillet B, Apotheloz F, Cordonier S, Staub O, Rotin D, Abriel H (2005) Molecular determinants of voltage-gated sodium channel regulation by the Nedd4/Nedd4-like proteins. *Am J Physiol Cell Physiol* **288**(3)**:** C692-701

Ryan MF (1991) The role of magnesium in clinical biochemistry: an overview. *Ann Clin Biochem* **28 (Pt 1):** 19-26

Saeki Y, Isono E, Toh EA (2005) Preparation of ubiquitinated substrates by the PY motif-insertion method for monitoring 26S proteasome activity. *Methods Enzymol* **399:** 215-227

Sahni J, Nelson B, Scharenberg AM (2007) SLC41A2 encodes a plasma-membrane Mg2+ transporter. *Biochem J* **401**(2)**:** 505-513

Samaj J, Baluska F, Voigt B, Schlicht M, Volkmann D, Menzel D (2004) Endocytosis, actin cytoskeleton, and signaling. *Plant Physiol* **135**(3)**:** 1150-1161

Saris NE, Mervaala E, Karppanen H, Khawaja JA, Lewenstam A (2000) Magnesium. An update on physiological, clinical and analytical aspects. *Clin Chim Acta* **294**(1-2)**:** 1-26

Scarpa A, Brinley FJ (1981) In situ measurements of free cytosolic magnesium ions. *Fed Proc* **40**(12)**:** 2646-2652

Scheiffele P, Peranen J, Simons K (1995) N-glycans as apical sorting signals in epithelial cells. *Nature* **378**(6552)**:** 96-98

Schekman R, Orci L (1996) Coat proteins and vesicle budding. *Science* **271**(5255)**:** 1526-1533

Schindl R, Weghuber J, Romanin C, Schweyen RJ (2007) Mrs2p forms a high conductance Mg2+ selective channel in mitochondria. *Biophys J* **93**(11)**:** 3872-3883

Schlingmann KP, Weber S, Peters M, Niemann Nejsum L, Vitzthum H, Klingel K, Kratz M, Haddad E, Ristoff E, Dinour D, Syrrou M, Nielsen S, Sassen M, Waldegger S, Seyberth HW, Konrad M (2002) Hypomagnesemia with secondary hypocalcemia is caused by mutations in TRPM6, a new member of the TRPM gene family. *Nat Genet* **31**(2)**:** 166-170

Schmitz C, Deason F, Perraud AL (2007) Molecular components of vertebrate Mg2+-homeostasis regulation. *Magnes Res* **20**(1)**:** 6-18

Schmitz C, Perraud AL, Johnson CO, Inabe K, Smith MK, Penner R, Kurosaki T, Fleig A, Scharenberg AM (2003) Regulation of vertebrate cellular Mg2+ homeostasis by TRPM7. *Cell* **114**(2)**:** 191-200

Schock I, Gregan J, Steinhauser S, Schweyen R, Brennicke A, Knoop V (2000) A member of a novel Arabidopsis thaliana gene family of candidate Mg2+ ion transporters complements a yeast mitochondrial group II intron-splicing mutant. *Plant J* **24**(4)**:** 489-501

Schwartz DC, Hochstrasser M (2003) A superfamily of protein tags: ubiquitin, SUMO and related modifiers. *Trends Biochem Sci* **28**(6)**:** 321-328

Schweigel M, Park HS, Etschmann B, Martens H (2006) Characterization of the Na+-dependent Mg2+ transport in sheep ruminal epithelial cells. *Am J Physiol Gastrointest Liver Physiol* **290**(1)**:** G56-65

Schweigel M, Vormann J, Martens H (2000) Mechanisms of Mg(2+) transport in cultured ruminal epithelial cells. *Am J Physiol Gastrointest Liver Physiol* **278**(3)**:** G400-408

Seaman MN (2005) Recycle your receptors with retromer. *Trends Cell Biol* **15**(2)**:** 68-75

Seeger M, Payne GS (1992) A role for clathrin in the sorting of vacuolar proteins in the Golgi complex of yeast. *The EMBO journal* **11**(8)**:** 2811-2818

Shaul O, Hilgemann DW, de-Almeida-Engler J, Van Montagu M, Inz D, Galili G (1999) Cloning and characterization of a novel Mg(2+)/H(+) exchanger. *The EMBO journal* **18**(14)**:** 3973-3980

Shearwin-Whyatt L, Dalton HE, Foot N, Kumar S (2006) Regulation of functional diversity within the Nedd4 family by accessory and adaptor proteins. *Bioessays* **28**(6)**:** 617-628

Sherman F (2002) Getting started with yeast. *Methods Enzymol* **350:** 3-41

Shim J, Lee J (2000) Molecular genetic analysis of apm-2 and aps-2, genes encoding the medium and small chains of the AP-2 clathrin-associated protein complex in the nematode Caenorhabditis elegans. *Mol Cells* **10**(3)**:** 309-316

Silver S (1969) Active transport of magnesium in escherichia coli. *Proceedings of the National Academy of Sciences of the United States of America* **62**(3)**:** 764-771

Silver S, Clark D (1971) Magnesium transport in Escherichia coli. *The Journal of biological chemistry* **246**(3)**:** 569-576

Simon DB, Lu Y, Choate KA, Velazquez H, Al-Sabban E, Praga M, Casari G, Bettinelli A, Colussi G, Rodriguez-Soriano J, McCredie D, Milford D, Sanjad S, Lifton RP (1999) Paracellin-1, a renal tight junction protein required for paracellular Mg2+ resorption. *Science* **285**(5424)**:** 103-106

Simons K, Ikonen E (1997) Functional rafts in cell membranes. *Nature* **387**(6633)**:** 569-572

Simons K, van Meer G (1988) Lipid sorting in epithelial cells. *Biochemistry* **27**(17)**:** 6197-6202

Singer-Kruger B, Nemoto Y, Daniell L, Ferro-Novick S, De Camilli P (1998) Synaptojanin family members are implicated in endocytic membrane traffic in yeast. *Journal of cell science* **111 (Pt 22):** 3347-3356

Siniossoglou S, Pelham HR (2002) Vps51p links the VFT complex to the SNARE Tlg1p. *The Journal of biological chemistry* **277**(50)**:** 48318-48324

Smith RL, Banks JL, Snavely MD, Maguire ME (1993) Sequence and topology of the CorA magnesium transport systems of Salmonella typhimurium and Escherichia coli. Identification of a new class of transport protein. *The Journal of biological chemistry* **268**(19)**:** 14071-14080

Smith RL, Kaczmarek MT, Kucharski LM, Maguire ME (1998) Magnesium transport in Salmonella typhimurium: regulation of mgtA and mgtCB during invasion of epithelial and macrophage cells. *Microbiology* **144 (Pt 7):** 1835-1843

Smith RL, Maguire ME (1998) Microbial magnesium transport: unusual transporters searching for identity. *Mol Microbiol* **28**(2)**:** 217-226

Smith RL, Thompson LJ, Maguire ME (1995) Cloning and characterization of MgtE, a putative new class of Mg2+ transporter from Bacillus firmus OF4. *J Bacteriol* **177**(5)**:** 1233-1238

Sollner T, Whiteheart SW, Brunner M, Erdjument-Bromage H, Geromanos S, Tempst P, Rothman JE (1993) SNAP receptors implicated in vesicle targeting and fusion. *Nature* **362**(6418)**:** 318-324

Spodsberg N, Alfalah M, Naim HY (2001) Characteristics and structural requirements of apical sorting of the rat growth hormone through the O-glycosylated stalk region of intestinal sucrase-isomaltase. *The Journal of biological chemistry* **276**(49)**:** 46597-46604

Springael JY, Andre B (1998) Nitrogen-regulated ubiquitination of the Gap1 permease of Saccharomyces cerevisiae. *Molecular biology of the cell* **9**(6)**:** 1253-1263

Stagljar I, Korostensky C, Johnsson N, te Heesen S (1998) A genetic system based on split-ubiquitin for the analysis of interactions between membrane proteins in vivo. *Proceedings of the National Academy of Sciences of the United States of America* **95**(9)**:** 5187-5192

Stamenova SD, Dunn R, Adler AS, Hicke L (2004) The Rsp5 ubiquitin ligase binds to and ubiquitinates members of the yeast CIN85-endophilin complex, Sla1-Rvs167. *The Journal of biological chemistry* **279**(16)**:** 16017-16025

Staub O, Rotin D (2006) Role of ubiquitylation in cellular membrane transport. *Physiological reviews* **86**(2)**:** 669-707

Sudol M (1996) Structure and function of the WW domain. *Prog Biophys Mol Biol* **65**(1-2)**:** 113-132

Sullivan JA, Lewis MJ, Nikko E, Pelham HR (2007) Multiple interactions drive adaptor-mediated recruitment of the ubiquitin ligase rsp5 to membrane proteins in vivo and in vitro. *Molecular biology of the cell* **18**(7)**:** 2429-2440

Surpin M, Raikhel N (2004) Traffic jams affect plant development and signal transduction. *Nat Rev Mol Cell Biol* **5**(2)**:** 100-109

Sutton RB, Fasshauer D, Jahn R, Brunger AT (1998) Crystal structure of a SNARE complex involved in synaptic exocytosis at 2.4 A resolution. *Nature* **395**(6700)**:** 347-353

Szegedy MA, Maguire ME (1999) The CorA Mg(2+) transport protein of Salmonella typhimurium. Mutagenesis of conserved residues in the second membrane domain. *The Journal of biological chemistry* **274**(52)**:** 36973-36979

Tan PK, Howard JP, Payne GS (1996) The sequence NPFXD defines a new class of endocytosis signal in Saccharomyces cerevisiae. *The Journal of cell biology* **135**(6 Pt 2)**:** 1789-1800

Tang HY, Munn A, Cai M (1997) EH domain proteins Pan1p and End3p are components of a complex that plays a dual role in organization of the cortical actin cytoskeleton and endocytosis in Saccharomyces cerevisiae. *Molecular and cellular biology* **17**(8)**:** 4294-4304

Tao T, Grulich PF, Kucharski LM, Smith RL, Maguire ME (1998) Magnesium transport in Salmonella typhimurium: biphasic magnesium and time dependence of the transcription of the mgtA and mgtCB loci. *Microbiology* **144 (Pt 3):** 655-664

Tevelev A, Cowan JA (1995) Metal substitution as a probe of the biological chemistry of magnesium ion. In: Cowan, J.A. (Ed.), The Biological Chemistry of Magnesium. VCH. 53-84

Townsend DE, Esenwine AJ, George J, 3rd, Bross D, Maguire ME, Smith RL (1995) Cloning of the mgtE Mg2+ transporter from Providencia stuartii and the distribution of mgtE in gram-negative and gram-positive bacteria. *J Bacteriol* **177**(18)**:** 5350-5354

Traub LM (2005) Common principles in clathrin-mediated sorting at the Golgi and the plasma membrane. *Biochimica et biophysica acta* **1744**(3)**:** 415-437

Traub LM, Lukacs GL (2007) Decoding ubiquitin sorting signals for clathrin-dependent endocytosis by CLASPs. *Journal of cell science* **120**(Pt 4)**:** 543-553

Trombetta ES, Parodi AJ (2003) Quality control and protein folding in the secretory pathway. *Annual review of cell and developmental biology* **19:** 649-676

Umebayashi K, Nakano A (2003) Ergosterol is required for targeting of tryptophan permease to the yeast plasma membrane. *The Journal of cell biology* **161**(6)**:** 1117-1131

Ungermann C, Sato K, Wickner W (1998) Defining the functions of trans-SNARE pairs. *Nature* **396**(6711)**:** 543-548

Varlamov O, Volchuk A, Rahimian V, Doege CA, Paumet F, Eng WS, Arango N, Parlati F, Ravazzola M, Orci L, Sollner TH, Rothman JE (2004) i-SNAREs: inhibitory SNAREs that fine-tune the specificity of membrane fusion. *The Journal of cell biology* **164**(1)**:** 79-88

Vashist S, Ng DT (2004) Misfolded proteins are sorted by a sequential checkpoint mechanism of ER quality control. *The Journal of cell biology* **165**(1)**:** 41-52

Vida TA, Huyer G, Emr SD (1993) Yeast vacuolar proenzymes are sorted in the late Golgi complex and transported to the vacuole via a prevacuolar endosome-like compartment. *The Journal of cell biology* **121**(6)**:** 1245-1256

Voets T, Nilius B, Hoefs S, van der Kemp AW, Droogmans G, Bindels RJ, Hoenderop JG (2004) TRPM6 forms the Mg2+ influx channel involved in intestinal and renal Mg2+ absorption. *The Journal of biological chemistry* **279**(1)**:** 19-25

Wabakken T, Rian E, Kveine M, Aasheim HC (2003) The human solute carrier SLC41A1 belongs to a novel eukaryotic subfamily with homology to prokaryotic MgtE Mg2+ transporters. *Biochem Biophys Res Commun* **306**(3)**:** 718-724

Wachek M, Aichinger MC, Stadler JA, Schweyen RJ, Graschopf A (2006) Oligomerization of the Mg2+-transport proteins Alr1p and Alr2p in yeast plasma membrane. *The FEBS journal* **273**(18)**:** 4236-4249

Walther TC, Brickner JH, Aguilar PS, Bernales S, Pantoja C, Walter P (2006) Eisosomes mark static sites of endocytosis. *Nature* **439**(7079)**:** 998-1003

Wang CY, Shi JD, Yang P, Kumar PG, Li QZ, Run QG, Su YC, Scott HS, Kao KJ, She JX (2003) Molecular cloning and characterization of a novel gene family of four ancient conserved domain proteins (ACDP). *Gene* **306:** 37-44

Wang W, Sacher M, Ferro-Novick S (2000) TRAPP stimulates guanine nucleotide exchange on Ypt1p. *The Journal of cell biology* **151**(2)**:** 289-296

Warren MA, Kucharski LM, Veenstra A, Shi L, Grulich PF, Maguire ME (2004) The CorA Mg2+ transporter is a homotetramer. *J Bacteriol* **186**(14)**:** 4605-4612

Watanabe R, Riezman H (2004) Differential ER exit in yeast and mammalian cells. *Current opinion in cell biology* **16**(4)**:** 350-355

Watson HA, Von Zastrow M, Wendland B (2004) Endocytosis. *Encyclopedia of Molecular Cell Biology and Molecular Medicine Second edition Edited by Robert A Myers Wiley-VCH* **4:** 181-224

Weber T, Zemelman BV, McNew JA, Westermann B, Gmachl M, Parlati F, Sollner TH, Rothman JE (1998) SNAREpins: minimal machinery for membrane fusion. *Cell* **92**(6)**:** 759-772

Weghuber J, Dieterich F, Froschauer EM, Svidova S, Schweyen RJ (2006) Mutational analysis of functional domains in Mrs2p, the mitochondrial Mg2+ channel protein of Saccharomyces cerevisiae. *The FEBS journal* **273**(6)**:** 1198-1209

Weissman AM (2001) Themes and variations on ubiquitylation. *Nat Rev Mol Cell Biol* **2**(3)**:** 169-178

Whyte JR, Munro S (2002) Vesicle tethering complexes in membrane traffic. *Journal of cell science* **115**(Pt 13)**:** 2627-2637

Wiesenberger G, Waldherr M, Schweyen RJ (1992) The nuclear gene MRS2 is essential for the excision of group II introns from yeast mitochondrial transcripts in vivo. *The Journal of biological chemistry* **267**(10)**:** 6963-6969

Williams RJP (1970) The biochemistry of sodium, potassium, magnesium and calcium. . *Q Rev Chem Soc* **24:** 331-365

Williams RJP (1993) Magnesium: an introduction to its biochemistry. . *In: Birch, NJ (Ed), Magnesium and the Cell Academic Press, NY***:** 15-30

Wilsbach K, Payne GS (1993) Vps1p, a member of the dynamin GTPase family, is necessary for Golgi membrane protein retention in Saccharomyces cerevisiae. *The EMBO journal* **12**(8)**:** 3049-3059

Wolf FI, Cittadini A (2003) Chemistry and biochemistry of magnesium. *Mol Aspects Med* **24**(1-3)**:** 3-9

Wood V, Gwilliam R, Rajandream MA, Lyne M, Lyne R, Stewart A, Sgouros J, Peat N, Hayles J, Baker S, Basham D, Bowman S, Brooks K, Brown D, Brown S, Chillingworth T, Churcher C, Collins M, Connor R, Cronin A, Davis P, Feltwell T, Fraser A, Gentles S, Goble A, Hamlin N, Harris D, Hidalgo J, Hodgson G, Holroyd S, Hornsby T, Howarth S, Huckle EJ, Hunt S, Jagels K, James K, Jones L, Jones M, Leather S, McDonald S, McLean J, Mooney P, Moule S, Mungall K, Murphy L, Niblett D, Odell C, Oliver K, O'Neil S, Pearson D, Quail MA, Rabbinowitsch E, Rutherford K, Rutter S, Saunders D, Seeger K, Sharp S, Skelton J, Simmonds M, Squares R, Squares S, Stevens K, Taylor K, Taylor RG, Tivey A, Walsh S, Warren T, Whitehead S, Woodward J, Volckaert G, Aert R, Robben J, Grymonprez B, Weltjens I, Vanstreels E, Rieger M, Schafer M, Muller-Auer S, Gabel C, Fuchs M, Dusterhoft A, Fritzc C, Holzer E, Moestl D, Hilbert H, Borzym K, Langer I, Beck A, Lehrach H, Reinhardt R, Pohl TM, Eger P, Zimmermann W, Wedler H, Wambutt R, Purnelle B, Goffeau A, Cadieu E, Dreano S, Gloux S, Lelaure V, Mottier S, Galibert F, Aves SJ, Xiang Z, Hunt C, Moore K, Hurst SM, Lucas M, Rochet M, Gaillardin C, Tallada VA, Garzon A, Thode G, Daga RR, Cruzado L, Jimenez J, Sanchez M, del Rey F, Benito J, Dominguez A, Revuelta JL, Moreno S, Armstrong J, Forsburg SL, Cerutti L, Lowe T, McCombie WR, Paulsen I, Potashkin J, Shpakovski GV, Ussery D, Barrell BG, Nurse P (2002) The genome sequence of Schizosaccharomyces pombe. *Nature* **415**(6874)**:** 871-880

Wuestehube LJ, Duden R, Eun A, Hamamoto S, Korn P, Ram R, Schekman R (1996) New mutants of Saccharomyces cerevisiae affected in the transport of proteins from the endoplasmic reticulum to the Golgi complex. *Genetics* **142**(2)**:** 393-406

Yeaman C, Le Gall AH, Baldwin AN, Monlauzeur L, Le Bivic A, Rodriguez-Boulan E (1997) The O-glycosylated stalk domain is required for apical sorting of neurotrophin receptors in polarized MDCK cells. *The Journal of cell biology* **139**(4)**:** 929-940

Yerushalmi H, Lebendiker M, Schuldiner S (1996) Negative dominance studies demonstrate the oligomeric structure of EmrE, a multidrug antiporter from Escherichia coli. *The Journal of biological chemistry* **271**(49)**:** 31044-31048

Yeung BG, Phan HL, Payne GS (1999) Adaptor complex-independent clathrin function in yeast. *Molecular biology of the cell* **10**(11)**:** 3643-3659

Zerial M, McBride H (2001) Rab proteins as membrane organizers. *Nat Rev Mol Cell Biol* **2**(2)**:** 107-117

Zsurka G, Gregan J, Schweyen RJ (2001) The human mitochondrial Mrs2 protein functionally substitutes for its yeast homologue, a candidate magnesium transporter. *Genomics* **72**(2)**:** 158-168

8. LIST OF ABBREVIATIONS

Table. List of abbreviations used in the text

Abbreviation	Term written out
aa	amino acid
Amp	ampicillin
ARH	autosomal recessive hypercholesterolemia adaptor
ARS	autonomously replicating sequences
ATP	adenosine triphosphate
BSA	bovine serum albumin
CEN	centromeric
COG	conserved oligomeric Golgi complex
DMSO	dimethyl sulfoxide
DNA	deoxyribonucleic acid
EDTA	ethylenediaminetetraacetat
EE	early endosome
e.g.	for example
ER	endoplasmatic reticulum
g	gram
GARP	golgi associated retrograde protein complex
GFP	green fluorescent protein
GPI	glycosyl-phosphatidylinositol
GTP	guanosine triphosphate
HA	hemagglutinin
HIS	histidine
HOPS	homotypic fusion and vacuole protein sorting complex
i.e.	that is
kDa	kilo Dalton
l	liter
LB	Luria-Bertani medium
LE	late endosome
LEU	leucine
LiAc	lithium acetate
m	mili
M	mol
mbSUS	mating-based split-ubiquitin system
MDCK	Madin Darby Canine Kidney
Min	minute

Abbreviation	Term written out
μ	micro
N	normal
OD$_{600}$	optical density at 600 nm
p	pico
PAGE	polyacrylamide gel electrophoresis
PCR	polymerase chain reaction
PEG	polyethylenglycol
PM	plasma membrane
PTB	phosphotyrosine binding domain
PVC	pre-vacuolar compartment
RNA	ribonucleic acid
rpm	revolutions per minute
s	second
SDS	sodium-dodecyl-sulfate
SNAP	soluble NSF attachment protein
TCA	trichloroacetic acid
TE	tris-EDTA buffer
TGN	trans-Golgi network
TM (TMD)	transmembrane (domain)
TRP	tryptophan
V	volt
VFT	Vps fifty-three complex
wt	wild-type
YPD	yeast extract-peptone-dextrose medium
YTH	yeast two-hybrid system

9. ACKNOWLEDGMENTS

10. CURRICULUM VITAE

Personal Information

Name: Marcin Krzysztof Wachek

Date of Birth: 20th March 1977

Place of Birth: Elblag, Poland

Nationality: Poland

Marital Status: Married

Education

1983-1992   Elblag, Poland (primary school)

1992-1996   Elblag, Poland (high school)

1996-2000   Bachelor of Science, Faculty of Animal Bioengineering, UWM in Poland.

2000-2001   Master of Science, Faculty of Animal Bioengineering, UWM in Poland.
Thesis – "Single-strand conformation polymorphism within the porcine growth hormone gene promoter". Prof. Dr. Hab. Stanislaw Kaminski.

2009   Ph.D., Molecular Biology, Institute for Genetics, University of Vienna
Thesis – "Functional Analysis of the Plasma Membrane Alr1 and Alr2 Proteins in Yeast *Saccharomyces cerevisiae*".
Lab of Prof. Dr. Rudolf J. Schweyen

Publications

Wachek M., Schweyen R.J., and Graschopf A. (submitted) An internal α-helix and sequence motifs are essential for vesicular transport and turnover of the plasma membrane Mg2+ transporter Alr1p.

Wachek M., Aichinger M.C., Stadler J.A, Schweyen R.J., and Graschopf A. (2006) Oligomerization of the Mg^{2+}-transport proteins Alr1p and Alr2p in yeast plasma membrane. *The FEBS Journal* **273**, 4236-4249.

Kaminski S., Wachek M. (2002) Single-strand conformation polymorphism within the porcine growth hormone gene promoter. *Animal Science Paper and Reports* **20**, 1:47 – 53.